Order Number 9009720

An internally consistent thermodynamic database on minerals: Application to the earth's crust and upper mantle

Chatterjee, Nilanjan, Ph.D.

City University of New York, 1989

U·M·I
300 N. Zeeb Rd.
Ann Arbor, MI 48106

AN INTERNALLY CONSISTENT THERMODYNAMIC DATA BASE ON MINERALS:

Application to the Earth's Crust and Upper Mantle

by

NILANJAN CHATTERJEE

A dissertation submitted to the Graduate Faculty in Earth and Environmental Sciences in partial fulfillment of the requirements for the degree of Doctor of Philosophy, The City University of New York.

1989

This manuscript has been read and accepted for the Graduate Faculty in Earth and Environmental Sciences in satisfaction of the dissertation requirement for the degree of Doctor of Philosophy.

5/2/89

Date

Chair of Examining Committee

8/29/89

Date

Executive Officer

Somdev Bhattacharji

Supervisory Committee

The City University of New York

Abstract

AN INTERNALLY CONSISTENT THERMODYNAMIC DATA BASE ON MINERALS:

Application to the Earth's Crust and Upper Mantle

by

Nilanjan Chatterjee

Advisor: Professor Surendra K. Saxena

An internally consistent thermodynamic data base with fifty two common minerals found in the earth's crust and upper mantle in the system Na_2O-K_2O-CaO-FeO-MnO-MgO-Al_2O_3-TiO_2-SiO_2-H_2O is created by systematization of available calorimetric data and experimental phase equilibrium data. An optimization of the two data sets is carried out through the program MINUIT, in which numerical techniques are used. These techniques include the Monte Carlo search, the simplex and the gradient methods. The data base also includes interaction parameters of forty four different binary solid solutions of common crustal and upper mantle minerals. The method adopted is to work on small sub-systems and then combine them to test for internal consistency. The sub-systems studied extensively are MgO-Al_2O_3-SiO_2, CaO-Al_2O_3-SiO_2, CaO-MgO-Al_2O_3-SiO_2, FeO-MgO-Al_2O_3-SiO_2, MgO-SiO_2-H_2O, K_2O-Al_2O_3-SiO_2-H_2O, Na_2O-Al_2O_3-SiO_2-H_2O and K_2O-FeO-MgO-Al_2O_3-SiO_2-H_2O. Recommended thermodynamic properties of most of the minerals studied are within their originally stated calorimetric error limits with the exception of the enthalpies, entropies and heat capacities of gehlenite and Ca-tschermak; the enthalpy and entropy of almandine; the enthalpies of anorthite, spinel, talc and anthophyllite; the entropy and heat capacity of monticellite;

the entropy of sanidine and the heat capacity of paragonite. The test of internal consistency is done through computation of phase equilibrium relations in a system of fixed composition by the technique of minimization of total Gibbs free energy of a system. This technique is implemented in Eriksson's program SOLGASMIX (Eriksson, 1975). The data base is managed through a program called RETR, which is used to inspect and retrieve thermodynamic properties of pure phases and solid solutions. The data base is used in thermometry and barometry of natural assemblages. It is also used in the calculation of phase equilibria. Two programs, THERMO and REAC, are presented for thermometry and barometry. Thirteen different thermometric reactions are considered in program THERMO. In program REAC, any reaction can be defined from the set of phases being considered. In both programs, the Bertrand-Kohler (Bertrand et al., 1983) model for multicomponent solid solutions is used. The fugacity models of Saxena and Fei (1987a,b), for real gases, are also incorporated in program REAC.

Acknowledgement

I wish to express my deepest gratitude to my advisor Prof. S.K. Saxena without whose guidance this study would never have been accomplished. I am also grateful to my advisory committee members Prof. Brian Bayly, Prof. S. Bhattacharji, Prof. Allan Ludman and Prof. C.E. Nehru for their critical reviews and helpful suggestions in improving this dissertation and their constant support and encouragement throughout the period in which this work was accomplished. I am very thankful to Prof. Saxena, Prof. Nehru, Prof. Daniel Habib, Prof. A. Strahler and Prof A. Ohan for lending me financial support in form of assistantship at some time or other during this period.

I express my thanks to G. Eriksson for letting me use his program in many of the calculations in this work. Special thanks are due to Yingwei Fei, my personal friend and a colleague for the last five years, whose help and suggestions and camaraderie at work and outside are very deeply appreciated.

Last, but not least by any means, I thank my parents and my family for their love and support and inspiration they have always provided during these five hectic years.

Content

List of Tables

List of Figures

CHAPTER 1

INTRODUCTION

The primary aim of this research was to understand the chemical and physical nature of the earth's crust and upper mantle through a thermodynamic study of phase equilibria. Chemical nature implies chemical equilibria in mineral assemblages. Physical nature implies the variation of pressure, temperature and density under the earth's surface. Both chemical and physical information are critically interdependent. However, it was soon realized that the thermodynamic data needed for this purpose were not consistent with many of the observed experimental equilibria. Therfore, the major goal of this research became the development of an internally consistent thermodynamic data base which would reproduce all experimental observed phase equilibria. Only equilibrium processes are considered in this study and secondary importance is given to kinetic factors.

The principles adopted in this study are those of equilibrium thermodynamics. In order to study phase equilibria in the earth's crust and upper mantle, the following research is essential:

a) Systematization of available thermochemical and thermophysical data on minerals (enthalpy, entropy, heat capacity, molar volume, thermal expansion and compressibility of phases, excess properties of solid solutions and fugacities of fluids).

b) Calculation and/or estimation of thermodynamic properties of

phases for which thermodynamic data are missing.

c) Modeling multicomponent solid solutions and estimating and/or calculating excess solution properties that are missing.

d) Modeling fluid fugacities.

e) Documentation of observed and calculated phase relations in the crust and upper mantle.

A) Thermodynamic Data Systematics.

Phase equilibria can be studied either through equilibrium experiments or through computation using thermodynamic data. The main sources of thermochemical and thermophysical data are calorimetry, X-ray measurements of unit cells and stress-strain experiments. However, computed equilibria using thermochemical data from calorimetric sources in most cases do not reproduce observations of equilibrium experiments. Examples of this kind of discrepancy are given in Chapter 4. The reason for this discrepancy varies from one case to another. For example, some minerals, such as spinel, show different degrees of intracrystalline disorder at different temperatures. The true state of disorder could be misinterpreted in a calorimetric experiment. Systematization in this case would involve a correction for disorder in the data of spinel. Hence, the emphasis of this work is to systematize the thermodynamic properties of important metamorphic minerals and to achieve an internally consistent data base with which all experimental equilibria may be reproduced satisfactorily. The major element chemistry of the earth's crust and upper mantle can be described by the system Na_2O-K_2O-CaO-FeO-MnO-MgO-Al_2O_3-TiO_2-SiO_2-H_2O. Other major components such as C,

Cr, Fe^{3+} and Mn^{3+} are not considered here. The method adopted is to study sub-systems and combine them finally to test for internal consistency. The sub-systems studied extensively are $MgO-Al_2O_3-SiO_2$, $CaO-Al_2O_3-SiO_2$, $CaO-MgO-Al_2O_3-SiO_2$, $FeO-MgO-Al_2O_3-SiO_2$, $MgO-SiO_2-H_2O$, $K_2O-Al_2O_3-SiO_2-H_2O$, $Na_2O-Al_2O_3-SiO_2-H_2O$ and $K_2O-FeO-MgO-Al_2O_3-SiO_2-H_2O$.

Discussion of Errors

The optimization technique used in evaluating the properties of the phases in this study is discussed in Chapter 2. The error associated with the final estimate of a thermodynamic property can be stated when it is calculated from a reaction showing reversed equilibria. The upper and lower bounds of the reversals correspond to the limits of the error. It is difficult to state the errors when several parameters are optimized simultaneously. For example, suppose the enthalpy and entropy of one of the phases participating in a group of reactions is calculated by optimization. The statistical error given by this procedure must be distributed between the enthalpy and the entropy. This is a difficult problem. The problem becomes more complex when four or five parameters are optimized simultaneously.

B) Applications.

Applications of the data base are considered in Chapter 5. One of the advantages of an internally consistent data base is that a large amount of physical and chemical information on a system can be stored in simple terms. Only a few thermodynamic terms are necessary to describe a

phase and its behavior under given physicochemical conditions. Phase relations can be easily calculated from the data base. A major use of the data base is to calculate equilibria outside the pressure, temperature and chemical composition bounds of the equilibrium experiments. Such extrapolations and interpolations, done frequently in thermometric and barometric calculations, can be achieved through the data base presented here. A similar approach may be followed in many ceramic and metallurgical calculations.

The free energy minimization technique (discussed in Chapter 2) can be applied to a given bulk chemical composition to calculate at a fixed pressure and temperature the equilibrium assemblage, the composition, proportion and density of each phase, the activities of the components of a solution, fugacities of gas phases, distribution coefficients of solid solutions and the average density of the assemblage.

CHAPTER 2

THERMODYNAMIC PRINCIPLES AND METHODS OF STUDY

1. FREE ENERGY AND VOLUME OF A PHASE UNDER SPECIFIED CONDITIONS

The Gibbs free energy of formation of a phase from elements at a given pressure and temperature is given by,

$$\Delta G^{o}(P,T) = [\Delta H^{o}_{298} + \int_{298}^{T} \Delta C_p dT] - T[\Delta S^{o}_{298} + \int_{298}^{T} \Delta C_p/T dT] + \int_{1}^{P} \Delta V(T) dP \qquad (2.1)$$

where, $\Delta G^{o}(P,T)$, ΔH^{o}_{298}, ΔS^{o}_{298}, ΔC_p and $\Delta V(T)$ are the Gibbs free energy of formation at pressure P and temperature T, enthalpy of formation at 298 K, entropy of formation at 298 K, heat capacity of formation at constant pressure and molar volume of formation at temperature T respectively.

The heat capacity expression for minerals used in this study is from Fei and Saxena (1987). The expression is as follows:

$$C_p = 3Rn(1 + k_1T^{-1} + k_2T^{-2} + k_3T^{-3}) + (A + BT) + C'_p \qquad (2.2)$$

which can be rewritten as

$$C_p = a + bT + cT^{-2} + eT^{-3} + gT^{-1} \qquad (2.2a)$$

where $a = 3Rn + A + C'_p$, $b = B$, $c = 3Rnk_2$, $e = 3Rnk_3$ and $g = 3Rnk_1$. R is the gas constant; n, the number of atoms in the chemical formula; A and B are related to the thermal expansion coefficient and the isothermal bulk modulus, at the temperature of interest as described below. Heat capacities at constant pressure and constant volume are related by the equation:

$$C_p - C_v = [\alpha(T)]^2 V(1,T) K_T T \qquad (2.3)$$

where $\alpha(T)$, $V(1,T)$ and K_T are the thermal expansion, molar volume and isothermal bulk modulus respectively. Equation (2.3) is simplified to fit an empirical expression such that

$$C_p - C_v = A + BT \qquad (2.3a)$$

The constants k_1, k_2 and k_3, along with A and B are determined by least squares analysis of calorimetric data. C'_p represents the contributions to the heat capacity for some substances due to factors such as cation disordering, electronic and magnetic contributions.

The thermal expansion equation used in this study is similar to the C_p equation and is as follows:

$$\alpha(T) = \alpha_0 + \alpha_1 T + \alpha_2 T^{-2} \qquad (2.4)$$

The molar volume is given by the Murnaghan equation which is as follows:

$$V(P,T) = V_{298} \exp\left[\int_{298}^{T} \alpha(T)dT\right] [1 + K'_T P/K_T]^{(-1/K'_T)} \qquad (2.5)$$

which upon integration becomes

$$\int_1^P V(T)dP =$$

$$V_{298}\exp[\alpha_0(T-298)+\alpha_1(T^2-298^2)/2-\alpha_2(1/T-1/298)]$$
$$[K_T/(K'_T-1)][(1+K'_TP/K_T)^{(1-1/K'_T)}-1] \qquad (2.6)$$

where K'_T is the pressure derivative of K_T.

II. FUGACITY OF WATER

The fugacity expression for H_2O used in this study is from Saxena and Fei (1987a,b) which is described below. The compressibility factor of water is expressed as

$$Z(1Kbar<P<=5Kbar) = A + BP + CP^2 \qquad (2.7)$$

where

$$A = 9.968E+1T^{-1} - 7.025E-1 + 1.160E-3T$$
$$B = 2.143E-1T^{-1} - 3.142E-14T^3$$
$$C = -1.459E-1T^{-3} - 2.249E-6T^{-1} + 2.169E-15T^2$$

$$Z(5Kbar<=P) = A + BP + CP^2 + DP^3 \qquad (2.8)$$

where

$$A = 2.17E+8T^{-3} - 7.80E+5T^{-2} + 4.045 - 3.941E-11nT$$
$$B = -1.10E+4T^{-3} + 4.57E+1T^{-2} + 1.24E-1T^{-1}$$
$$C = 1.24E-1T^{-3} - 5.27E-4T^{-2} - 1.20E-8T^{-1} - 6.943E-11 + 1.073E-111nT$$
$$D = -3.27E-7T^{-3} + 1.60E-9T^{-2} - 4.61E-13T^{-1} - 2.16E-36T^3$$

Fugacity of water is calculated from the following relation:

$$RTlnf(P,T) =$$

$$RTlnf(1Kbar,T)$$

$$+ RT\left(\int_{1000}^{5000} Z_{(2.7)}/PdP + \int_{5000}^{P} Z_{(2.8)}/PdP\right) \qquad (2.9)$$

An expression for water fugacity at 1 Kbar that reproduces the data of Burnham et al. (1969), Halbach and Chatterjee (1982), Haar et al. (1984), etc. is:

$$RT\ln f(1Kbar,T) = 1000(-222.943 + 2.9865E\text{-}2T + 35.9794\ln T) \qquad (2.10)$$

III. SOLID SOLUTION MODELS

All binary solid solutions are modeled using the Margules formulation, which is as follows:

$$\Delta G^{ex}_{12} = X_1X_2[W_{12}X_2 + W_{21}X_1] \qquad (2.11)$$

where, ΔG^{ex}_{12} is the excess free energy associated with the 1-2 binary solution and W_{12} and W_{21} are the asymmetric interaction parameters for the same join. The interaction parameters can be further expressed as:

$$W_{12} = W_{12}^{H} - TW_{12}^{S} + PW_{12}^{V} \qquad (2.11a)$$

and

$$W_{21} = W_{21}^{H} - TW_{21}^{S} + PW_{21}^{V} \qquad (2.11b)$$

The above two expressions are analogous to the free energy expression.

The multicomponent solutions are modeled using the Bertrand-Kohler formulation (Bertrand et al., 1983), which is as follows:

$$\Delta G^{ex}_{12...N} = \Sigma^{N}_{i=1} \Sigma^{N}_{j>i} (X_i + X_j) (f_i + f_j) (\Delta G^{ex}_{ij})^{*} \qquad (2.12)$$

where, $(\Delta G^{ex}_{ij})^{*}$ is the molar excess free energy of the binary system with components at the same molar ratio as the multicomponent system and f_i and f_j are weighted mole fractions using weighting factors based on the excess properties of the binary systems. X_i is used as the mole fraction in the multicomponent system.

IV. MINIMIZATION OF TOTAL FREE ENERGY

A useful technique in computing phase equilibria is the method of minimization of the total Gibbs free energy employing linear algebraic methods as discussed by Eriksson (1975) and Smith and Missen (1982). It forms the basis of the computer program SOLGASMIX which is employed many times in this study and is described in Chapter 5.

The total Gibbs free energy of a chemical system can be expressed as

$$G = \Sigma \mu_i n_i \qquad (2.13)$$

where, μ is the chemical potential. Chemical potential and activity are related by the expression

$$\mu = \mu^{o} + RT\ln a \qquad (2.14)$$

where, μ^{o} denotes the standard state potential. For a real gas component in an ideal gas solution, a solid component in a non-ideal solid solution and a stoichiometric solid respectively, we have

$$\mu_i = \mu^o_i + RT\ln f_i + RT\ln x_i \qquad (2.15)$$

$$\mu_i = \mu^o_i + RT\ln \gamma_i + RT\ln x_i \qquad (2.16)$$

$$\mu_i = \mu^o_i \qquad (2.17)$$

where, x_i is the mole fraction of real gas or solid component 'i', γ_i, the activity coefficient of solid component 'i' and f_i, the fugacity of real gas component 'i'.

The minimization of G in equation (2.13) at constant pressure and temperature is achieved with the constraints imposed by the mass balance relationships represented as

$$\Sigma a_{ij} n_i = b_j (j=1,2,..,l) \qquad (2.18)$$

where, a_{ij} is the number of atoms of the jth element in a molecule of the ith species, l, the total number of elements and b_j, the total amount of the jth element. This is a simple form of a constrained optimization problem which may be solved by the Lagrange method of undetermined multipliers. For this, we define a function,

$$F = G + {}^{l}\Sigma_{j=1} \lambda_j (b_j - \Sigma a_{ij} n_i) \qquad (2.19)$$

where, λ_j denotes the Lagrangian multiplier, for which the necessary conditions, at an extremum of F, are

$$(\partial F/\partial n_i)_{n_k=i,\lambda} = \mu_i - \Sigma a_{ij} \lambda_j = 0 \qquad (2.20)$$

$$(\partial F/\partial \lambda_j)_{\lambda_k=j,n} = b_j - \Sigma a_{ij} n_i = 0 \qquad (2.21)$$

$$n_i >= 0 \qquad (2.22)$$

Combination of equations (2.15) to (2.17) with equation (2.20) gives

$$\mu^{o}_{i} + RT\ln f_i + RT\ln x_i - \Sigma a_{ij}\lambda_j = 0 \qquad (2.23)$$

$$\mu^{o}_{i} + RT\ln \gamma_i + RT\ln x_i - \Sigma a_{ij}\lambda_j = 0 \qquad (2.24)$$

$$\mu^{o}_{i} - \Sigma a_{ij}\lambda_j = 0 \qquad (2.25)$$

Equation (2.23) is valid for real gases in ideal gas solutions while equations (2.24) and (2.25) hold for components of solid solution phases and stoichiometric phases respectively.

The system consisting of equations (2.18) and (2.23) to (2.25), with the unknowns n_i and λ_i, is nonlinear because of the logarithmic term in equations (2.24) and (2.25). The next step is, therefore, a linearization of these equations by expansion in a Taylor series around an estimated equilibrium composition upto and including the term of the first order. This is equivalent to making a quadratic approximation to the free energy surface, and we can obtain an expression which relates n_i linearly to λ_j and the estimated equilibrium amounts. Incorporation of this expression into equation (2.18) gives then the final linear set of equations. The number of unknowns is reduced to the sum of elements and phases are assumed to be present at equilibrium.

Parameterized activity coefficient expressions to be inserted into equation (2.24) are supplied by the user. In order to avoid the need of also specifying derivatives, $\ln\lambda$ is treated as constant when calculating the partial derivative with respect to n_i in the Taylor expansion. The

partial derivative is, therefore, approximate as long as the equilibrium composition does not correspond to a free energy minimum.

The approximation to the free energy surface implies an iterative algorithm and, if positive, the calculated n_i values are used as improved estimates in the subsequent iterative cycle. If some n_i values are negative, these are set to zero before being used as the starting-point for a new Taylor expansion. The iterative procedure ends when the calculated values coincide with the starting estimates.

The condensed phases included in the initial estimate are constrained by the Gibbs phase rule, but need not necessarily be the correct ones of the final equilibrium state. Another phase combination might yield a lower free energy, and condensed phases need to be withdrawn or added to the previous combination until the set of equilibrium phases is found. This set has the characteristic feature that the activity for an omitted stoichiometric phase must be less than one as must the sum of mole fractions for an omitted solution phase.

A more detailed description of the method is described in Eriksson and Rosen (1973).

V. COMPUTATIONAL TECHNIQUES

Various techniques are adopted, depending upon the complexity of a problem, to construct the internally consistent data base. The phases considered in this study can be characterized into four distinct groups:

i) Phases with well determined calorimetric data. E.g., MgO.

ii) Phases whose thermochemical properties have been measured from calorimetry by different workers with different results. E.g., enstatite, forsterite.

iii) Phases whose thermochemical properties are not available, but experimental reversals, including data on distribution of major elements between coexisting phases, are available. E.g., ferrosilite.

iv) Phases for which neither calorimetric nor experimental data are available.

In the first case, the calorimetric data are accepted as they are and the phases are used as a foundation for the data base. In the second and third cases, a method of optimization is adopted to find the best set of data which reproduce the experimental data within their uncertainty limits. In the fourth case, an estimate based on theoretical considerations is made.

a) The Manual Adjustment Approach.

This method is mainly followed when experimental data are on a single reaction and are too few to run an optimization. Only enthalpy and entropy are adjusted within their stated uncertainties. The method is also useful to obtain start values for an optimization when a lot of

experimental data are available on a single reaction.

The procedure involves a repeated computation of phase diagrams and adjustments of the thermochemical values. This is an optimization procedure conducted manually. Adjustments are made in the enthalpy and/or entropy data of the phase whenever the initially selected data fail to reproduce the experiments within the stated uncertainty. Constraints from other reactions are used so that the need for adjusting data on more than one of the phases in a reaction should not arise.

For computation of phase equilibrium, the method of minimization of the total Gibbs free energy of an assemblage as discussed by Eriksson (1975), Smith and Missen (1982) and used by Saxena and Eriksson (1983a,b, 1985), Saxena and Chatterjee (1986) and Fei and Saxena (1986) is used. This computational procedure has the advantage of considering the entire data set in each calculation and therefore the results reflect the internal consistency of the whole data set. Thus each datum is tested in a multireaction environment. For example, in the system $MgO\text{-}SiO_2$, we have the following possible reactions:

$MgO + SiO_2 = MgSiO_3$ (2.a)

periclase quartz enstatite

$2MgO + SiO_2 = Mg_2SiO_4$ (2.b)

periclase quartz forsterite

$Mg_2SiO_4 + SiO_2 = 2MgSiO_3$ (2.c)

forsterite quartz enstatite

$SiO_2 = SiO_2$ (2.d)

α-quartz β-quartz

$MgSiO_3$ = $MgSiO_3$ (2.e)

enstatite clinoenstatite

Let us assume that there exist experimental phase equilibrium relations for the above system and a set of thermochemical data which reproduce some of the experimental results but not all. If the experiments are all reversed and the thermochemical data do not reproduce the equilibrium pressure and temperature of the reactions (2.a), (2.c) and (2.e), the offending species is enstatite and its data should be adjusted. If, in addition to the three reactions, reaction (2.b) is also not reproduced, then the data on MgO would also need adjustment. While the above procedure can easily be performed by hand calculation, the total Gibbs free energy minimization method expedites the computation on multicomponent systems with additional information on divariant fields. Furthermore, each computation involves all the data on the phases of the system (not just the ones used in each individual reaction). When we compute the equilibrium of a single reaction, only the total free energy of the phases participating in the reaction is minimized. Such a procedure may result in a spurious value of enthalpy of a phase. This cannot happen with the method used here, since all phases that can form compositionally in the system are included in the possible assemblages for which the total free energy is computed and compared by the minimization technique.

Note that this procedure in certain cases is not apparently more useful than simple hand calculation. Such may be the case, for example, if we wish to determine the standard free energy of formation of

Al_2O_3orthopyroxene according to the reaction:

$$MgSiO_3 + Al_2O_3 = MgAl_{2/3}SiO_4 \qquad (2.f)$$

Orthopyroxene Pyrope

With the standard free energy of formation of pyrope and enstatite known and the standard free energy change of the reaction being $RT\ln(X_{Al}X_{En})$, where X_{Al} and X_{En} are mole fractions of Al_2O_3 and $MgSiO_3$ in orthopyroxene, the standard free energy of formation of Al_2O_3-orthopyroxene can be determined if experimental data on X_{Al} and X_{En} are available. However, with hand calculation, the condition that the standard free energy of formation of Al_2O_3orthopyroxene should always be greater than the standard free energy of formation of corundum is not automatically enforced as it is with the total free energy minimization method. The situation becomes more complex in multicomponent-multiphase systems. Since it is equally easy to compute both simple and complex systems with the installed program, all computations are done with the free energy minimization program.

b) The Regression Technique.

Thermochemical data for phases are mostly determined from calorimetric experiments. In theory, one should be able to reproduce experimentally observed equilibria using these thermochemical data. However, due to errors in both calorimetric and equilibrium experiments, this is often not the case. Many techniques of curve fitting have been suggested by different workers such as Haas and Fisher's (1976) regression analysis method and the linear and mathematical programming

methods of Gordon (1973), Halbach and Chatterjee (1982), Berman et al. (1986), Day and Kumin (1980), etc.. In this study available thermochemical data are systematized by adjusting them within their uncertainties. The method followed is described in the following paragraph. The final data set is compatible with most of the experimental equilibrium data.

In some cases, thermochemical data for phases are not available. In such cases, they are calculated from equilibrium data involving the phase. When data for only one phase in a reaction is unknown, it is calculated as follows. The change in free energy of a reaction

$$A + B = C + D \qquad (2.g)$$

at equilibrium is zero and can be written as

$$\Delta G^{o} = G^{o}_{f,C} + G^{o}_{f,D} - G^{o}_{f,A} - G^{o}_{f,B} = 0 \qquad (2.26)$$

where, G^{o}_{f} is the free energy of formation of a phase. If $G^{o}_{f,C}$ is unknown, it is easily calculated from equation (2.26). If several equilibrium pressures and temperatures are known for reaction (2.g), $G^{o}_{f,C}$ is regressed according to equation (2.1) and enthalpy, entropy and heat capacity functions for phase 'C' are obtained. In many cases, one or two quantities among H, S, and C_p are known from calorimetry. This makes the regression procedure much simpler.

In some cases there may be more than one uncertain quantity. For example, suppose in reaction (2.g) 'D' is a component of a solid

solution and the excess property of the solution is not well determined. The free energy of 'D' will then be expressed as $G^{o}_{f,D} + RT\ln a_D$, where a_D is the activity of 'D' in the solid solution. Suppose, the free energy of 'C' is available, but is also not well determined. Then, it is necessary to adjust both quantities (activity of 'D' and free energy of 'C') by trial and error until a reasonable result is achieved. Let us call the two uncertain quantities 'x' and 'y' with errors of δx and δy associated with them. First, the value of y is calculated keeping x constant. If y^c (the calculated value of y) lies within δy, the result is accepted. If it does not, x is adjusted (to let us say, x^c) within δx and y^c is redetermined. The procedure is repeated several times. In the final calculation, both x^c and y^c should lie within δx and δy respectively.

The data set obtained is finally tested in a multiphase-multicomponent environment for global consistency. This is done by the method of minimization of total Gibbs free energy of an assemblage as described before.

c) The Optimization Technique.

An internally consistent data base is constructed by considering all the experimentally determined data and theoretically or empirically extrapolated values for the system under consideration. These include phase equilibrium data, calorimetric and volume data and values extrapolated by theoretical methods such as that of heat capacity by

equation (2.2). Thermodynamic relationships described above link these data together and constrain as a set. Evaluation of thermodynamic properties of a phase by refinement involves a large number of data. A standard optimization technique may be used to solve this problem.

The thermodynamic properties of a phase can be evaluated by using the relations given in sections I through IV and constraining the free energy change of the reaction in which the phase participates to zero under equilibrium conditions. When both the thermodynamic properties and the equilibrium conditions have uncertainties, the optimization technique is employed. The optimization program used in this study is called MINUIT, which is written for the general purpose of function minimization and the analyses of errors and correlations. The program consists of several parts. In the first part, initial values of the parameters to be optimized are chosen. This is done by the Monte Carlo search method in which the values are chosen randomly according to the uniform distributions centered at the best previous values with widths equal to the starting parameter errors. In the next part, a combination of several numerical methods are used in minimizing the function including stepping methods for many variables and gradient methods. The simplex method has proved to be one of the best stepping methods. Gradient methods have the advantage of producing a fall covariance matrix, whereas the simplex method gives estimates of only the diagonal elements. A combined use of the simplex and gradient methods is always recommended in function minimization.

The program MINUIT has the advantage of flexibility. The functions, the data base and the parameters to be optimized can be entered in the most convenient way. Errors (including half brackets), if available, can be considered for all the data points and the parameters to be optimized. These parameters include thermochemical and thermophysical data and phase equilibrium data. The errors in pressure and temperature in the phase equilibrium data can be directly entered. In multireaction optimizations, the inconsistencies in equilibrium P-T data between different reactions can be easily detected through chi-square values. Discrepancies between phase equilibrium and thermodynamic data can be identified by either high chi-square values or optimized parameter values beyond the given limits.

A physical constraint on the heat capacity is placed while optimizing parameters through free energy minimization. The equation that constrains the heat capacity at high temperatures is equation (2.3). When C_p, α, K_T and V are optimized together (Saxena, 1989b), the values obtained satisfy equation (2.3). This additional constraint ensures the consistency between thermochemical and thermophysical data.

CHAPTER 3

THERMODYNAMIC DATA ON MINERAL PHASES

Stability of minerals is a function of pressure, temperature and bulk chemistry. Fluid pressure is also an important factor. In recent years, through experimental study, much data has accumulated on the stability of minerals. Many of the reactions studied in the laboratory involve pure solid and fluid phases. Other experimental investigations involve solid solutions. In this chapter, important experimental equilibrium data along with the details of the thermodynamic data systematized in this study are given. For some phases, such as the oxides, the thermodynamic data are directly adopted from calorimetric sources. These data are taken as a standard for the calculation of properties of other phases which are either determined poorly or not determined.

I. PURE PHASES AND END-MEMBERS

a) Steam, Calcium oxide, Ferrous oxide, Periclase, Corundum, α -Quartz and β -Quartz

The thermochemical values on these oxides are from Robie et al. (1978). All the values were determined through calorimetry. The heat capacity expression of α-quartz above 848 K and the enthalpy and entropy of β-quartz are determined through optimization of the phase equilibrium

TABLE 3.1. INDEX AND ABBREVIATIONS FOR MINERALS AND SOLID SOLUTIONS

Akermanite	Aker	(c)	Grossular	Gr	(k)
Albite	Ab	(p)	Grunerite	Grun	(u)
Almandine	Alm	(l)	Hedenbergite	Hed	(j)
Al_2O_3-cpx		(d)	Hercynite	Her	(l)
Al_2O_3-opx		(d)	Hydrous cordierite		(x)
Andalusite	And	(b)	Ilmenite	Ilm	(n)
Annite	Ann	(r)	Jadeite	Jd	(p)
Anorthite	An	(k)	Kyanite	Ky	(b)
Anthophyllite	Anth	(s)	Magnetite	Mag	
Antigorite	Ant	(t)	Monticellite	Mont	(c)
Brucite	Br	(t)	Muscovite	Ms	(o)
Calcium Oxide		(a)	Orthodiopside	Odi	(g)
Ca-Tschermak	CaTs	(k)	Orthohedenbergite	Ohed	(g)
Chrysotile	Chr	(t)	Orthopyroxene	opx	
Clinoenstatite	Cen	(h)	Paragonite	Pg	(p)
Clinoferrosilite	Cfer	(g)	Periclase	Per	(a)
Clinopyroxene	cpx		Phlogopite	Phl	(q)
Cordierite	Cord	(v)	Pyrope	Pyr	(d)
Corundum	Cor	(a)	Quartz	Q	(a)
Diopside	Di	(i)	Rutile	Ru	(n)
Enstatite	En	(d)	Sanidine	San	(o)
Fayalite	Fay	(f)	Sillimanite	Sill	(b)
Ferrocordierite	Fcord	(w)	Spessartine	Spess	(m)
Ferrosilite	Fer	(f)	Spinel	Sp	(d)
Ferrous Oxide		(a)	Steam		(a)
Forsterite	Fo	(e)	Talc	Tc	(s)
Gehlenite	Ge	(c)	Wollastonite	Woll	(c)

Solid solutions:

Almandine - Grossular	(xv)
Almandine - Spessartine	(xvi)
Albite - Sanidine	(xxi)
Anorthite - Albite	(xxi)
Anorthite - Sanidine	(xxi)
Al_2O_3-cpx - Jadeite	(ix)
Clinoenstatite - Al_2O_3-cpx	(ix)
Clinoenstatite - Clinoferrosilite	(vi)
Clinoenstatite - Diopside	(vii)
Clinoenstatite - Hedenbergite	(viii)
Clinoenstatite - Jadeite	(xi)
Clinoferrosilite - Al_2O_3-cpx	(ix)
Clinoferrosilite - Diopside	(viii)
Clinoferrosilite - Hedenbergite	(viii)
Clinoferrosilite - Jadeite	(xi)
Cordierite - Ferrocordierite	(xix)
Cordierite - Hydrous cordierite	(xx)
Diopside - Al_2O_3-cpx	(x)
Diopside - Hedenbergite	(viii)
Diopside - Jadeite	(xii)

Enstatite - Al_2O_3-opx	(ix)
Enstatite - Ferrosilite	(vi)
Enstatite - Orthodiopside	(vii)
Enstatite - Orthohedenbergite	(viii)
Ferrocordierite - Hydrous cordierite	(xxi)
Ferrosilite - Al_2O_3-opx	(ix)
Ferrosilite - Orthodiopside	(viii)
Ferrosilite - Orthohedenbergite	(viii)
Forsterite - Fayalite	(iii)
Gehlenite - Akermanite	(i)
Grossular - Spessartine	(xvi)
Hedenbergite - Al_2O_3-cpx	(x)
Hedenbergite - Jadeite	(xii)
Muscovite - Paragonite	(xvii)
Orthodiopside - Al_2O_3-opx	(x)
Orthodiopside - Orthohedenbergite	(viii)
Orthohedenbergite - Al_2O_3-opx	(x)
Phlogopite - Annite	(xviii)
Pyrope - Almandine	(xiii)
Pyrope - Grossular	(xiv)
Pyrope - Spessartine	(xvi)
Spinel - Hercynite	(ii)

letter or number in parentheses correspond to the section under which the mineral or the solid solution is described.

data on the transformation

α-quartz = β-quartz. (3.a)

The experimental data on this transformation are from Fenner (1913), Cohen and Klement (1967) and Mirwald and Massonne (1980). The calculated curve is shown in Figure 3.2a.

b) Andalusite, Kyanite and Sillimanite

Several experiments on the following equilibria

andalusite = kyanite (3.b-a)

kyanite = sillimanite (3.b-b)

sillimanite = andalusite (3.b-c)

relating the three polymorphs have been performed. However, the results obtained by different workers are very different. Experiments were done by Evans (1965), Newton (1966, 1969), Althaus (1967), Richardson et al. (1968, 1969) and Holdaway (1971). The reason behind this discrepancy is the small difference in the free energies of formation of the three polymorphs which leads to metastability.

Robie and Hemingway (1984b) determined the heat capacities of the three aluminosilicates in the range 10-380 K. The slopes of phase boundaries among these phases match the experimental data of Evans (1965), Newton (1966, 1969) and Holdaway (1971). Robie and Hemingway concluded that since Evans's, Newton's and Holdaway's results are consistent with their independently derived calorimetric data, the

equilibrium results of these three workers must be correct. The thermodynamic properties given by Robie and Hemingway are adopted in this work. Robie and Hemingway also concluded that Al and Si are ordered in sillimanite to at least 1100 K. Calculated positions of these polymorphic transformations and the experimental data of Evans, Newton and Holdaway are shown in Figure 3.1.

c) Wollastonite, Gehlenite, Akermanite and Monticellite

Wollastonite and Gehlenite participate in reactions involving the breakdown of anorthite. These reactions, studied by various workers (see Figure 3.2a,b), are as follows:

$$An + Woll = Gr + Q \qquad (3.c)$$

$$An + Ge = Gr + Cor \qquad (3.d)$$

$$An + Ge + Woll = Gr \qquad (3.e)$$

Reaction (3.c) was also studied by Huckenholz et al. (1975). Stability of these minerals and akermanite and monticellite was also studied by Yoder (1968).

The properties of wollastonite are as listed in Haas et al. (1981) and are closely similar to those of Charlu et al. (1981).

For the reaction (3.d) involving gehlenite, Gasparik (1984b) evaluated the experimental data of Boettcher (1970) and Huckenholz et al. (1975) and found the equilibrium pressure as

$$P = 23.8T(^{o}C) - 17440 \qquad (3.1)$$

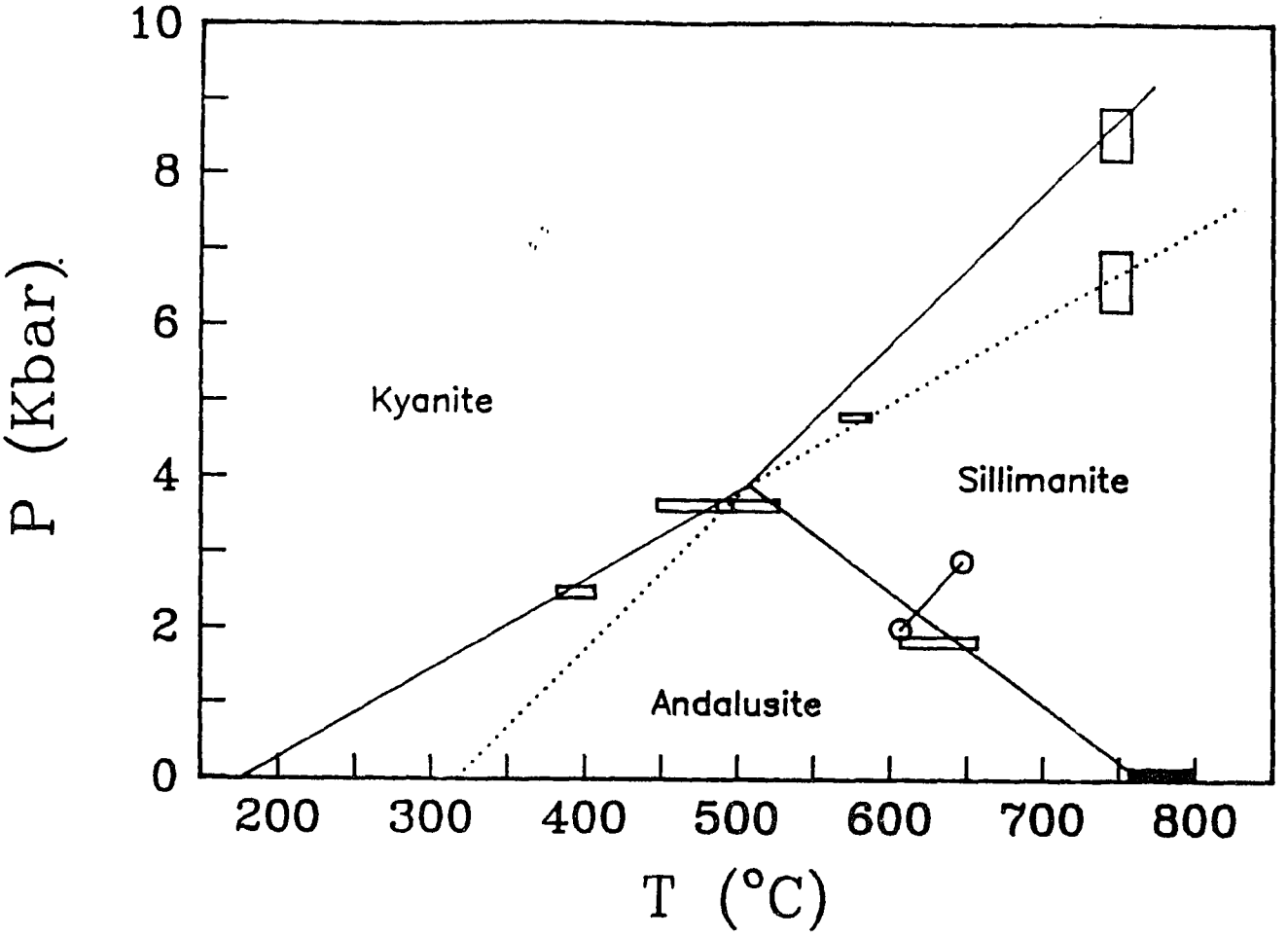

Figure 3.1: Phase equilibria for the aluminosilicate polymorphs. Experimental results are from Holdaway (1971, open horizontal rectangles); Newton (1966,1969, vertical rectangles); Evans (1965, open circles) and unpublished data of Weill as reported by Holdaway (1971, filled horizontal rectangle). The lines are calculated by Robie and Hemingway (1984) from their calorimetric data (adopted in this study).

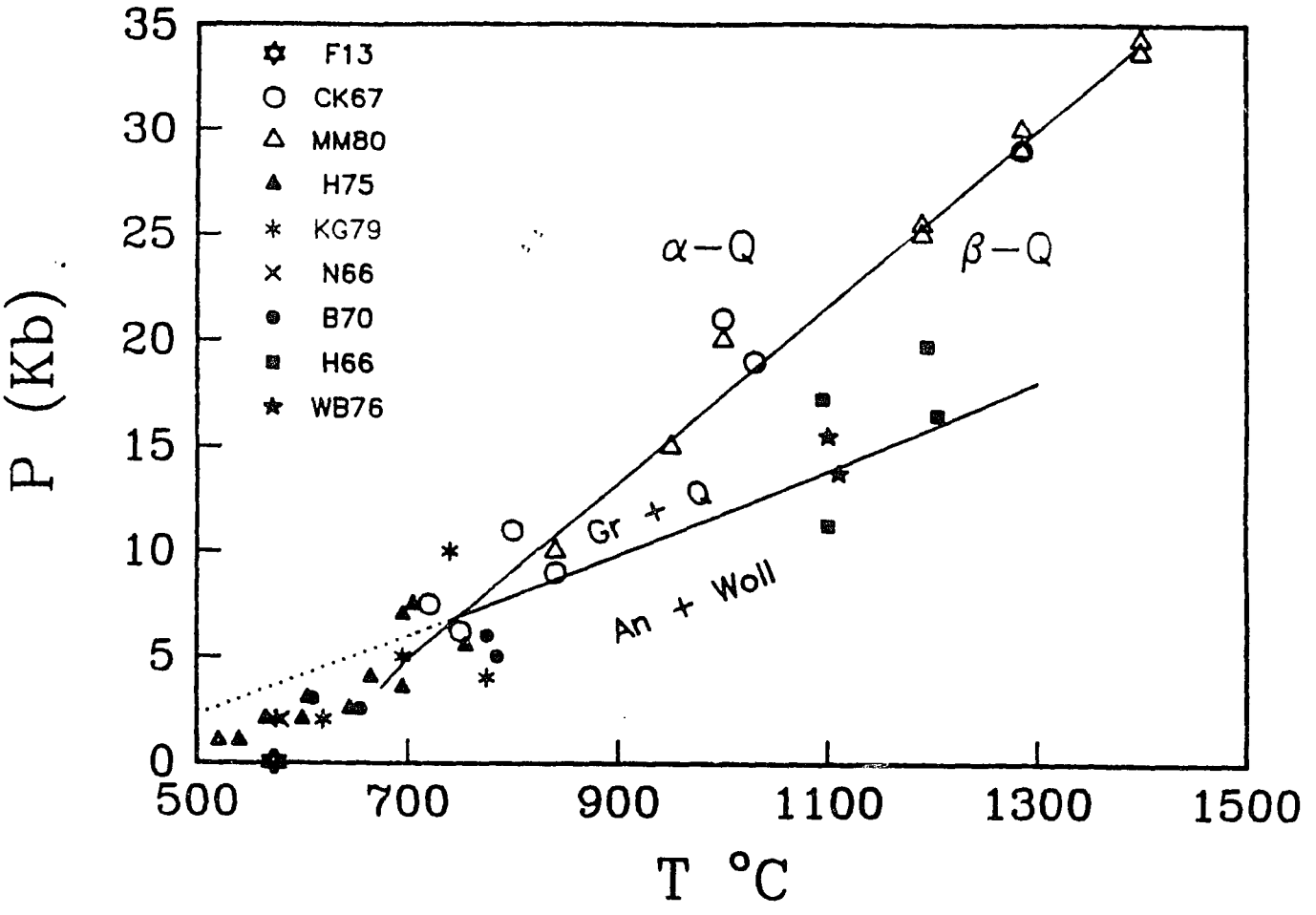

Figure 3.2a: Calculated equilibrium curves for reactions in the CaO-Al_2O_3-SiO_2 system. Experimental data are as follows: B70: Boettcher (1970), CK67: Cohen & Klement (1967), F13: Fenner (1913), H66: Hays (1966), H75: Huckenholz et al. (1975), KG79: Kerrick & Ghent (1979), MM80: Mirwald & Massone (1980), N66: Newton (1966), WB76: Windom & Boettcher (1976).

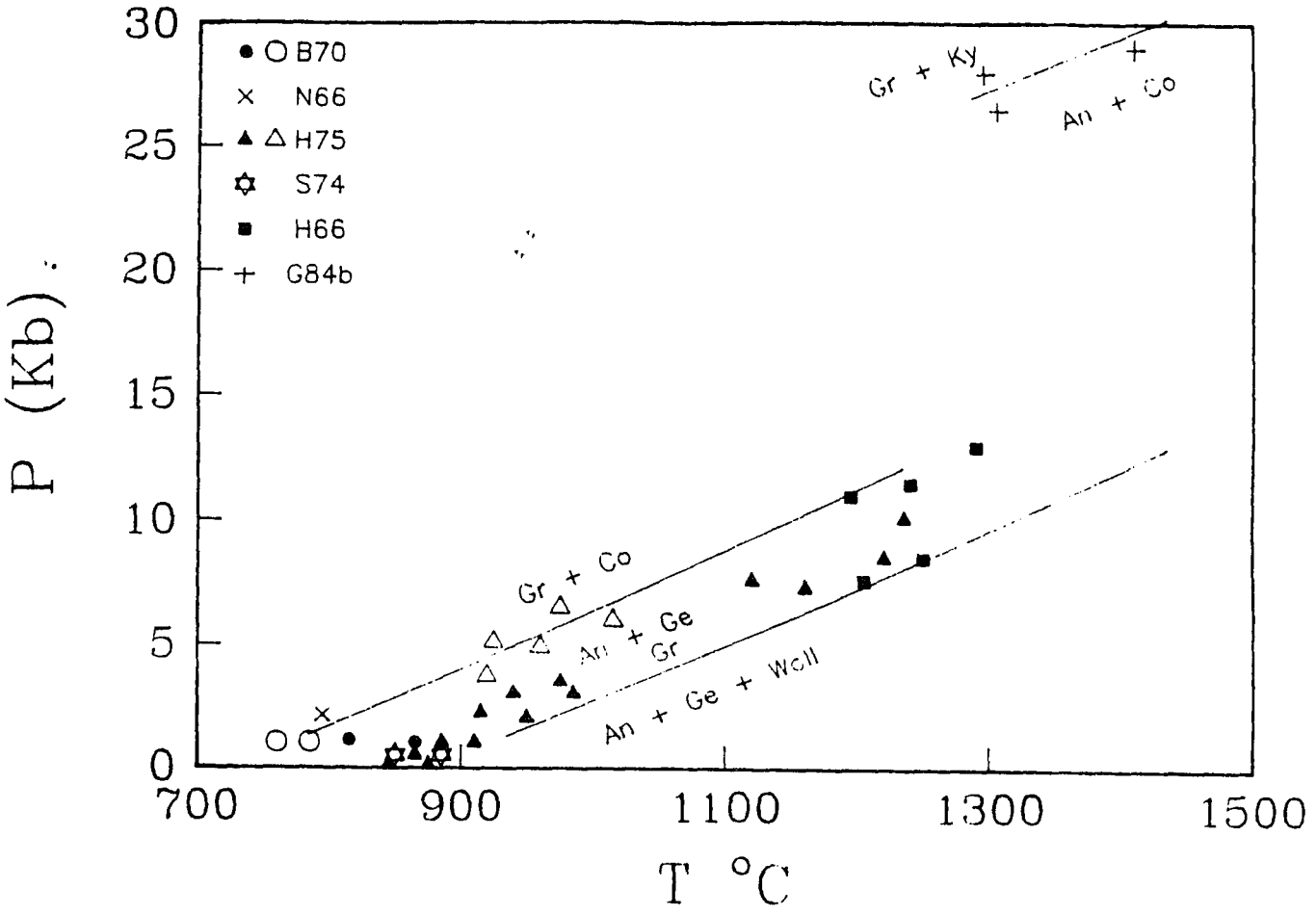

Figure 3.2b: Calculated equilibrium curves for reactions in the $CaO\text{-}Al_2O_3\text{-}SiO_2$ system. Experimental data are as follows: B70: Boettcher (1970), G84b: Gasparik (1984b), H66: Hays (1966), H75: Huckenholz et al. (1975), N66: Newton (1966), S74: Shmulovich (1974).

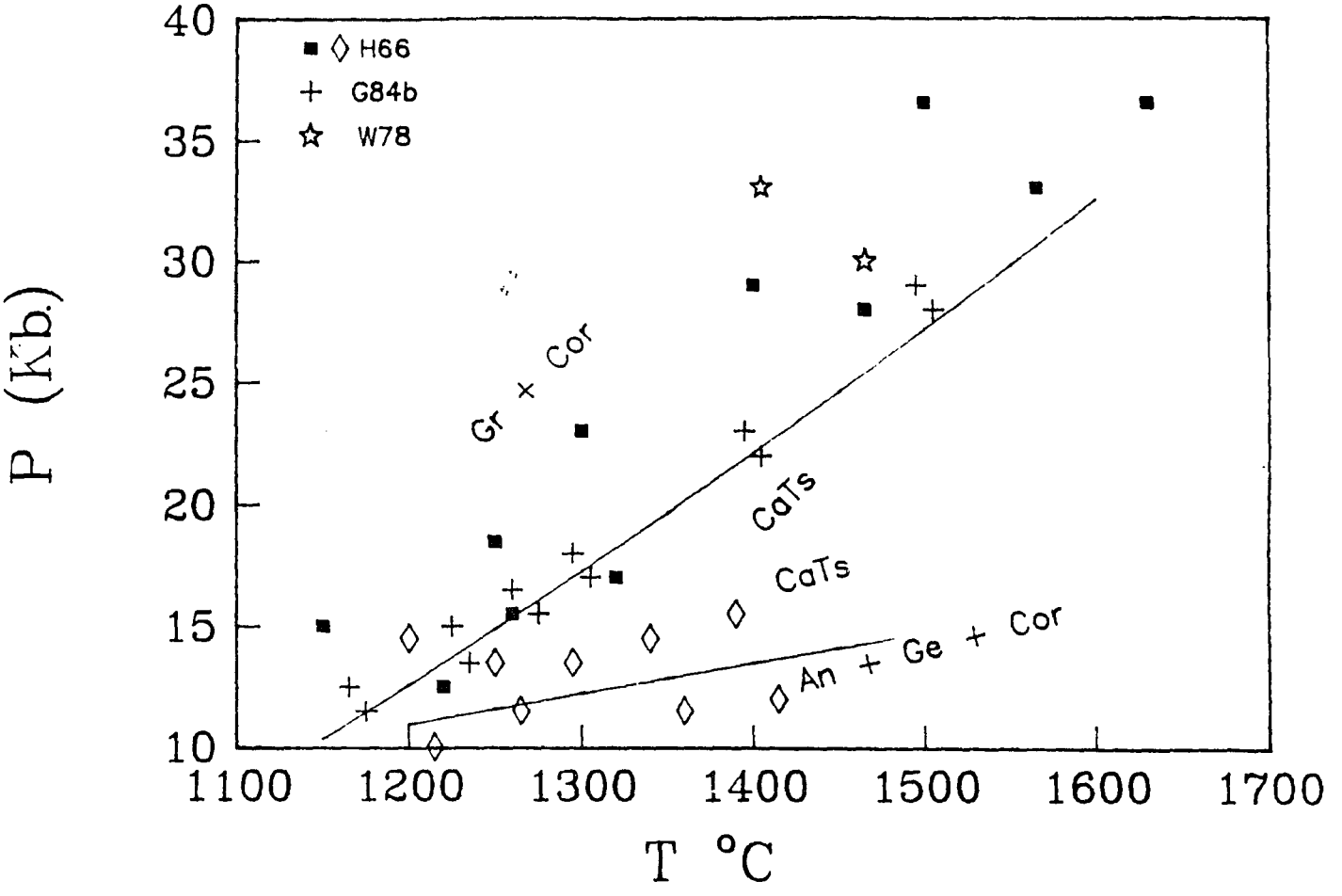

Figure 3.2c: Calculated equilibrium curves for reactions in the CaO-Al_2O_3-SiO_2 system. Experimental data are as follows: G84b: Gasparik (1984b), H66: Hays (1966), W78: Wood (1978).

Using these data, $\Delta C'_p$, the difference between the experimental and the calculated heat capacities, for gehlenite is found to be

$$\Delta C'_p = 7.5491(\pm 0.134) + 0.0027126(\pm 0.00019)T \qquad (3.2)$$

and a corresponding ΔH^o_f as -3980763 J/mol. This value is comparable to -3979046 J/mol derived from the $\Delta H^o_{f,970}$ value of Charlu et al. (1981) using the C_p expression from Robie et al. (1978). The entropy of gehlenite is selected as 204.35 J/mol-K following Woodhead (1977), who considers a progressively increasing disorder in gehlenite with temperature. In Figures 3.2a and 3.2b the calculated curves for reactions (3.c), (3.d) and (3.e) along with the experimental data are shown.

The experimental data of Yoder (1968) involving wollastonite, monticellite and akermanite are used to calculate the enthalpy of akermanite. The entropy and heat capacity data are from Robie et al. (1978). The data are closely similar to the calorimetric data of Haas et al. (1981) and Charlu et al. (1981). Calculated curves for reactions (3.c) through (3.e) and the experimental data are shown in Figure (3.2a,b).

The enthalpy of monticellite is adjusted by about 1 KJ from Brousse et al. (1984) so that an improved fit to Yoder's (1968) experimental data involving wollastonite, monticellite and akermanite is obtained. The entropy is from Robie et al. (1978) and the heat capacity equation is as recommended by Helgeson et al. (1978).

d) Spinel, Enstatite, Al_2O_3-Orthopyroxene and Pyrope

Experiments involving spinel, orthopyroxene and pyrope were done by Haselton (1979), Lane and Ganguly (1980), Danckwerth and Newton (1978) and Gasparik and Newton (1984). The reaction is as follows:

$$En + Sp = Pyr + Fo \qquad (3.f)$$

Kawasaki and Matsui (1983) also studied the aluminum solubility in enstatite-ferrosilite orthopyroxenes.

Another reaction with excess silica is as follows:

$$En + Sill = Pyr + Q \qquad (3.g)$$

This reaction was studied by Perkins (1983) and Hensen (1972).

For pyrope, the enthalpy is from Charlu et al. (1975), the entropy is from Haselton & Westrum (1980) and the heat capacity is from Haselton (1979). The values are calorimetric.

The enthalpy of enstatite is from Brousse et al. (1984). Although there are other determinations of the enthalpy, the value of Brousse et al. is close to the average of all the values. So, their value is adopted. Entropy and heat capacity of enstatite are from Haselton (1979). All these values are calorimetric.

Aluminous orthopyroxene and pyrope can be related by reaction (2.f). Experimental phase equilibrium data on the Al content of orthopyroxene as shown in Figure 5.1 are used to estimate the thermodynamic properties of Al_2O_3-orthopyroxene. At each given pressure and temperature, the standard free energy of formation from elements of Al_2O_3-orthopyroxene is determined by computing the phase relations in the divariant field

with coexisting pyrope and orthopyroxene. From several estimates of ΔG^{o}_{f}, the other thermochemical properties ($\Delta H^{o}_{f,298}$, S^{o}_{298} and C_p) are derived by regression analysis. It is assumed that the data on compressibility and thermal expansion are the same as for enstatite and the $MgSiO_3$-Al_2O_3 orthopyroxene solution is ideal. This was the approach followed by Saxena and Chatterjee (1986). The free energy of Al_2O_3-orthopyroxene is revised in this work. Experimental data on the Al_2O_3 content of orthopyroxene are in the temperature range of 900 to 1600°C and care should be taken when the free energy of Al_2O_3-orthopyroxene derived here is extrapolated outside this range.

Free energy of spinel is calculated from the reaction (3.f). Heat capacity of spinel is from Robie et al. (1978). Enthalpy and entropy of spinel are adjusted in order to reproduce reaction (3.f). The adjusted entropy value (81.5 J/mol.K) lies close to the value in Robie et al. (1978) (80.63 J/mol.K). However, the enthalpy value ($\Delta H^{o}_{f,970}$ from oxides = -30.659 KJ/mol) is much lower than the calorimetric value ($\Delta H^{o}_{f,970}$ from oxides = -22.51±0.75 KJ/mol) of Charlu et al. (1975). Wood and Holloway (1984) pointed out that Charlu et al. prepared their sample at 1698 K. Hence, the sample they used had a built-in Mg-Al disorder as the experiment was done at 970 K. The energy due to disorder is reflected in their result. Wood et al. (1986) studied the disordering behavior of spinel and concluded that above 1173 K disordering is negligible. Thus, the difference between the value of Charlu et al. (1975) and this study (appoximately 8 KJ/mol) could be due to the difference between the disorder state of spinel at 1173 K and 970 K. Thus, as also concluded by Wood and Holloway (1984), the enthalpy of spinel should be a lot less than the value of Charlu et al. (1975). The

value obtained here is similar to that obtained by Wood and Holloway (1984). In Figure 5.1, the calculated curve for reaction (3.f) along with the various experimental data and calculated isopleths of Al_2O_3 in orthopyroxene are shown.

e) Forsterite

Brousse et al. (1984) discussed the calorimetric data on enthalpy of forsterite which range from a high of -57.823 to a low of -63.262 (KJ/mol, $\Delta H^{o}_{f,298}$ from oxides). The value recommended here is -60.68 KJ/mol. Most of the calorimetric data are close to this value. The entropy and C_p of forsterite are from Robie et al. (1978). Robie et al. (1982b) determined the heat capacity of forsterite in the range 5-380 K. The C_p recommended here is closely similar to the C_p determined by them.

f) Fayalite and Ferrosilite

Ferrosilite breaks down to give fayalite and quartz according to the following reaction:

$$Fer = Fay + Q \qquad (3.h)$$

This reaction was studied experimentally by Bohlen et al. (1980). However, when orthopyroxene solutions break down there is a three phase stability field where orthopyroxene solution is present along with olivine solution and quartz. This phenomenon was recently investigated by Bohlen and Boettcher (1981).

Free energy of fayalite is adopted from Robie et al. (1982a) which is determined by calorimetry.

Free energy of ferrosilite is closely constrained by reaction (3.h). Enthalpy (adjusted by 300 J) and entropy are the recommended values of Bohlen and Boettcher (1981) and the heat capacity is calculated from reaction (3.h). In Figure 3.3, a calculated curve for the reaction (3.g) along with the experimental data is shown.

g) Orthodiopside, Orthohedenbergite and Clinoferrosilite

The properties of these phases are adopted from Saxena et al. (1986). Their evaluations are based on the phase equilibrium data compiled by Lindsley (1983) on quadrilateral pyroxenes. These properties and the properties of clinoentatite and hedenbergite and the solution properties of the binaries involved are being currently revised (Saxena, 1989a) in light of the recent experiments done on the pyroxene quadrilateral by Carlson and Lindsley (1988).

h) Clinoenstatite

The enthalpy and entropy are evaluated from the experimental data of Lindsley et al. (1981) on enstatite-diopside equilibria. These values are close to the values of Kiseleva et al. (1979). The heat capacity is assumed to be the same as that of enstatite.

i) Diopside

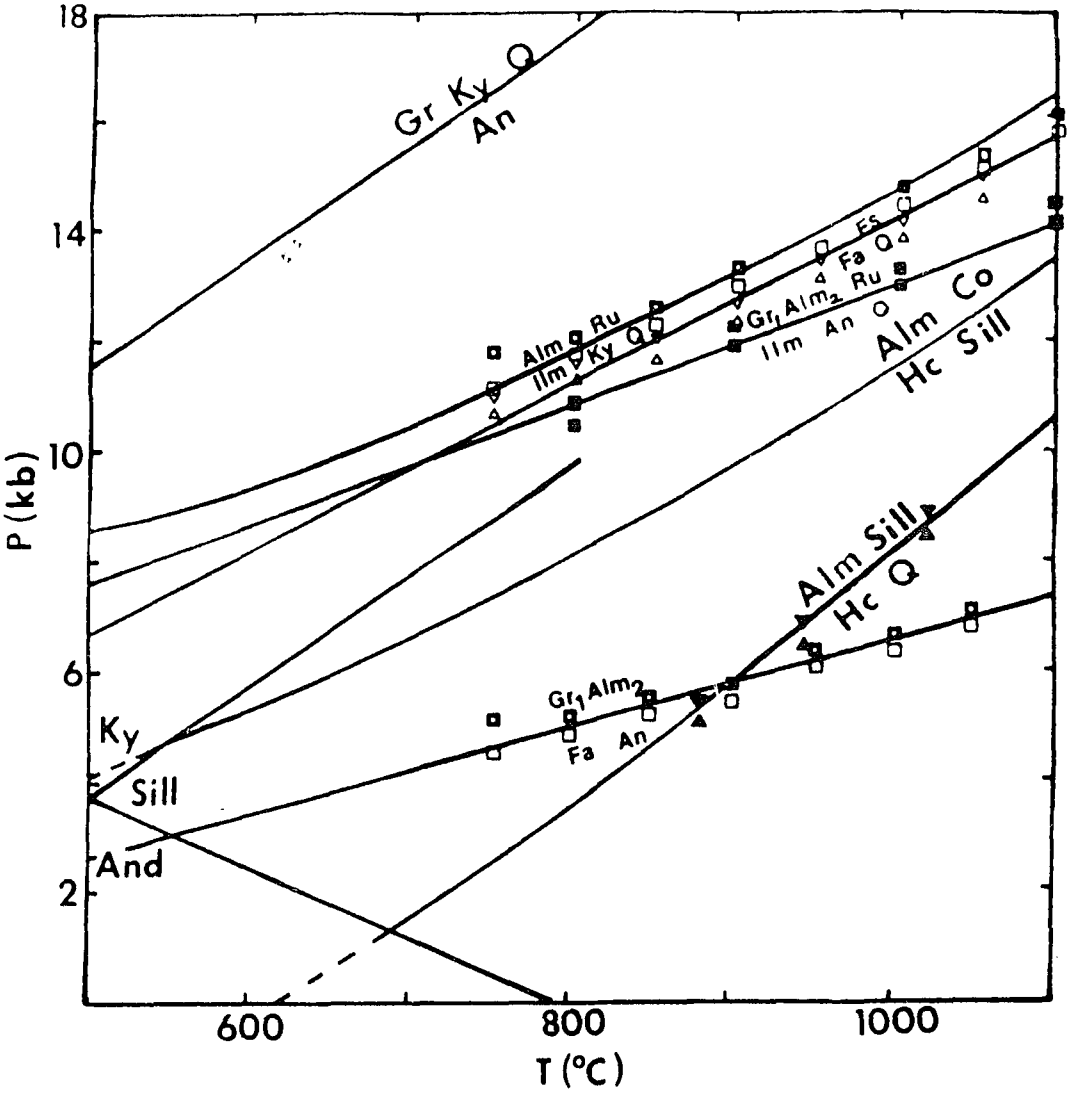

Figure 3.3: Calculated equilibrium curves for some reactions in the CaO-FeO-MgO-Al_2O_3-SiO_2-TiO_2 system. Curves for Al_2SiO_5 phase change reactions are from Robie & Hemingway (1984b). Filled squares are from Bohlen & Liotta (1986), filled triangles are from Bohlen et al. (1986), open squares are from Bohlen et al. (1983a,b) and open triangles are from Bohlen et al. (1980).

The properties listed in Robie et al. (1978) are adopted. These data are from calorimetric sources.

j) Hedenbergite

The values are as recommended by Saxena et al. (1986). All values in their study were adjusted from the recommended values of Helgeson et al. (1978) to fit the equilibrium data on quadrilateral pyroxenes from Lindsley (1983). Recently, Haselton et al. (1987) determined the heat capacity of hedenbergite by low-temperature adiabatic and differential scanning calorimetry in the range 9-647 K. The heat capacity recommended by Saxena et al. (1986) is consistent with this later experimental determination. The difference between the heat capacity of Saxena et al. and Haselton et al. at 647 K is 0.8 J/cation.

k) Ca-tschermak, Anorthite and Grossular

Ca-Tschermak is related to grossular and anorthite by the following equilibrium reactions:

$$Gr + Cor = CaTs \qquad (3.i)$$

$$An + Ge + Cor = CaTs \qquad (3.j)$$

Reaction (3.i) was studied by Gasparik (1984b), Hays (1966) and Wood (1978), and reaction (3.j) was studied by Hays (1966).

The equilibria involving anorthite and grossular is given by the reaction:

$$An = Gr + Ky + Q \qquad (3.k)$$

which was studied by many workers (see Figure 3.5). Koziol and Newton's (1988a) results constrains the boundary within tight reversal brackets. Gasparik's (1984c) results place the reaction boundary a few kbars above that of Goldsmith's (1980).

Another reaction involving anorthite and grossular is for the silica unsaturated system and is:

$$Gr + Ky = An + Cor \qquad (3.l)$$

This reaction was studied experimentally by Gasparik (1984b).

The following reaction is an important mechanism in the plagioclas-lherzolite to spinel-lherzolite transition

$$An + Fo = Sp + opx + cpx \qquad (3.m)$$

This reaction was studied by Herzberg (1976) and Kushiro and Yoder (1966).

Another reaction involving anorthite with excess silica is as follows:

$$opx + An + Sill = garnet + Q \qquad (3.n)$$

This reaction was studied by Perkins (1983). The equilibria are approximately 14 kbar/1000^{o}C and 14.7 kbar/1100^{o}C.

Equilibria of anorthite with gehlenite and wollastonite are described in section (c).

For grossular, the enthalpy is from Charlu et al. (1975), the entropy is from Haselton & Westrum (1980) and the heat capacity is from Haselton (1979). The values are calorimetric.

Free energy of Ca-Tschermak was calculated by Saxena and Chatterjee (1986) using Gasparik's (1984b) data on reaction (3.i) and (3.j) which yielded

$$\Delta C'_p = 2220824(\pm 130)T^{-2} \qquad (3.3)$$

with a corresponding $\Delta H^{\circ}_{f,298}$ of -3300902 J/mol, where, $\Delta C'_p$ is the difference between the experimental and the calculated heat capacities. This $\Delta H^{\circ}_{f,298}$ is comparable to the $\Delta H^{\circ}_{f,298}$ (calculated from $\Delta H^{\circ}_{f,970}$) of -3297994 J/mol determined by Charlu et al. (1978). The enthalpy and entropy needed adjustment in this study while the heat capacity of Saxena and Chatterjee (1986) is retained. The data on C_p listed in Table 3.2 represents the addition of $\Delta C'_p$ to the C_p expression of Haselton et al. (1984). In Figure 3.2c, calculated curves for reaction (3.i) and (3.j) and the experimental data of Gasparik (1984b), Hays (1966) and Wood (1978) are shown.

The heat capacity of anorthite, as listed in Robie et al. (1978) upto 1800 K, shows an anomalous extrapolation above 1200 K (see Figure 3.4). In this study, the data upto 1200 K are fitted to the Fei-Saxena equation for high-temperature extrapolation. The resulting equation gives very similar results when compared to the equation of Holland (1981). Entropy of anorthite is from Robie et al. (1978) and enthalpy is calculated from reaction (3.k). The calculated curve along with the experimental data is shown in Figure 3.5.

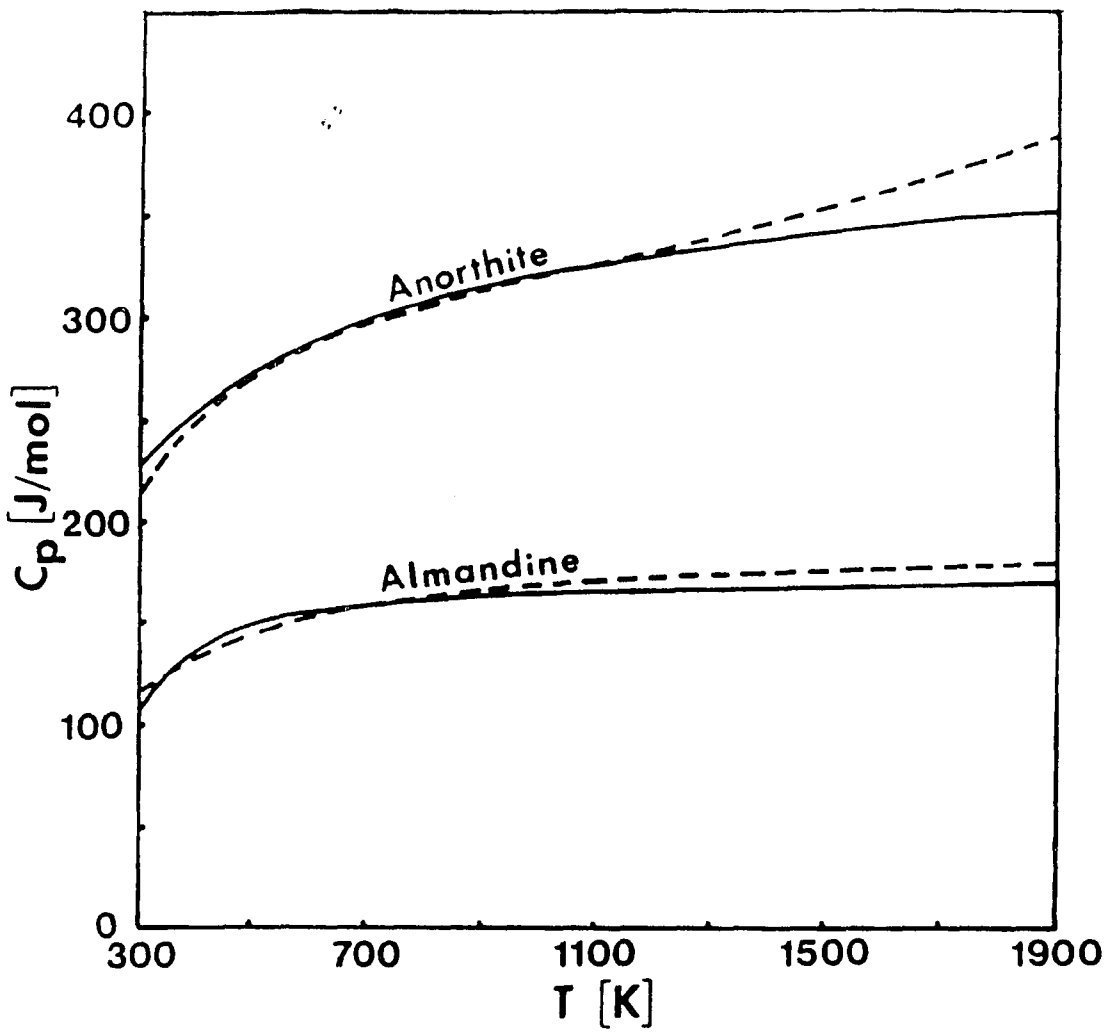

Figure 3.4: Calorimetric and extrapolated (using equations from this study) heat capacities of almandine and anorthite. Dashed lines are from calorimetry from Metz et al. (as in Bohlen et al. (1986)) for almandine (upto 1000 K) and as in Robie et al. (1978) for anorthite (upto 1800 K).

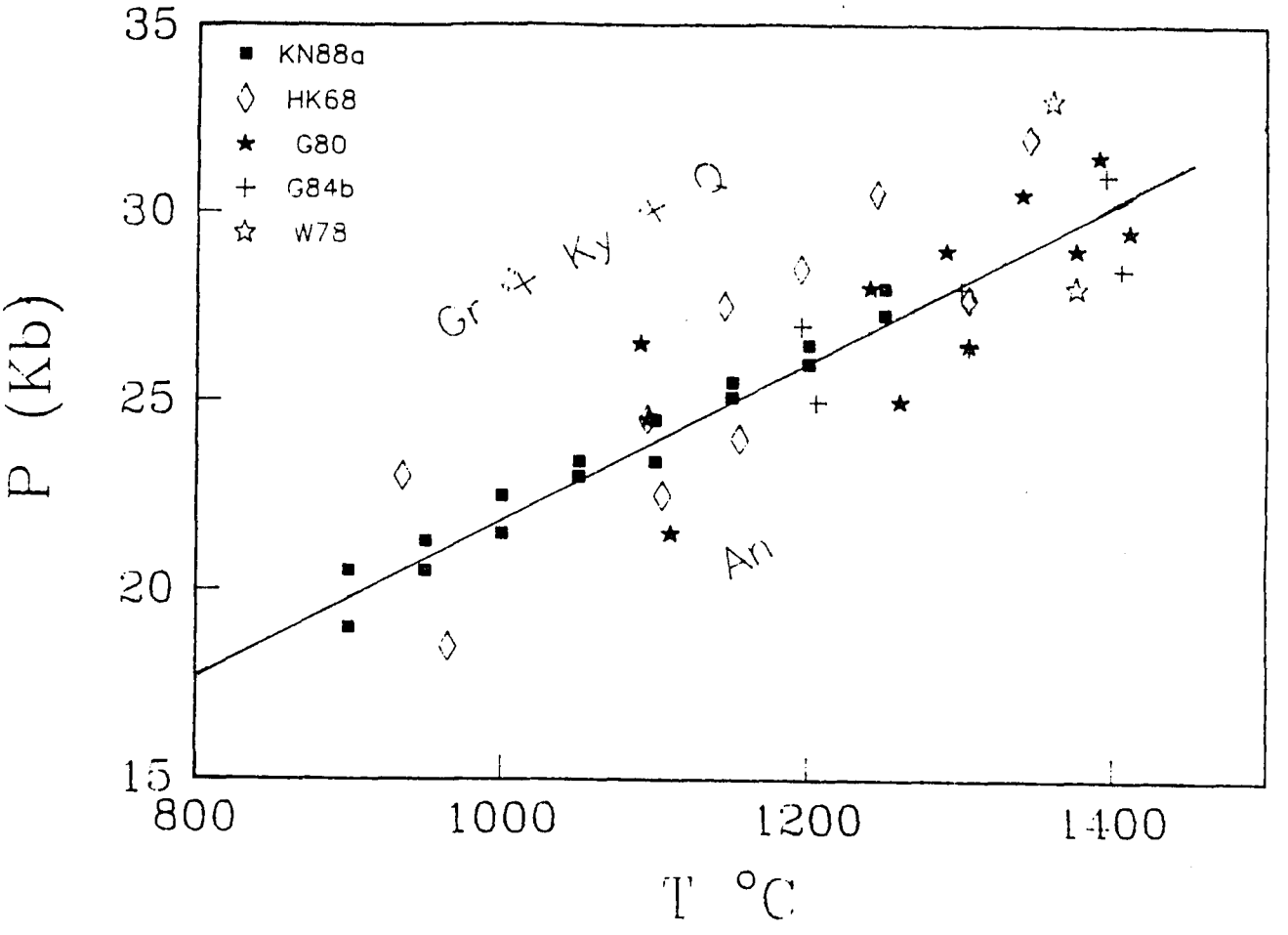

Figure 3.5: Calculated and experimental equilibria for reaction (3.k). Experimental data are as follows: G80: Goldsmith (1980), G84b: Gasparik (1984b), HK68: Hariya & Kennedy (1968), KN88a: Koziol & Newton (1988a), W78: Wood (1978).

The low pressure equilibria of anorthite in the CaO-MgO-Al_2O_3-SiO_2 system (reaction (3.m)) are reproduced by the data recommended in this study (see Figure 5.2). In the silica saturated system, for reaction (3.n), pressures are calculated at temperatures of 1273, 1373 and 1573 K respectively. While the first two pressures are close to the experimental data of Perkins (1983), the third lies at a pressure several kilobars above. Wood and Holloway (1984) faced a similar problem and point to Perkins's (1983) discussion of possible metastable reactions in these experimental runs.

Other equilibria involving anorthite in conjunction with wollastonite and gehlenite, discussed in section (c), are also shown in Figures 3.2a and 3.2b.

l) Almandine and Hercynite

The following reaction involving almandine and hercynite was recently investigated by Bohlen et al. (1986):

Alm + Sill = Her + Q (3.o)

Bohlen et al. (1983a) also studied the following reaction involving the garnet composition $grossular_1 almandine_2$:

garnet = Fay + An (3.p)

Heat capacity of almandine is estimated from the Fe-Mg exchange reaction

En + Alm = Fer + Pyr (3.q)

by assuming that ΔC_p of the reaction is zero. Although this is normally not true, it is preferred over the C_p determined by Metz et al. (as in Bohlen et al. (1986)) for the following reason. When their determined C_p values are extrapolated to high temperatures such as the range of experiments of Lee and Ganguly (1987) (see Ganguly and Saxena, 1988) they become too high to fit the observed equilibria. In Figure 3.4 the C_p equation of Metz et al. (as given in Bohlen et al. (1986) and converted into the Fei-Saxena form for extrapolation) and the equation used in this study are plotted for comparison. Note that the upper limit of calorimetric experiment of Metz et al. is 1000 K.

Distribution data for the exchange reaction (3.q) were determined from the synthesis experiments of Kawasaki and Matsui (1983) and the reversal experiments of Lee and Ganguly (1987) (see Ganguly and Saxena, 1989). They both suggest a relative ideal behavior of the orthopyroxene and garnet solutions. A condition for this behavior would be

$$RT\ln K_{\gamma(3.q)} = 0 \qquad (3.4)$$

where, $K_{\gamma(3.q)}=K_{(3.q)}/K_{D(3.q)}$, $K_{(3.q)}$ being the equilibrium constant for reaction (3.q). Thus, the free energy of almandine is calculated from reaction (3.q) according to the following equilibrium relation

$$\Delta G^{\circ} + RT\ln K_{D(3.q)} = 0 \qquad (3.5)$$

Free energies of enstatite, ferrosilite and pyrope are discussed under sections (d) and (f). Enthalpy and entropy of almandine are available from calorimetric experiments of Chatillon-Colinet et al. (1983a) (-1749.9±3.6 KJ/mol of cation, an average of two different methods) and Metz et al. (1983) (113.39 J/K/mol of cation). Enthalpy and entropy of

almandine are adjusted in order to reproduce the available distribution data by satisfying relation (3.5).

Free energy of hercynite is determined from the reaction (3.o). The heat capacity expression for hercynite used by Saxena and Eriksson (1983b) is adjusted here. The entropy is from Robie et al. (1978). Enthalpy is adjusted within the error limits of Robie et al. (1978) (-1966.48±8.5 KJ/mol). Calculated position of reaction (3.o) and the experimental results on the reaction are shown in Figure 3.3.

m) Spessartine

Free energy is from Bokreta (1989). The values were calculated from lattice energy consideration.

n) Rutile and Ilmenite

The following reactions involving rutile and ilmenite were experimentally reversed by Bohlen et al. (1983a) and Bohlen and Liotta (1986) respectively:

$$Alm + Ru = Ilm + Ky + Q \qquad (3.r)$$

$$garnet + Ru = Ilm + An + Q \qquad (3.s)$$

Reaction (3.s) involves the garnet composition $grossular_1 almandine_2$. These reactions are also known as GRAIL and GRIPS respectively.

Enthalpy and entropy of rutile are adjusted within the error limits of Robie et al. (1978) to fit the experimental data on reaction (3.r).

The heat capacity of rutile is from Robie et al. (1978). Entropy and heat capacity of ilmenite are from Anovitz et al. (1985). The enthalpy of both ilmenite and rutile and the entropy of rutile are adjusted within their stated errors (Robie et al., 1978). The data on ilmenite and rutile thus adjusted, along with the solution data on the grossular-almandine solution discussed in a later section, reproduce the experimental data on reaction (3.s) well. The calculated curves for reactions (3.r) and (3.s) along with the experimental data are shown in Figure 3.3.

o) Sanidine and Muscovite

The equilibrium relations between these two minerals have been studied by many workers. Important reactions are as follows:

$$Ms = Cor + San + H_2O \qquad (3.t)$$

$$Ms + Q = San + Al_2SiO_5 + H_2O \qquad (3.u)$$

The muscovite breakdown reactions mark the boundary between medium and high grade metamorphism. Experimental work has been done on reaction (3.t) by Velde (1966) and Chatterjee and Johannes (1974) and on reaction (3.u) by Evans (1965), Althaus et al. (1970), Day (1973) and Chatterjee and Johannes (1974).

Experimental information available on the stability of sanidine and muscovite are from the reactions (3.t) and (3.u). Krupka et al. (1979) attempted to calculate the enthalpy and free energy of muscovite from the experimental data of Chatterjee and Johannes (1974) on the above

reactions. Their calculations were based on the fugacity values of steam from Chatterjee and Johannes (1974) and Fisher and Zen (1971) and the heat capacity data on muscovite determined by them and the unpublished data on sanidine listed in Robie et al. (1978). In this work the more general equation for water fugacity of Saxena and Fei (1987a,b) and the published heat capacity data on sanidine by Hemingway et al. (1981) are used. The enthalpy of sanidine is from Robie et al. (1978). The thermal expansion of muscovite is also optimized from a combination of the phase equilibrium and heat capacity data. The optimized entropy of sanidine is found to be 7.09 J/mol-K higher than that determined by Openshaw et al. (1976). This amount can be considered as the disorder entropy of sanidine. Sanidine shows an Al/Si disorder and since, at very low temperatures, the heat capacity is not well characterized, this treatment is reasonable. However, it should be kept in mind that the zero-point Al/Si disorder entropy of muscovite is also unknown. Calculated curves for reactions (3.t) and (3.u) (for sillimanite and andalusite) along with the experimental data are shown in Figure 3.6.

p) Jadeite, Albite and Paragonite

The following reaction relating jadeite and albite

$$Ab = Jd + Q \qquad (3.v)$$

was studied by Holland (1979).

Reactions involving jadeite, albite and paragonite are as follows:

$$Pg = Ab + Cor + H_2O \qquad (3.w)$$

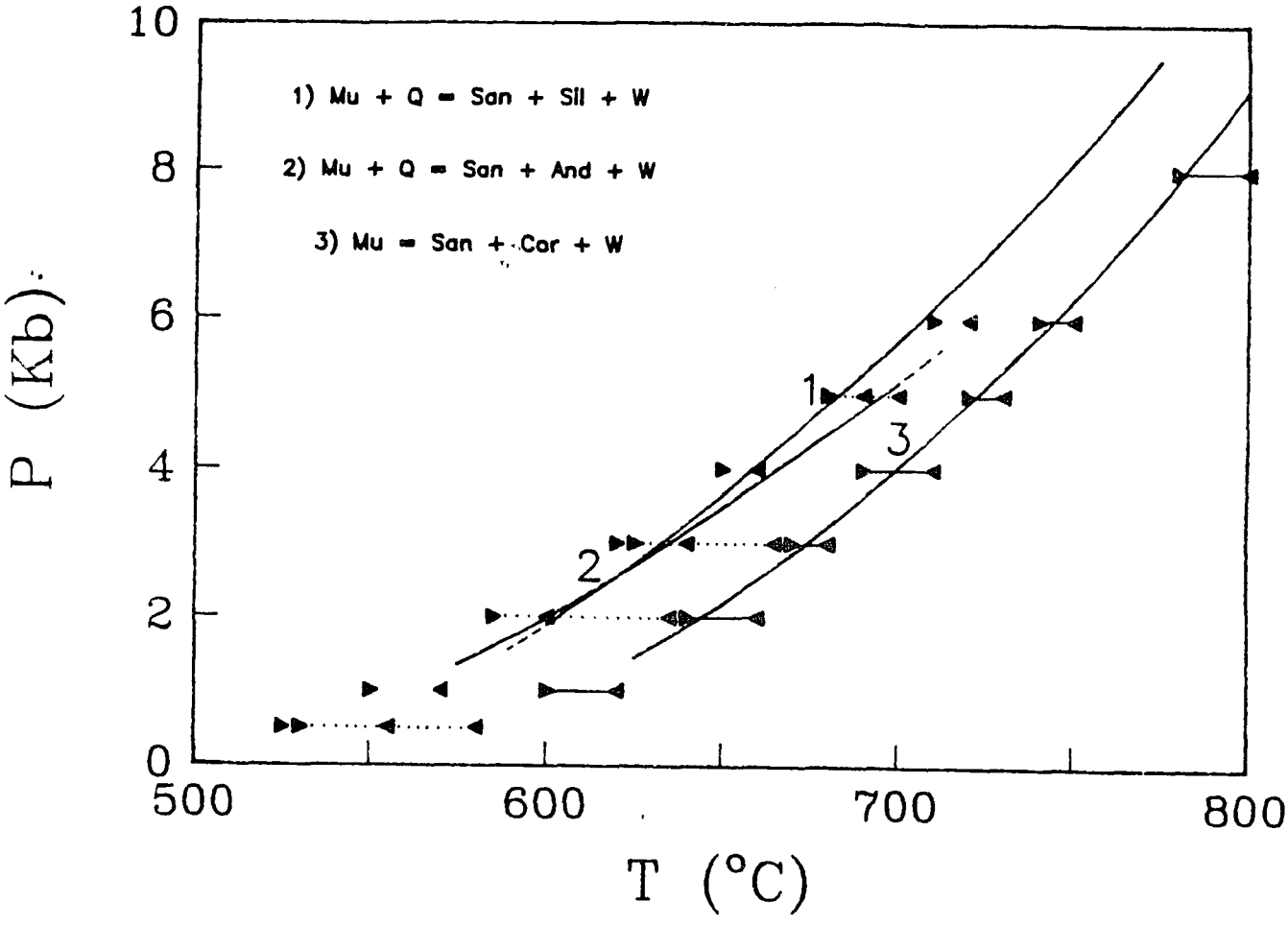

Figure 3.6: Calculated curves for reactions (3.t) and (3.u). The experimental data are summarized from Evans (1965), Velde (1966), Ivanov et al. (1973), Chatterjee & Johannes (1974), Huang & Wyllie (1974), Althaus et al. (1970), Kerrick (1972) and Day (1973). The dotted lines and bars represent metastable equilibria.

$$Pg + Q = Ab + Al_2SiO_5 + H_2O \qquad (3.x)$$

$$Pg = Jd + Ky + Q \qquad (3.y)$$

Experimental work has been done on reaction (3.w) by Chatterjee (1970); on reaction (3.x) by Chatterjee (1972) and on reaction (3.y) by Holland (1979).

Entropy and C_p of jadeite are as listed in Robie et al. (1978). The evaluated enthalpy of jadeite from Hemingway et al. (1981) is adopted.

Albite and jadeite are related by the equilibrium (3.v). The free energies of albite and jadeite were evaluated by Hemingway et al. (1981). Holland (1979) also attempted to evaluate the free energy of albite on the basis of reaction (3.v). Hemingway et al.'s values on albite are based on a careful consideration of the low-albite -> albite transition. Their values on jadeite and albite are thus consistent with both the transition and the reaction (3.v). However, they did not consider the effect of thermal expansion and bulk modulus of these two phases. When these two parameters are considered, their second model, which assumes that the aluminum avoidance principle holds for albite, fits the experimental equilibria the best. Thus, the values recommended by Hemingway et al. (1981) are adopted for albite.

The stability limit of paragonite is defined by the experimentally investigated reactions (3.w), (3.x) and (3.y). In this work different approaches were made to calculate the free energy of paragonite. Assuming that the value for jadeite is correct, the enthalpy and entropy of paragonite were optimized from reaction (3.y) (heat capacity of paragonite being from the calometric measurement of Robie and Hemingway

(1984a)). Enthalpy and entropy of albite was then optimized from reactions (3.w), (3.x) and (3.v). However, this gave way to convergence problem. In the second approach, the free energies of albite and jadeite were adopted from Hemingway et al. (1981). Using the heat capacity of paragonite from Robie and Hemingway (1984a), the enthalpy and entropy of paragonite were calculated. The same problem of convergence was encountered again. In the final approach, the second approach is repeated; only this time instead of the entropy (which is taken from Robie and Hemingway, 1984a), the heat capacity of paragonite is optimized. The thermal expansion and bulk modulus are also optimized simultaneously. The resulting value of the bulk modulus was not different from that of muscovite. The molar volume of paragonite is from Flux and Chatterjee (1986). The results, listed in Tables 3.2 and 3.3, perfectly reproduce the reactions (3.w), (3.x) (for sillimanite and andalusite) and (3.y) Calculated curves for reactions (3.w), (3.x), (3.y) and (3.v) and the experimental data are shown in Figure 3.7.

In all the approaches above and the approaches of Hemingway et al. (1981) and Holland (1979), it was assumed that the free energy of jadeite is correct. Hemingway et al. (1981) pointed out that heat capacity of jadeite has not been determined in the temperature range 5-50 K. This could have led to a spurious value of the entropy of jadeite. Enthalpy and entropy of jadeite can be determined from reaction (3.v) if the free energy of albite were known independently or from reaction (3.y) if the free energy of paragonite were known independently. Since this is not the case, the approach adopted here is the best. The difference between the calculated and the calorimetric values (enthalpy being the recommended value of Robie and Hemingway,

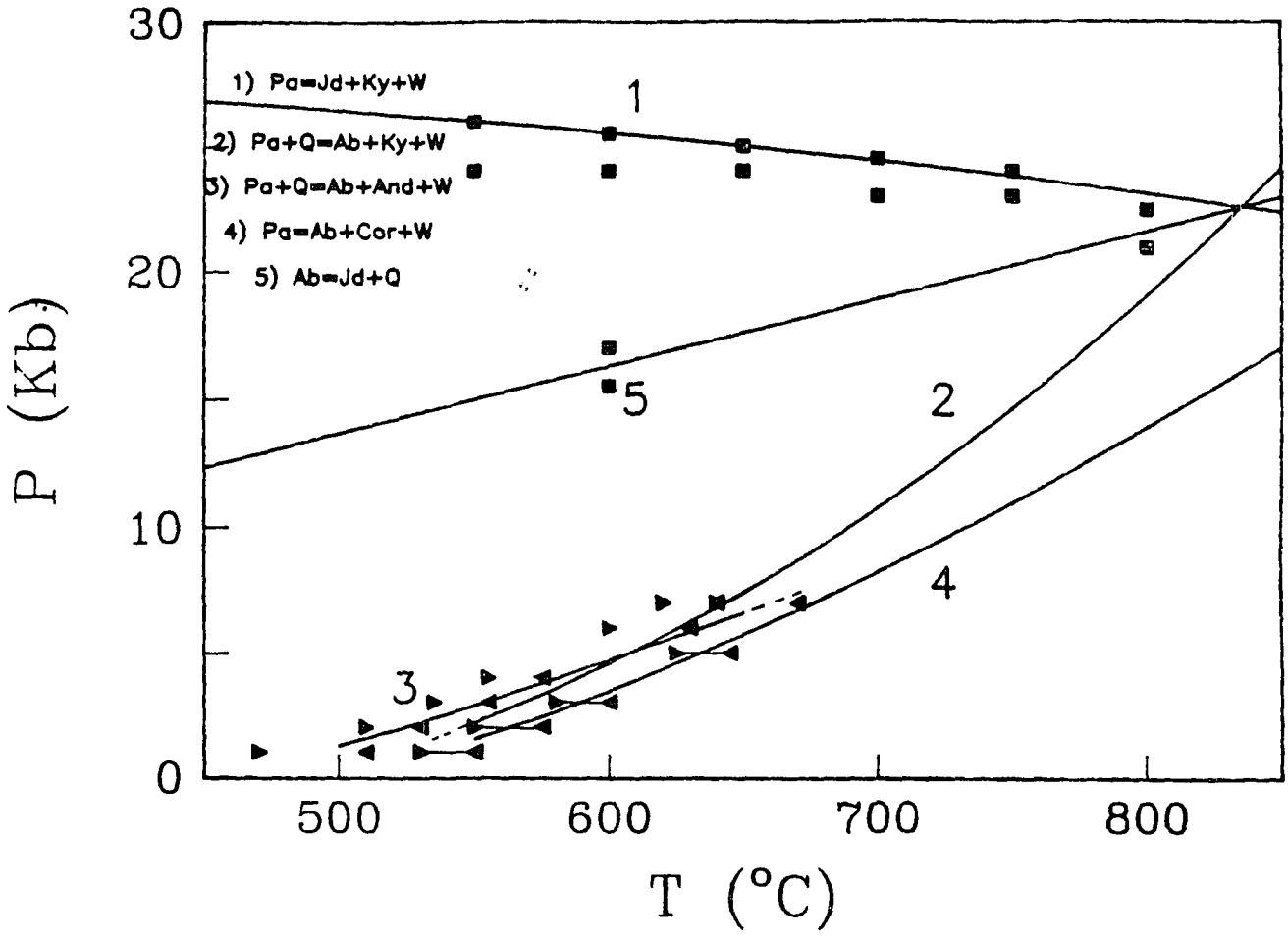

Figure 3.7: Calculated curves for reactions (3.v) through (3.y). The experimental data are from Chatterjee (1970, 1972), Ivanov & Gusynin (1970) and Holland (1979). The dotted lines represent metastable equilibria.

1984a) of the free energy of paragonite (0.23, 1.027 and 5.327 KJ/mol at 298, 500 and 800 K respectively) can be attributed to various types of energies associated with the paragonite structure, one of which could be the the entropy of disorder. Paragonite probably has some zero-point entropy as indicated by Schottky anomaly at lower temperatures (Robie and Hemingway, 1984a). However, more investigation is needed to characterize this energy from the theoretical point of view. The conclusion reached here can only be ascertained through a more accurate determination of the free energy of jadeite.

q) Phlogopite

The following phlogopite breakdown reaction was studied by Wood (1976), Wones and Dodge (1977) and Bohlen et al. (1983c):

$$Phl + Q = En + San + H_2O \qquad (3.z)$$

Enthalpy of phlogopite was determined by Clemens et al. (1987) by solution calorimetry. Their value of -6215.33 KJ/mol was derived by considering a calorimetric cycle for the reaction:

$$Per + Br + San = Phl \qquad (3.aa)$$

and using the free energies of periclase, brucite and sanidine from Robie et al. (1978) and the heat capacity of phlogopite from Robie and Hemingway (1984a). The same procedure is repeated here. A different value for the enthalpy of phlogopite is obtained for the following reason. Saxena (1989b) and Fei and Chatterjee (1988) using the experimental data on the reaction (3.jj) from Irving et al. (1977),

which are upto a temperature of 1400 K, obtained an optimized heat capacity expression for brucite. The heat capacities of brucite obtained from this expression differ from the original data of King et al. (1975) (used by Clemens et al.) by 0.8 and 1.35 J/mol at 500 and 700 K respectively. Also, the enthalpy of brucite obtained from optimization by Saxena (1989b) and Fei and Chatterjee (1988) is 0.08 J/mol less than the value quoted in Robie et al. (1978). The enthalpy of phlogopite obtained using these enthalpy and heat capacities of brucite is -6203.9 KJ/mol. The entropy of phlogopite is also from Robie and Hemingway (1984a). This includes a configurational entropy of 18.7 J/mol.K assuming total Al-Si disorder.

Clemens et al. (1987) found that there is a considerable discrepancy between the experimental data of Bohlen et al. (1983c) and those of Wood (1976) and Wones and Dodge (1977) on reaction (3.z). The enthalpy of phlogopite calculated by Robie and Hemingway (1984a) on the basis of the data of Wood (1976) and Wones and Dodge (1977) is -6226 KJ/mol. However, the measured value of Clemens et al. (1987) (recalculated here) agrees well with the data of Bohlen et al. (1983c).

r) Annite and the Phlogopite-Annite solution

Reversed distribution data of Fe and Mg between biotite and garnet are available from Ferry and Spear (1978) and Perchuk and Lavrent'eva (1983). These data, along with the free energy data of phlogopite as discussed above, are used to calculate the free-energy and volume data of annite and the solution properties of the biotite solution. The relevant reaction is as follows:

Alm + Phl = Pyr + Ann (3.bb)

Free energy of almandine is from Chatterjee (1987) (as discussed in section (1)) and of pyrope as discussed in section (d). The enthalpy, entropy and volume of annite and the interaction parameters of the phlogopite-annite solution are calculated assuming ΔC_p of reaction (3.bb) as zero and from the following equilibrium relation:

$$\Delta G^{o}_{(3.bb)}(P,T) + RTLnK_{D(3.bb)} + RTLnK_{\gamma(3.bb)} = 0 \qquad (3.6)$$

the only unknown quantities in the term $\Delta G^{o}_{(3.bb)}(P,T)$ being the enthalpy, entropy and volume of annite at P and T and where, K_D is from Ferry and Spear (1978) or Perchuk and Lavrent'eva (1983) and K_γ is as follows:

$$K_{\gamma(3.bb)} = (\gamma_{Mg}^{gar}.\gamma_{Fe}^{bio})/(\gamma_{Fe}^{gar}.\gamma_{Mg}^{bio}) \qquad (3.7)$$

The activity formulations for phlogopite and annite, following the Margules formulation for asymmetric solutions, are as follows:

$$RTLn\gamma_{Ph} = X_{An}^{2}[W_{Ph-An}+2X_{Ph}(W_{An-Ph}-W_{An-Ph})] \qquad (3.8)$$

$$RTLn\gamma_{An} = X_{Ph}^{2}[W_{An-Ph}+2X_{An}(W_{Ph-An}-W_{Ph-An})] \qquad (3.9)$$

where, W's are the interaction parameters.

When the data of Ferry and Spear (1978) and Perchuk and Lavrent'eva (1983) are used in conjunction, convergence is not achieved. It is concluded that the two sets of data are inconsistent. When only the data of Ferry and Spear (1978) are used, the fit obtained is not satisfactory. Also, the solution parameters obtained suggest an extremely asymmetric solution. This could be due to the fact that the

data are only in the Fe-rich end of the binary. When only the data of Perchuk and Lavrent'eva (1983) are used, a much better fit is obtained. Also, the solution parameters show a closely symmetric, not very non-ideal solution. Since Perchuk and Lavrent'eva's data cover a wide range of the binary and the results obtained are much better, the free-energy of annite and the interaction parameters of the phlogopite-annite solution obtained from their data are recommended for use in calculations. An uncertainty of 700 joules is found in the enthalpy of annite. The values for W obtained are as follows:

$$W_{Phl\text{-}Ann} = 5540.7 \quad J/mol$$

$$W_{Ann\text{-}Phl} = 5068.5 \quad J/mol$$

The molar volume of annite is from Robie and Bethke (1963). The bulk modulus is optimized with a start value equal to that of phlogopite. The resulting value is the same as that of phlogopite. This is because the experiments were performed only upto a higher pressure limit of 6 Kbar. Thermal expansion was not optimized as no data was found for the thermal expansion of phlogopite.

s) Talc and Anthophyllite

The stability limits of anthophyllite and talc were recently studied in details by Chernosky et al. (1985) under silica saturated and silica undersaturated conditions. The following reactions were studied:

$$Tc = 3En + Q + H_2O \qquad (3.cc)$$

$$Tc + Fo = 5En + H_2O \qquad (3.dd)$$

$$Anth = 7En + Q + H_2O \qquad (3.ee)$$

$$Anth + Fo = 9En + H_2O \qquad (3.ff)$$

$$Tc + 4En = Anth \qquad (3.gg)$$

$$9Tc + 4Fo = 5Anth + 4H_2O \qquad (3.hh)$$

$$7Tc = 3Anth + 4Q + 4H_2O \qquad (3.ii)$$

The three silica undersaturated reactions (3.dd), (3.ff) and (3.hh) along with the reaction (3.gg) intersect to give an invariant point at 7.7 kbar and 955 K. The three silica saturated reactions (3.cc), (3.ee) and (3.ii) along with the reaction (3.gg) intersect to give an invariant point at 10.5 kbar and 1067 K. Greenwood (1963) studied the same reactions. However, his results gave different locations of the invariant points.

Experimental data on reactions (3.cc) through (3.ii) are used to determine the free energy data of talc and anthophyllite. These seven reactions involve talc and two of them, (3.cc) and (3.dd), contain no other hydrous phases. The optimization of thermodynamic data for talc is started with these two reactions since the other three anhydrous phases, quartz, enstatite and forsterite, are well evaluated (Saxena and Chatterjee, 1986 and Chatterjee, 1987; see above). It is found that the phase equilibrium data for reactions (3.cc) and (3.dd) are not consistent with each other. There is no way to adjust thermodynamic data on talc to fit the experimental data on both reactions simultaneously. Optimization of thermodynamic data for anthophyllite from the five anthophyllite related reactions, (3.ee) through (3.ii), indicates that

the data on talc optimized from reaction (3.cc) are more consistent with other talc related equilibrium data than that from reaction (3.dd). Therefore, the final optimized results on talc and anthophyllite are obtained from reactions (3.cc) and (3.ee) through (3.ii). Berman et al. (1986) faced the same problem in their work. They ignored the data of Kitihara et al. (1966) on reactions (3.cc) and (3.dd) in their analysis. In this work also, the data of Kitihara et al. (1966) are found to be inconsistent with the other experimental data on reaction (3.dd). The reason for this may be that reaction (3.cc) takes place at higher temperatures than reaction (3.dd) and so is less influenced by kinetic factors. The heat capacity data of talc and anthophyllite in the temperature range 300-700 K are from Krupka et al. (1985a,b). These measured data are also included in the optimization for thermal expansion and bulk modulus.

Figure 3.8 shows equilibrium curves for reactions (3.cc) and (3.dd) calculated from the optimized parameters. The curve for reaction (3.dd) lies outside the experimental error limits in the higher pressure region (Kitihara et al., 1966) for the reasons mentioned above.

The curves in Figures 3.9 (reactions (3.ee), (3.ff) and (3.gg)) and 3.10 (reactions (3.hh) and (3.ii)) are calculated on the basis of the optimized parameters for anthophyllite. The curves agree well with the experimental data on reactions (3.ee) through (3.ii). The two triple points are consistent with the experiments of Greenwood (1963) and Chernosky et al. (1985) and the solubility experiments of Hemley et al. (1977a,b).

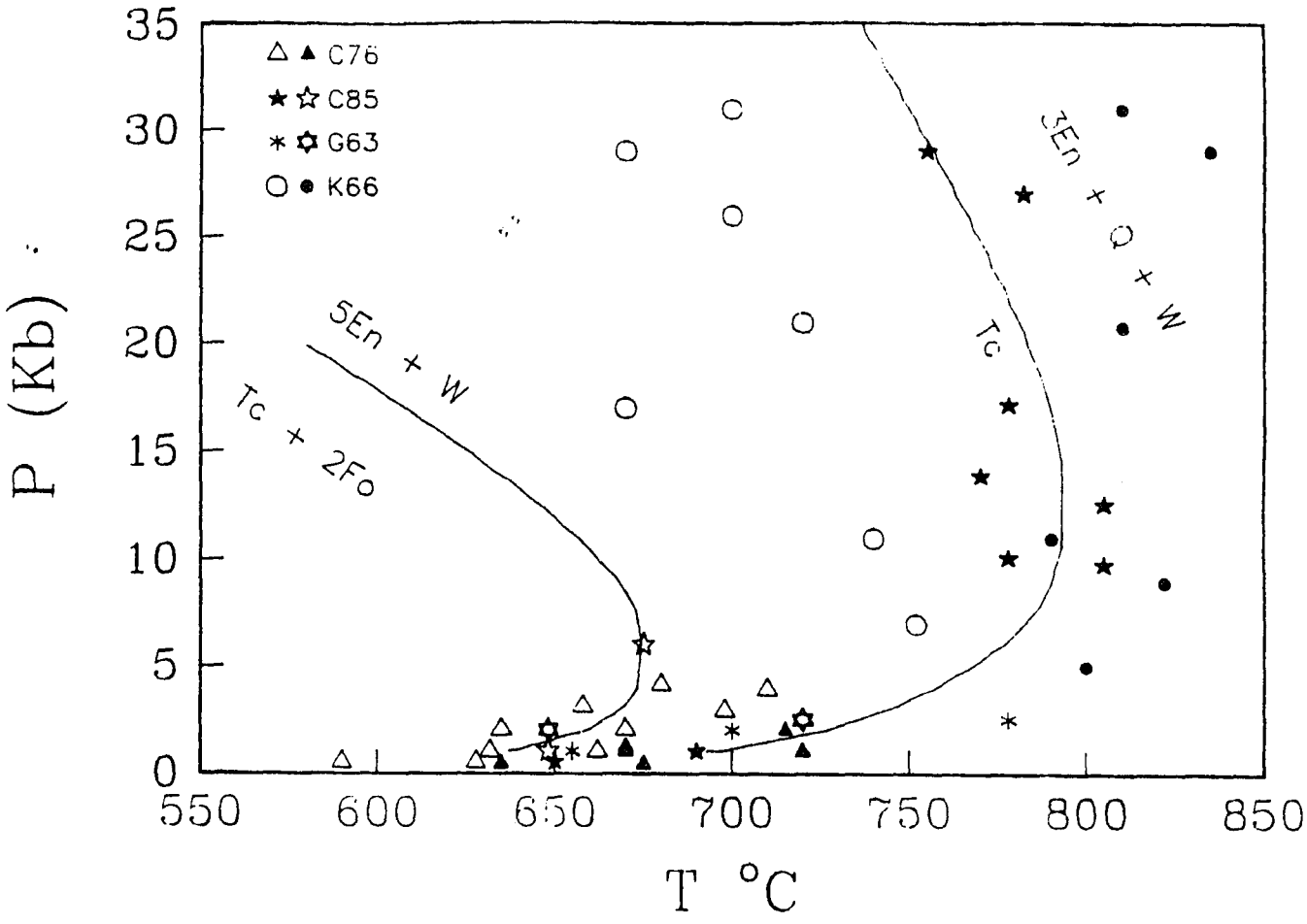

Figure 3.8: Calculated equilibria for reactions (3.cc) and (3.dd). The experimental data are from Chernosky (1976) (C76), Chernosky et al. (1985) (C85), Greenwood (1963) (G63) and Kitihara et al. (1966) (K66).

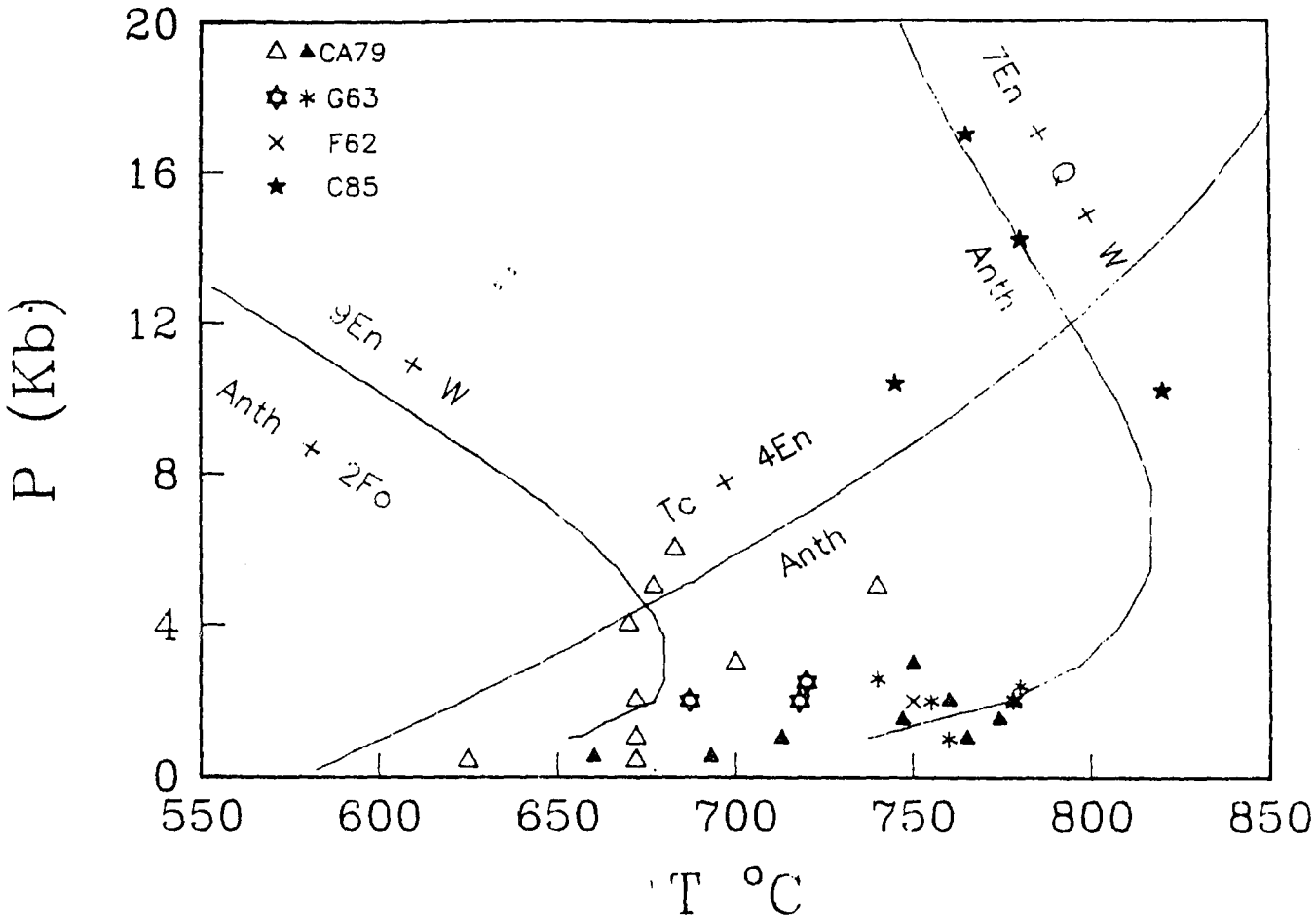

Figure 3.9: Calculated equilibria for reactions (3.ee) through (3.gg). The experimental data are from Chernosky & Autio (1979) (CA79), Greenwood (1963) (G63), Fyfe (1962) (F62), and Chernosky et al. (1985) (C85).

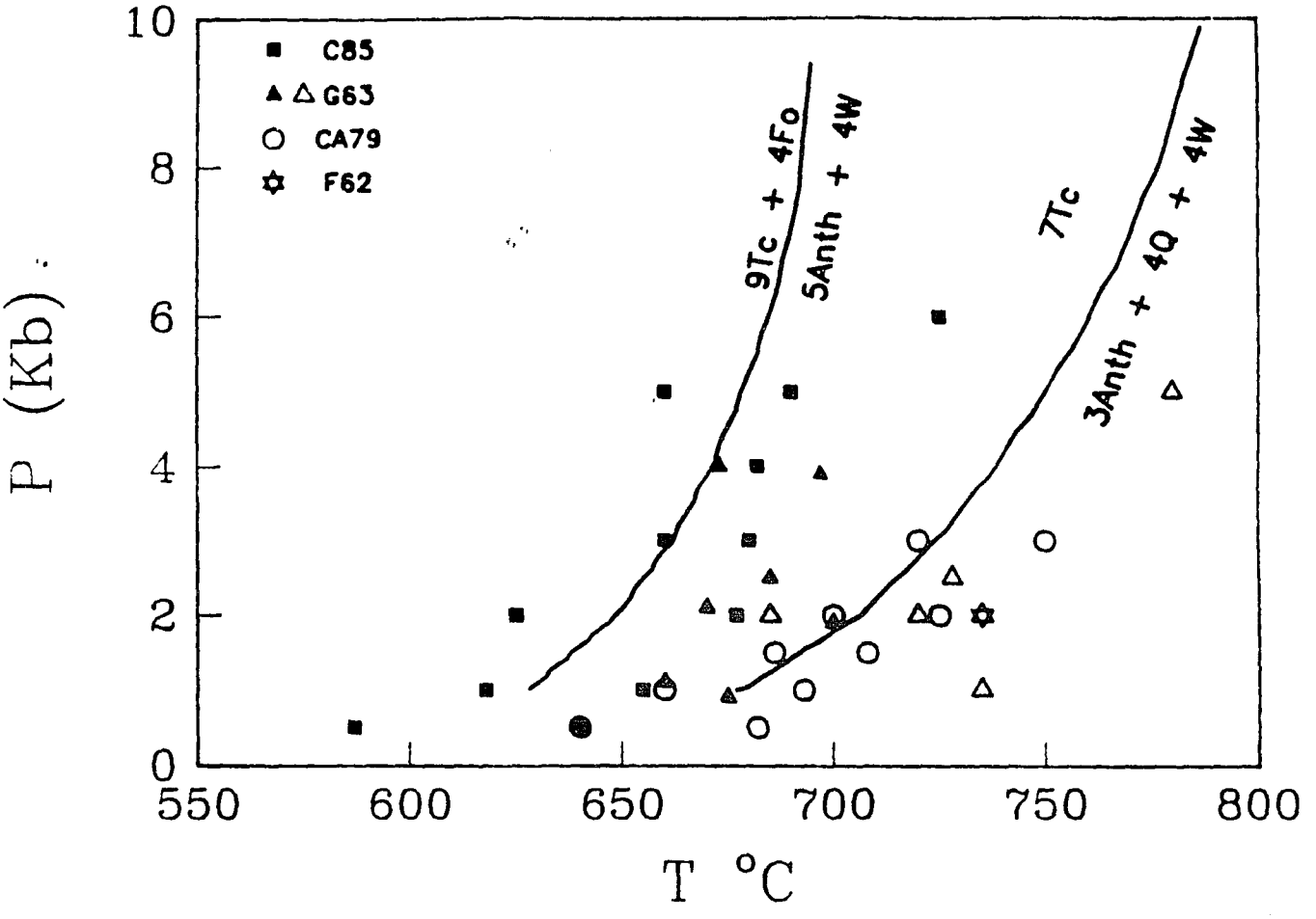

Figure 3.10: Calculated equilibria for reactions (3.hh) and (3.ii). The experimental data are from Chernosky et al. (1985) (C85), Greenwood (1963) (G63), Chernosky & Autio (1979) (CA79) and Fyfe (1962) (F62).

t) Brucite, Chrysotile and Antigorite

The equilibrium data on the following reaction were determined by Barnes and Ernst (1963), Irving et al. (1977) and Schramke et al. (1982):

$$Br = Per + H_2O \qquad (3.jj)$$

The following reactions involve chrysotile:

$$Chr + Br = 2Fo + 3H_2O \qquad (3.kk)$$

$$5Chr = 6Fo + Tc + 9H_2O \qquad (3.ll)$$

The experimental data on these two reactions are from Kitihara et al. (1966), Johannes (1968) and Chernosky (1982).

The stability of antigorite is defined by the following reaction:

$$Ant = 18Fo + 4Tc + 27H_2O \qquad (3.mm)$$

The equilibria for this reaction were experimentally determined by Evans et al. (1976).

Experimental data on reaction (3.jj) are used to determine the free energy data of brucite. The heat capacity data of brucite are available up to temperatures of 700 K (King et al., 1975). The equilibrium data of Irving et al. are upto a temperature of approximately 1400 K. Thus it is necessary to extrapolate the heat capacity using the Fei-Saxena formulation. The heat capacities obtained from the new expression

(optimized by Saxena, 1989b) deviates in small amounts from the original data of King et al. (-0.68, 0.8 and 1.35 J/mol at 298, 500 and 700 K respectively). Enthalpy, entropy, thermal expansion and bulk modulus of brucite are optimized from the experimental data. A detailed discussion of data evaluation on brucite is given in Saxena (1989b). Figure 3.11 shows the calculated curve for the reaction (3.jj) along with the experimental data.

Experimental data on reactions (3.kk) and (3.11) are used to optimize the free energy of chrysotile. The data of some other workers at low pressures on reaction (3.11) (see figure caption for details) were also included in the analysis. All these data are well reproduced from the results obtained. No heat capacity data for chrysotile are available. Therefore, the optimized parameters may not be very well constrained.

Experimental data on reaction (3.mm) are used to optimize the free energy of antigorite. The heat capacity data for antigorite were measured up to a temperature of 850 K by King et al. (1967). The equilibria for reaction (3.mm) were experimentally determined by Evans et al. (1976). The optimized parameters for antigorite include enthalpy, entropy, thermal expansion and bulk modulus.

The curves in Figures 3.11 and 3.12 involving brucite, chrysotile and antigorite are calculated from the optimized values. They agree very well with the experimental data of Johannes (1968), Kitihara et al. (1966), Chernosky (1982), Scarfe and Wyllie (1967), Kalinin and Zubkov (1981), Evans et al. (1976), Irving et al. (1977), Schramke et al. (1982) and Barnes and Ernst (1963). Berman et al. (1986) put an

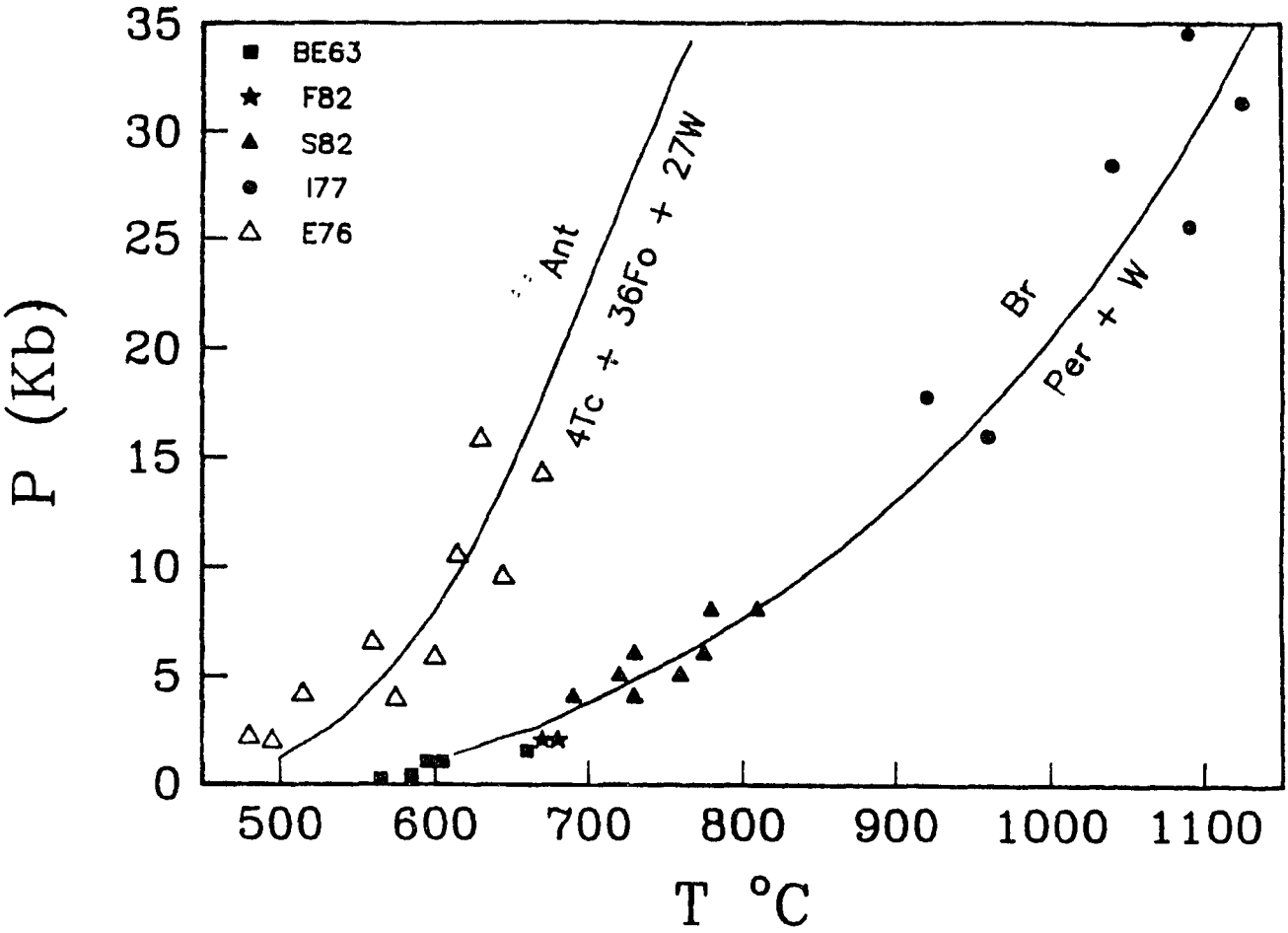

Figure 3.11: Calculated equilibria for reactions (3.jj) and (3.mm). The experimental data are from Barnes & Ernst (1963) (BE63), Franz (1982) (F82) Schramke et al. (1982) (S82), Irving et al. (1977) (I77) and Evans et al. (1976) (E76).

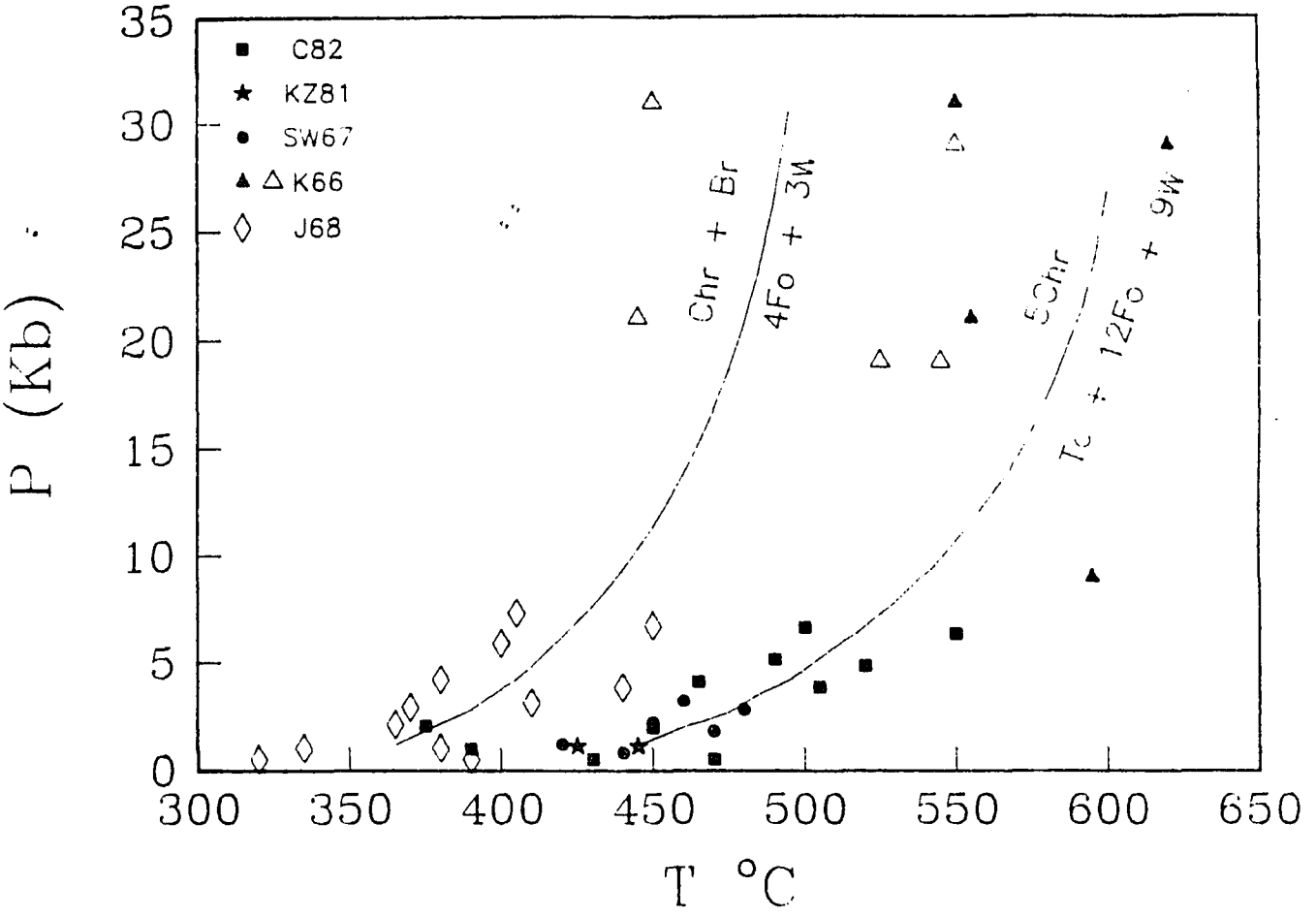

Figure 3.12: Calculated equilibria for reactions (3.kk) and (3.11). The experimental data are from Johannes (1968) (J68), Kitihara et al. (1966) (K66), Kalinin & Zubkov (1981) (KZ81), Scarfe & Wyllie (1967) (SW67) and Chernosky (1982) (C82).

artificial constraint on the basis of the solubility data of Hemley et al. (1977a,b) and some field observations (Evans et al., 1976; Evans, 1977) on the equilibrium at 523 K and 2 Kbar. In doing so they could not reproduce the higher pressure equilibrium data of Kitihara et al. (1966) for the reactions (3.kk) and (3.11). Since the results reproduce the low pressure-temperature points of the above mentioned workers except Hemley et al. (1977a,b) just as well, the data of Hemley et al. were not considered. There is clearly a major inconsistency between the data of Hemley et al. and the data of the other workers. Berman et al. (1986) suggest that the hydrothermal data of Chernosky (1982) and Evans et al. (1976) are more reliable than the solubility data of Hemley et al. which were probably affected by kinetic factors.

u) Grunerite

The grunerite breakdown reaction was studied by Mel'nik and Radchuk (1977) and Forbes (1977). Their results agree at the WM buffer. The reaction is as follows:

$$Grun = Fay + Q + H_2O \qquad (3.nn)$$

Experimental data on the reaction (3.nn) are used to optimize the free energy of grunerite. Miyano and Klein (1983) determined the free energy of grunerite by the same method. However, since they used different free energy values of fayalite and quartz than the values used in this study, the procedure had to be repeated. Their heat capacity equation is accepted in this work while calculating the enthalpy and entropy of grunerite. The molar volume of grunerite is from Klein and

Waldbaum (1967). A calculated curve for the reaction (3.nn) is shown in Figure 3.13 along with the experimental data.

v) Cordierite

The upper stability limit of Mg-cordierite is given by the following reaction studied by Seifert (1974) and more recently by Herzberg (1983):

Cord + Fo = En + Sp (3.oo)

This reaction is influenced by Al solubility in enstatite.

The heat capacity of cordierite is from Robie et al. (1978). The enthalpy and entropy are adjusted within the error limits of Robie et al. (1978) to fit the experimental data on reaction (3.oo). Enstatite is considered an ideal solution between $MgSiO_3$ and Al_2O_3 In Figure 3.14, the calculated curve for reaction (3.oo) is shown along with the experimental data.

w) Ferrocordierite and the Cordierite-Ferrocordierite solution

Experimental data on the distribution of Fe and Mg between garnet and cordierite were obtained by Hensen and Green (1973), Holdaway and Lee (1977) and Perchuk and Lavrent'eva (1983). The reaction is as follows:

Fcord + Pyr = Cord + Alm (3.pp)

The equation given below represents the average of all available experimental data:

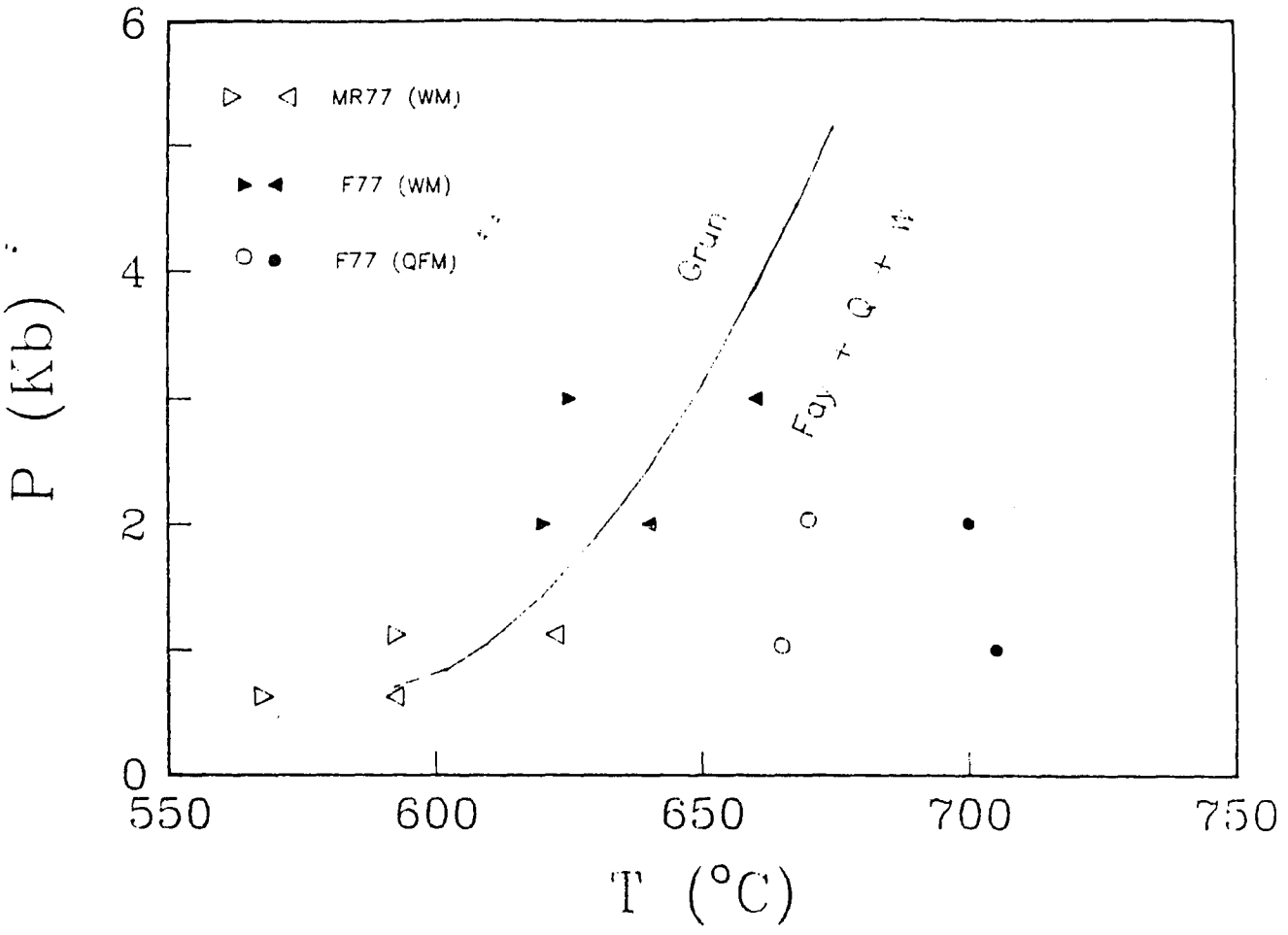

Figure 3.13: Calculated curve for the grunerite breakdown reaction. The experimental results are from Mel'nik and Radchuk (1977) (MR77) and Forbes (1977) (F77) studied under the WM and the QFM buffers.

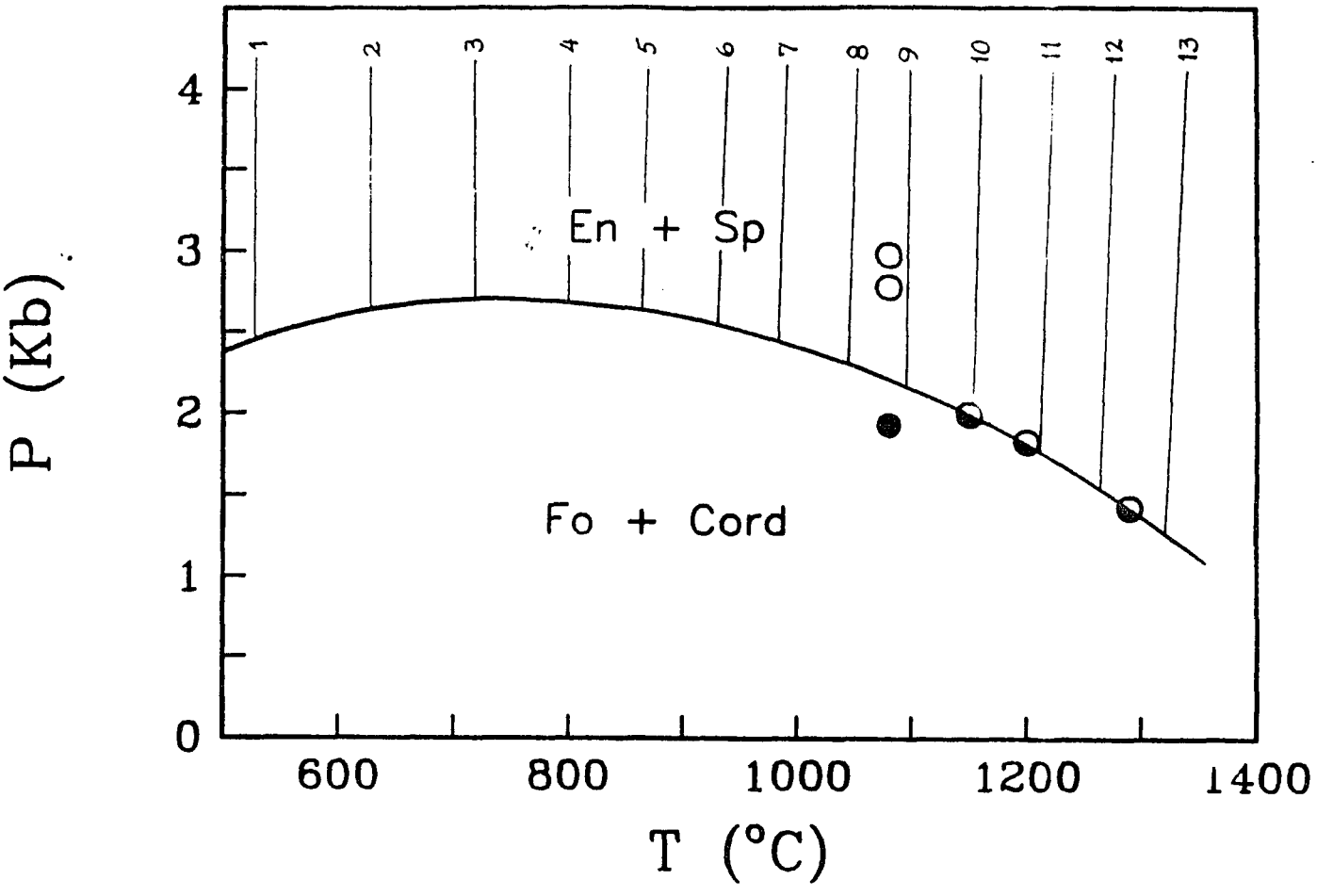

Figure 3.14: Calculated equilibria and experimental data involving Mg-cordierite. Half filled circles are from Herzberg (1983). Open circles are from Fawcett & Yoder (1966) and Seifert (1974). Isopleths of Al_2O_3 % in orthopyroxene are from Danckwerth & Newton (1978).

$$LnK_{D(3.pp)} = 3039.06/T(K) - 1.242 \qquad (3.10)$$

where,

$$K_{D(3.pp)} = (X_{Mg}^{cord}.X_{Fe}^{gar})/(X_{Fe}^{cord}.X_{Mg}^{gar}) \qquad (3.11)$$

The free energy and volume of ferrocordierite and the interaction parameters of the cordierite-ferrocordierite solution are calculated assuming ΔC_p of reaction (3.pp) as zero and from the following equilibrium relation:

$$\Delta G^{o}_{(3.pp)}(P,T) + RTLnK_{D(3.pp)} + RTLnK_{\gamma(3.pp)} = 0 \qquad (3.12)$$

the only unknown quantity in the term $\Delta G^{o}_{(3.pp)}(P,T)$ being the free energy of ferrocordierite at P and T and where, LnK_D is given by equation (3.10) and K_γ is as follows:

$$K_{\gamma(3.pp)} = (\gamma_{Mg}^{cord}.\gamma_{Fe}^{gar})/(\gamma_{Fe}^{cord}.\gamma_{Mg}^{gar}) \qquad (3.13)$$

The activity formulations for cordierite and ferrocordierite, following the Guggenheim formulation for simple mixtures, are as follows:

$$RTLn\gamma_{Mg.cord} = X_{Fe.cord}^{2}W \qquad (3.14)$$

$$RTLn\gamma_{Fe.cord} = X_{Mg.cord}^{2}W \qquad (3.15)$$

where, W is the interaction parameter. The solution shows a near-ideal behavior (W = 1830.6 J/mol) in the temperature range considered (600-1100°C). The thermodynamic properties obtained for ferrocordierite are consistent with the results of Richardson (1968) and Holdaway and Lee (1977), who studied the upper stability limit of ferrocordierite given by the following reaction:

Fcord = Alm + 4Sill + 5Q (3.qq)

x) Hydrous cordierite

For the reaction

Cord + H_2O = Hydrous-cord (3.rr)

Bhattacharya and Sen (1985) give the following relations in the range 773-1073 K:

$\Delta G_{solids}(1,T) = -271018.6 + 134.976xT$ J/mol (3.16)

$\Delta V_{solids}(1,T) = -3.7656x10^{-3}xT - 2.1514$ J/bar/mol (3.17)

Using these relations, the enthalpy, entropy, molar volume and thermal expansion of hydrous cordierite are calculated. The heat capacity is assumed to be the same as that of cordierite.

II. SOLID SOLUTIONS

i) Gehlenite - Akermanite

This solution has a positive deviation from ideality. The asymmetric model of Charlu et al. (1981) determined from calorimetric experiments is adopted.

ii) Spinel - Hercynite

Fe-Mg distribution data for the exchange reaction

$$Fay + Sp = Fo + Her \qquad (3.ss)$$

were experimentally determined by Engi (1983) and Jamieson and Roeder (1984). A mixing model for spinel is obtained using the distribution data of Engi (1983). This is done by a multiple regression of the relation

$$\Delta G^{o}(P,T) + RT\ln K_{D(3.ss)} + RT\ln K_{\gamma(3.ss)} = 0 \qquad (3.18)$$

which can be rewritten as

$$\Delta G^{o} + RT\ln K_{D(3.ss)} + (2X_{Fe}^{Ol}-1)W^{Ol} = W_{MgFe}^{Sp}[X_{Fe}^{Sp}(3X_{Fe}^{Sp}-2)] + W_{FeMg}^{Sp}[-1+4X_{Fe}^{Sp}-3(X_{Fe}^{Sp})^{2}] \qquad (3.19)$$

The W values obtained from equation (3.19) are as follows:

$$W_{MgFe}^{Sp} = 9124 + 1145 \text{ J/mol}$$
$$W_{FeMg}^{Sp} = 0.0 \text{ J/mol}$$

with a standard deviation of 1283.9.

According to Jamieson and Roeder (1984), $\ln K_{D(3.ss)}$ at $X_{Fe}^{Sp} = 0.5$ is zero. In such a case equation (3.19) reduces to

$$\Delta G^{o} = W_{MgFe}^{Sp}(-0.25) + W_{FeMg}^{Sp}(0.25) = -2281 \text{ J}.$$

Using the free energy data from this study, $\Delta G^{o}(1,1573) = -7537.5$ J. Hence, their data are not reproduced. This discrepancy of -5.2 KJ remains to be solved.

iii) Forsterite - Fayalite

Fe-Mg distribution data for the exchange reaction

$$Fay + En = Fo + Fer \qquad (3.tt)$$

were determined by Matsui and Nishizawa (1974). Experiments involving Fe-rich olivine and quartz in equilibrium with Fe-rich orthopyroxene were done by Bohlen and Boettcher (1981).

A symmetric model for the Fe-Mg mixing in olivine with a W value of 4500 J/mol of cation fits best with the experiments of Bohlen and Boettcher (1981) (Figure 3.15). The fit with the synthesis data of Matsui and Nishizawa (1974) is shown in Figure 3.16. If the measurements of Wood and Kleppa (1981) are fitted to a symmetric solution model, the value of the interaction parameter will agree closely with the one recommended here.

iv) Forsterite - Monticellite

Interaction parameters for this solution were determined from experiments conducted by Adams and Bishop (1985). These are adopted here.

v) Fayalite - Monticellite

The interaction parameter for the solution fayalite - kirschsteinite ($[CaFeSi]_{0.5}O_2$) was determined experimentally by Mukhopadhyay and Lindsley (1983). The value obtained by them is 10933+72 J/mol. An

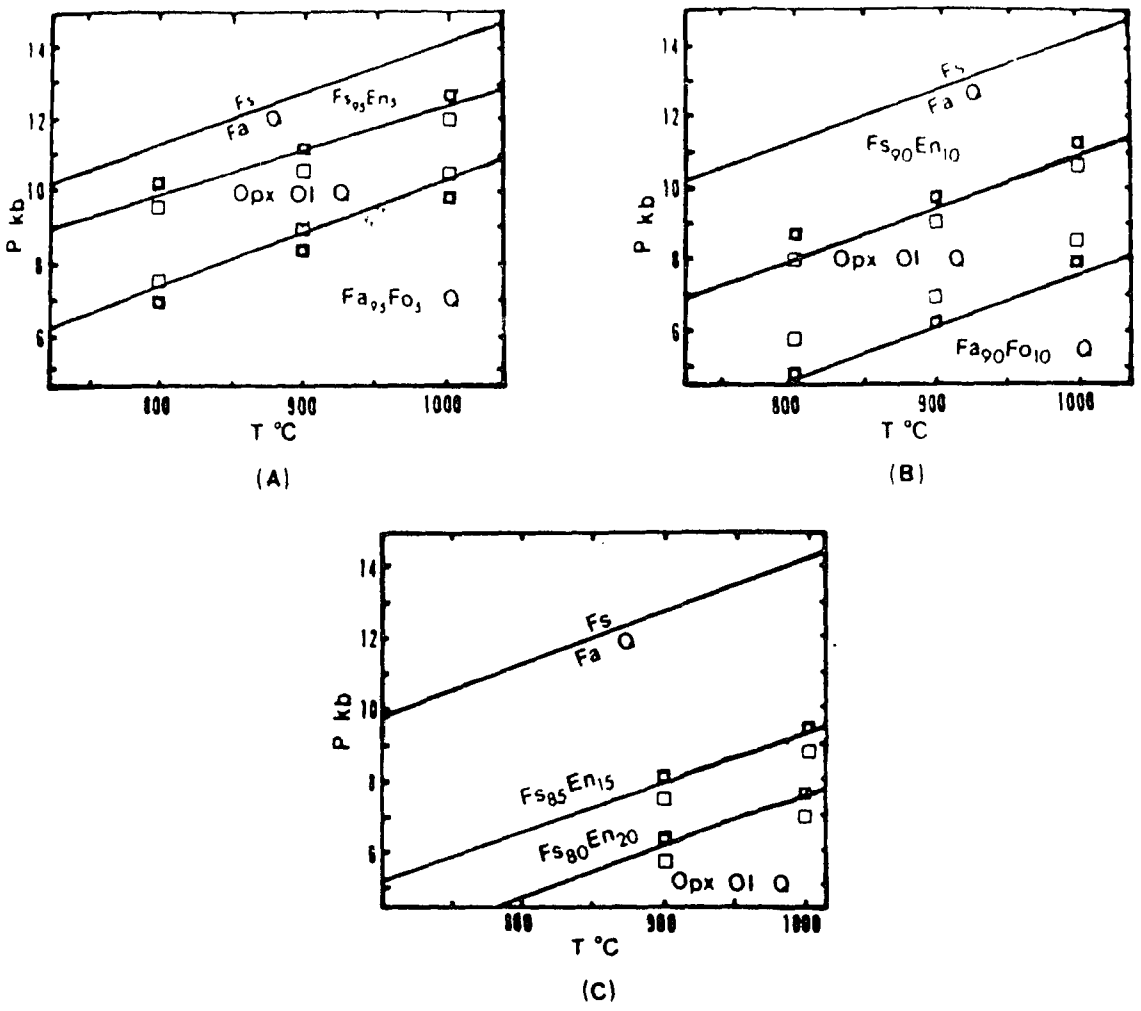

Figure 3.15: Calculated curves showing the effect of increasing enstatite content on the stability of orthopyroxene. All data points are from the experiments of Bohlen & Boettcher (1981). Bold squares indicate the stability field of either orthopyroxene or olivine and quartz. Light squares indicate the stability field of all three minerals at the same time. The reaction involving pure ferrosilite is from Bohlen et al. (1980).

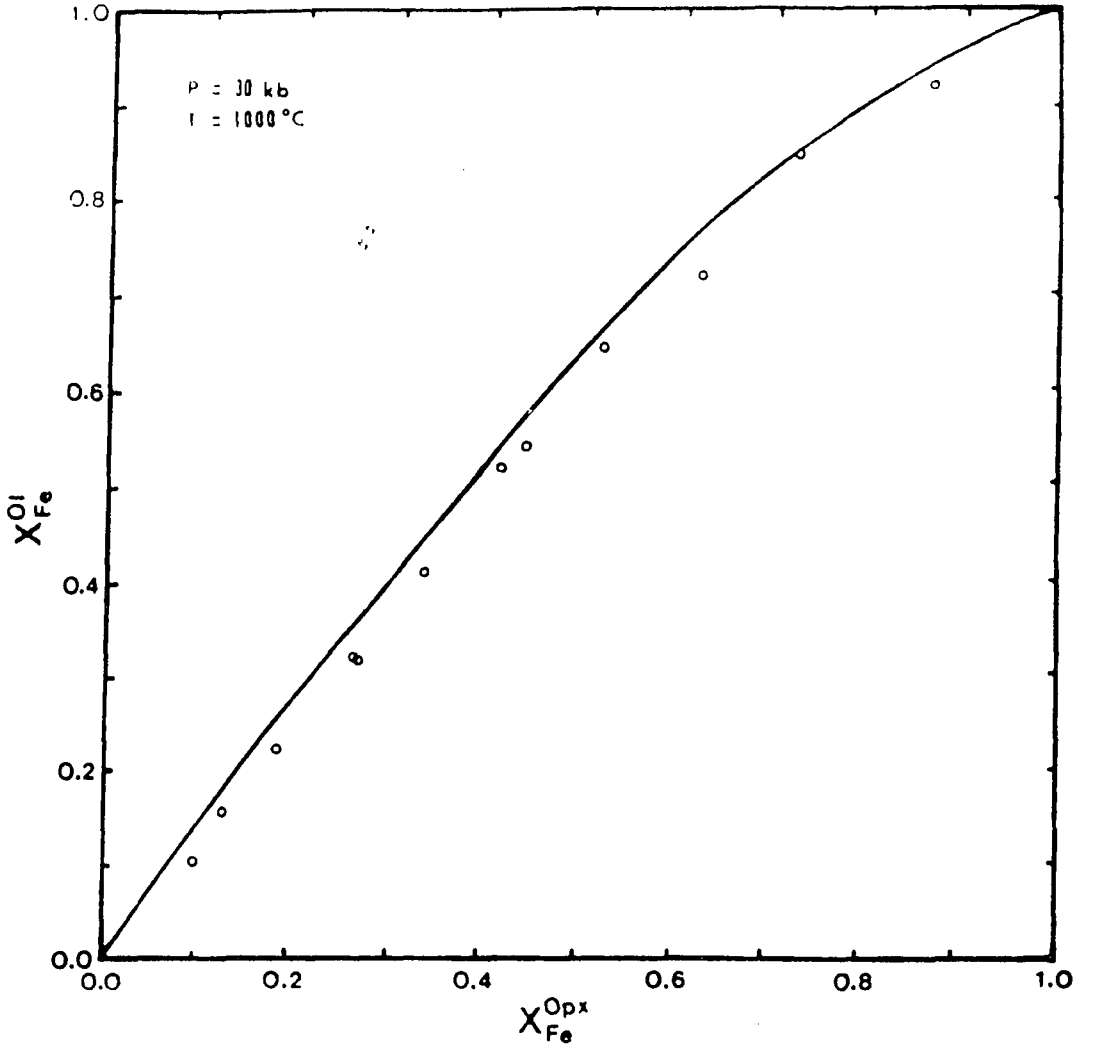

Figure 3.16: Roozeboom diagram for the exchange of Fe^{2+} and Mg^{2+} between olivine and orthopyroxene. All data points are from the experiments of Matsui & Nishizawa (1974). Curves are calculated from the data in this study.

average of this and the interaction parameter of the forsterite - fayalite solution is taken as the interaction parameter of the fayalite - monticellite solution.

vi) Enstatite - Ferrosilite (Ortho- and Clino-)

The enthalpy of solution measurements of Chatillon-Colinet et al. (1983b) indicate a slight positive deviation from ideality of the orthopyroxene solution. However, the site-occupancy data of Saxena and Ghose (1971) indicate a slight excess entropy of mixing which, in calculating the excess free energy, will approximately cancel out the excess enthalpy obtained by Chatillon-Colinet et al. (1983b). The orthopyroxene solution is taken as ideal above 873 K in this study. Below this temperature the solution shows a negative deviation as found by Saxena et al. (1986). This result is accepted in this study below 873 K for enstatite-ferrosilite and 673 K for ferrosilite-enstatite. The clinoenstatite-clinoferrosilite solution is assumed to be ideal.

vii) Enstatite - Diopside (Ortho- and Clino-)

The binary enstatite-diopside solid solutions have been discussed by Saxena (1973), Holland et al. (1979), Lindsley et al. (1981) and Nickel and Brey (1984). Although the latter have fitted a one constant symmetric model to clinopyroxene, the model of Lindsley et al. (1981) is retained here. The difference between the two models does not significantly affect the thermochemical data in Table 3.2, which reproduce the experimentally determined phase equilibrium data as

reviewed by Lindsley et al. (1981) very well. The properties of this solution are being currently revised (Saxena, 1989a) in light of the recent experiments done on the pyroxene quadrilateral by Carlson and Lindsley (1988).

viii) Enstatite-Orthohedenbergite, Ferrosilite-Orthodiopside, Ferrosilite-Orthohedenbergite, Orthodiopside-Orthohedenbergite, Clinoenstatite-Hedenbergite, Clinoferrosilite-Diopside, Clinoferrosilite-Hedenbergite and Diopside-Hedenbergite

The solution data on the above binaries are as recommended by Saxena et al. (1986) from their evaluation of the phase equilibrium data of Lindsley (1983) on quadrilateral pyroxenes.

ix) Enstatite - Al_2O_3-pyroxene (Ortho- and Clino-), Ferrosilite - Al_2O_3-pyroxene (Ortho- and Clino-) Al_2O_3-clinopyroxene - Jadeite

Enstatite solid solution may be modeled by using any of the three possible components besides $MgSiO_3$. These are orthopyrope ($Mg_3Al_2Si_3O_{12}$) recommended by Ganguly and Ghose (1979), Mg-Tschermak ($MgAl_2SiO_6$) used by Gasparik and Newton (1984) and Wood and Holloway (1984) and the Al_2O_3-Opx used by Saxena (1982). For computational convenience, Al_2O_3 is recommended as a component of the orthopyroxene solution mixing ideally with enstatite. The clinoenstatite-Al_2O_3 solution is also considered as ideal. Solutions of Al_2O_3 with ferrosilite, clinoferrosilite and jadeite are also considered ideal.

x) Diopside - Al_2O_3-pyroxene (Ortho- and Clino-) and Hedenbergite - Al_2O_3-pyroxene (Ortho- and Clino-)

The solutions of Al_2O_3 with orthodiopside and diopside are as recommended by Saxena and Chatterjee (1986). The solutions of Al_2O_3 with orthohedenbergite and hedenbergite are considered to have the same properties as their diopside counterparts.

xi) Clinoenstatite - Jadeite and Clinoferrosilite - Jadeite

Windom and Boettcher (1981) worked on the phase relations for the join clinoenstatite-jadeite and found a large miscibility gap at low temperatures. The interaction parameter for this solution is estimated from their result. The same value is assumed for the clinoferrosilite-jadeite solution.

xii) Diopside - Jadeite and Hedenbergite - Jadeite

The model adopted here is that of Gasparik (1985) who did phase equilibrium experiments on the diopside-jadeite join and found a large asymmetric non-ideality. For the hedenbergite-jadeite solution, the same model is assumed.

xiii) Pyrope - Almandine

The enthalpy of mixing of garnet is from the heat of solution measurements of Newton et al. (1986). The excess volume of mixing of the garnet solution is also from Newton et al. (1986).

Relation (3.4) can be rewritten as

$$RT\ln\gamma_{Fe}^{Gar} - RT\ln\gamma_{Mg}^{Gar} = RT\ln\gamma_{Fe}^{Opx} - RT\ln\gamma_{Mg}^{Opx} \qquad (3.20)$$

However, this relation is not satisfied unless some excess entropy is added to the garnet solution. The W^S values of garnet are obtained by multiple regression of equation (3.20), which can be rewritten as follows:

$$\begin{aligned}
&(W^H+PW^V)_{FeMg}^{Gar}[(1-X_{Fe}^{Gar})(1-3X_{Fe}^{Gar})] \\
&+ (W^H+PW^V)_{MgFe}^{Gar}[X_{Fe}^{Gar}(2-3X_{Fe}^{Gar})] \\
&- W_{MgFe}^{Opx}[(1-X_{Fe}^{Opx})(1-3X_{Fe}^{Opx})] \\
&- W_{FeMg}^{Opx}X_{Fe}^{Opx}(2-3X_{Fe}^{Opx})] \\
&\qquad = W_{FeMg}^{S,Gar}[T(1-X_{Fe}^{Gar})(1-3X_{Fe}^{Gar})] \\
&\qquad\quad + W_{MgFe}^{S,Gar}[TX_{Fe}^{Gar}(2-3X_{Fe}^{Gar})] \qquad (3.21)
\end{aligned}$$

The values obtained are as follows:

$$W_{MgFe}^{S} = 11.76 - 0.0016T \quad J/mol.K$$
$$W_{FeMg}^{S} = -10.146 + 0.0037T \quad J/mol.K$$

In the above analysis, Lee and Ganguly's (1987) reversed data for X_{Fe}^{Gar} and X_{Fe}^{Opx} are used. The compensation is best achieved in the range X_{Fe} = 0.3 to 0.8. The data of Lee and Ganguly (1987) (quoted in Ganguly and Saxena, 1987) are in the temperature range 1248-1673 K. The fit obtained is shown in Figure 3.17. Results obtained using the above parameters fit well with the data of Kawasaki and Matsui (1983) (Figure 3.18).

xiv) Pyrope - Grossular

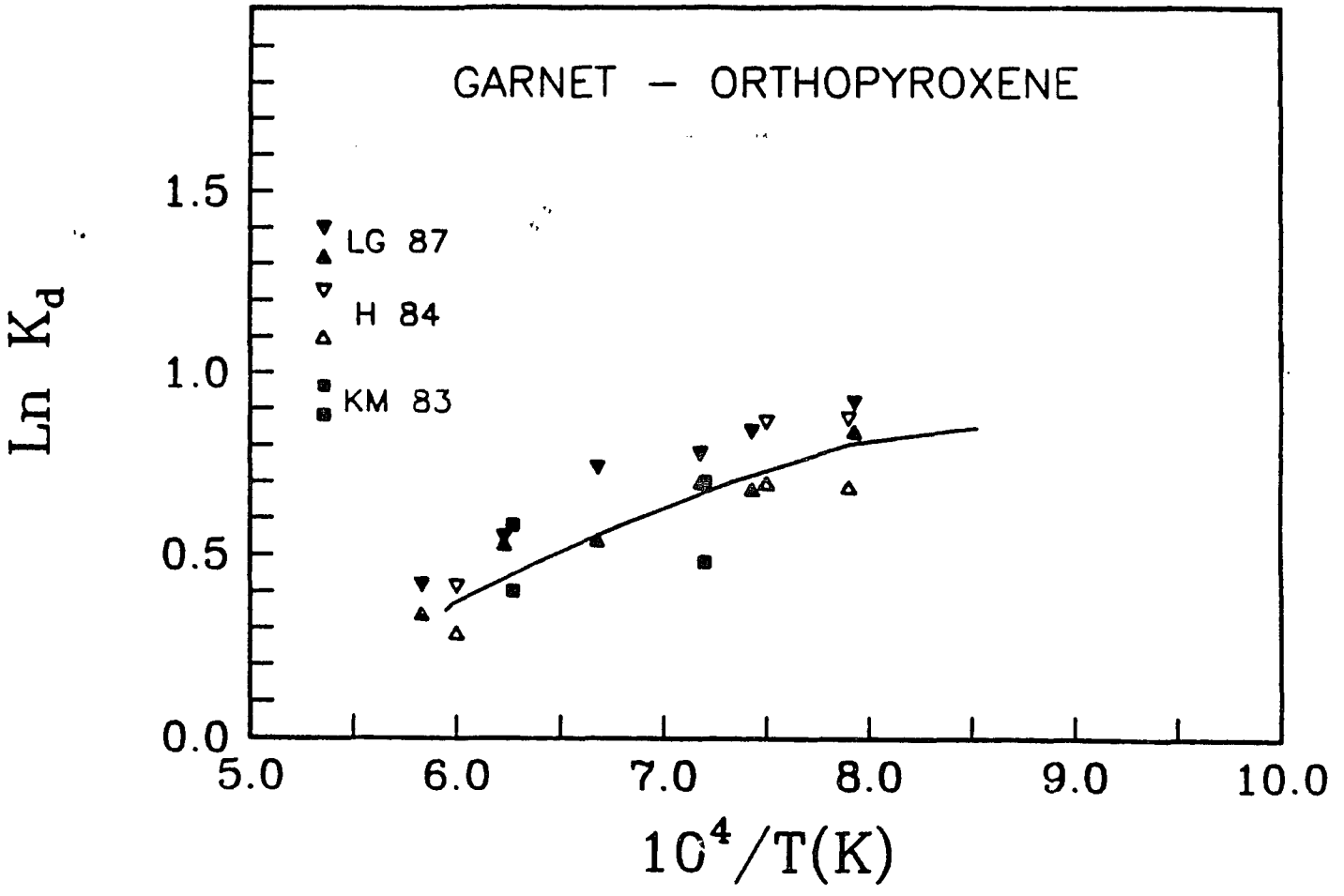

Figure 3.17: Calculated variation of Ln K_D with reciprocal temperature. The experimental data are from Lee & Ganguly (1987) (as quoted in Ganguly & Saxena, 1987) (LG 87), Harley (1984) (H 84) and Kawasaki & Matsui (1983) (KM 83).

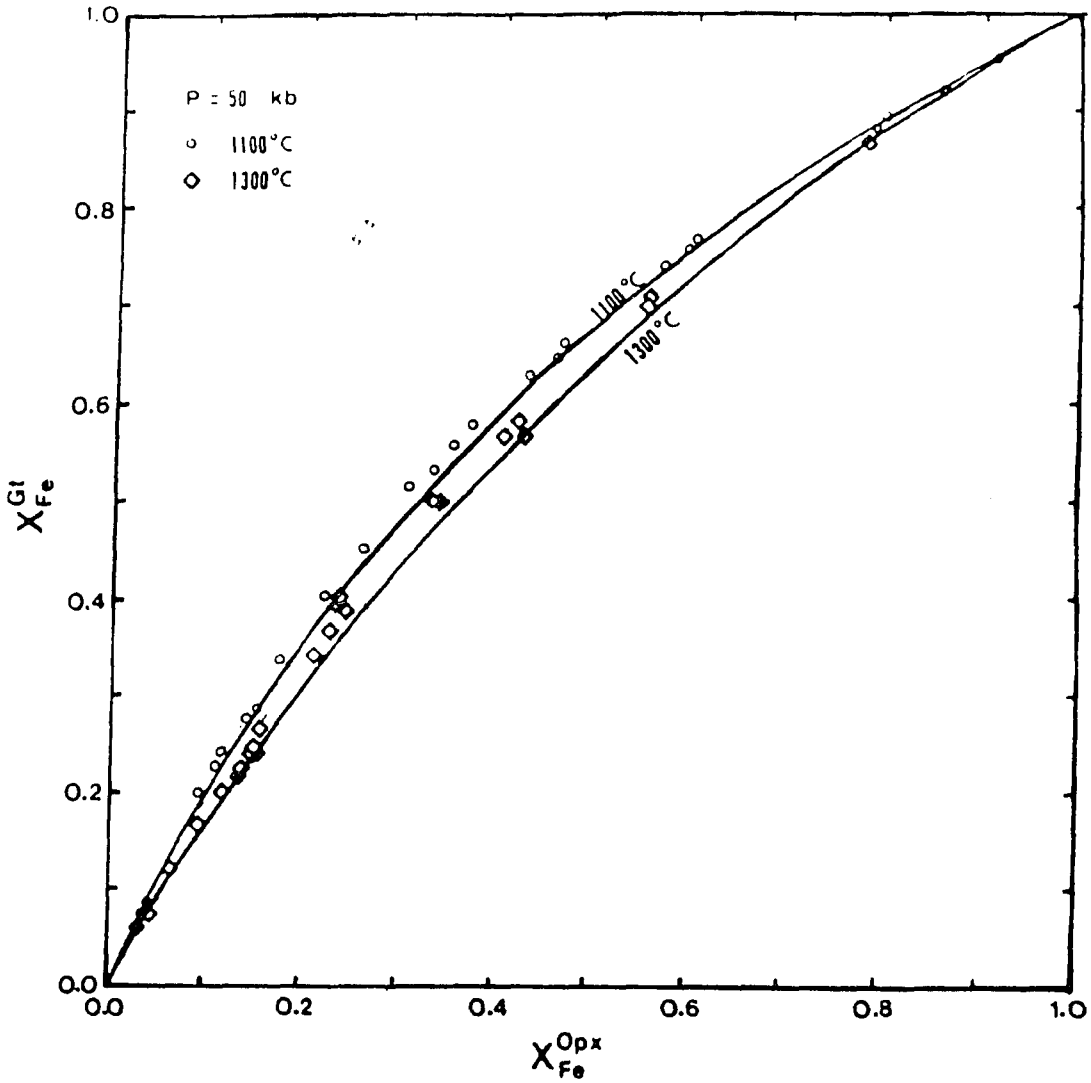

Figure 3.18: Roozeboom diagram for the exchange of Fe^{2+} and Mg^{2+} between orthopyroxene and garnet. All data points are from the experiments of Kawasaki & Matsui (1983). Curves are calculated from the data in this study.

The excess enthalpy values are as recommended by Ganguly & Saxena (1984). The excess entropy is as evaluated and the excess volume is as determined by unit cell measurement by Newton et al. (1986).

xv) Almandine - Grossular

The reaction (3.p) and the GRIPS reaction (3.s) were experimentally reversed by Bohlen et al. (1983a) and Bohlen and Liotta (1986) (see Figure 3.3). The excess enthalpy and volume of the grossular-almandine solution are from Newton et al. (1986). The excess entropy of the solution is calculated from the equilibrium relation

$$\Delta G^{o} + RT\ln K_{D(3.p)} + RT\ln K_{\gamma(3.p)} = 0 \qquad (3.22)$$

where,

$$RT\ln K_{\gamma(3.p)} = -RT\ln \gamma_{Ca}^{Gar} - 2RT\ln \gamma_{Fe}^{Gar} \qquad (3.23)$$

The result obtained is as follows:

$$W^{S} = -16.07 + 0.0126T \qquad J/mol.K$$

This value, when applied to reaction (3.s) (the GRIPS reaction) reproduces its equilibrium location well. The result is valid in the range 1023-1323 K and for a composition $X_{Ca}^{Gar} = 0.33$.

Fe-Mg distribution data for the reaction

$$Fay + Pyr = Fo + Alm \qquad (3.uu)$$

were experimentally determined by Kawasaki and Matsui (1977), Kawasaki (1979) (both at 50 Kb and 1373 K) and O'Neill and Wood (1979) (at 30 Kb and 1273-1473 K). The latter authors also studied the effect of

increasing calcium in garnet on the distribution coefficient. The data presented in this study reproduce the experimental results very well in the calcium-free system (Figure 3.19). However, the fit is poor (Figure 3.20), specially at 1400°C, with experiments involving calcic garnets. In these calculations, an asymmetric excess entropy parameter for the grossular-pyrope join recommended by Newton et al. (1986) is preferred. If a symmetric model for the excess entropy, as recommended by Ganguly and Saxena (1984) and used by Saxena and Chatterjee (1986), is used, the fit to the experimental data becomes worse as shown by the dashed lines in Figure 3.20. Also, note that the solution data in the grossular-almandine solution is only for a composition of $X_{Ca}^{Gar} = 0.33$ along the join.

xvi) Pyrope-Spessartine, Almandine-Spessartine and Grossular-Spessartine

Because of the similar behaviour of the Fe and the Mn atoms, the almandine-spessartine solution is considered as ideal. The interaction parameters for the pyrope-spessartine and the grossular-spessartine solutions are considered same as those of the pyrope-almandine and the grossular-almandine solutions.

xvii) Muscovite - Paragonite

The muscovite-paragonite solution was studied extensively in the past by Eugster et al. (1972) and Chatterjee and Froese (1975) and recently by Flux and Chatterjee (1986) and Chatterjee and Flux (1986).

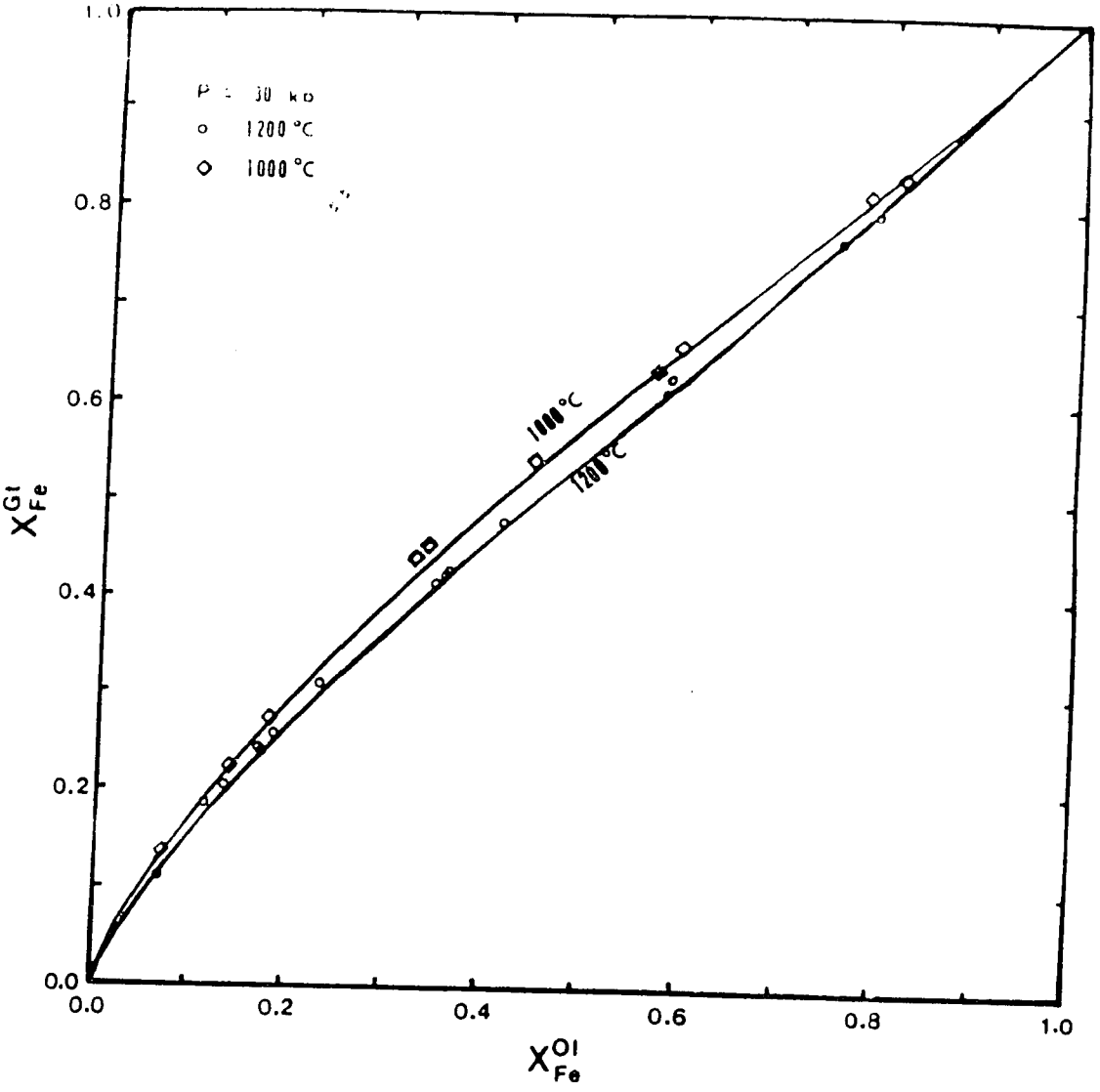

Figure 3.19: Roozeboom diagram for the exchange of Fe^{2+} and Mg^{2+} between olivine and garnet in the Ca-free system. All data points are from the experiments of O'Neill & Wood (1979). Curves are calculated from the data in this study.

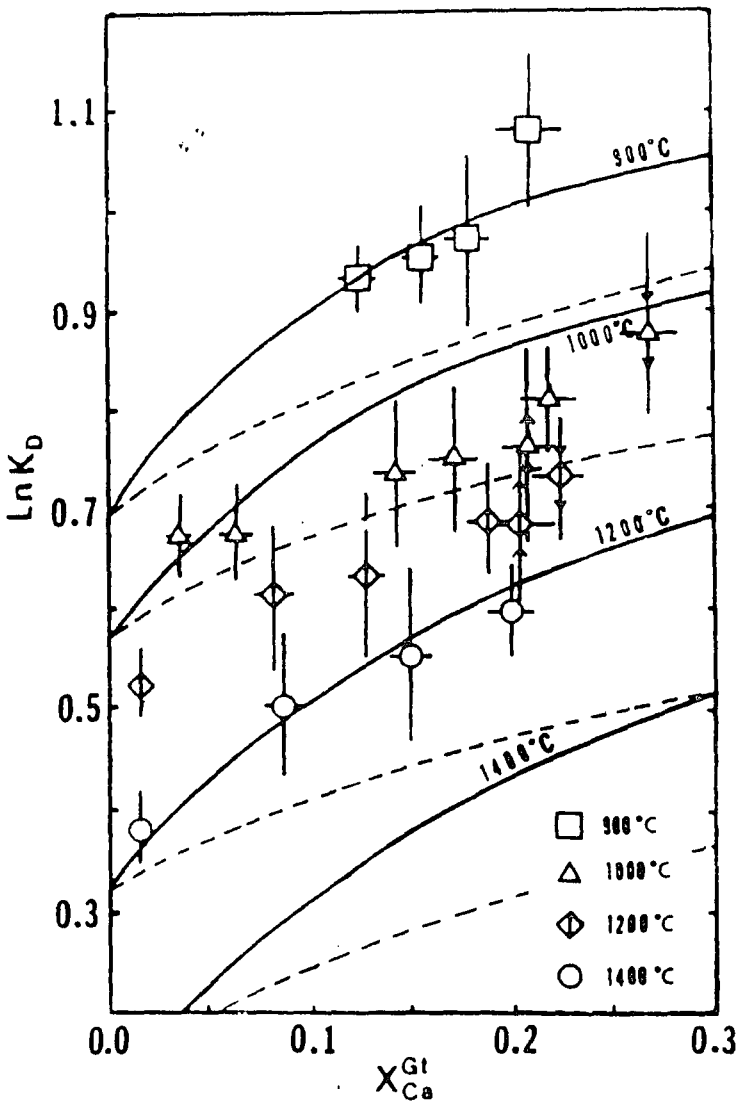

Figure 3.20: Calculated curves showing the effect of increasing calcium content of garnet on K_D [= $(Fe/Mg)^{Gar}/(Fe/Mg)^{Ol}$] at 30 Kb and different temperatures. All data points with error bars are from the experiments of O'Neill & Wood (1979). Points with arrows are from reversal experiments, while others are from synthesis experiments. The bulk value of [Mg/(Mg+Fe)] is close to 0.9. Dashed lines are calculated curves using a symmetric excess entropy model for garnet with W^S=6.276 J/mol for one cation.

Flux and Chatterjee (1986) determined the mixing properties of this binary by studying the exchange of K and Na between muscovite-paragonite and KCl-NaCl salts. They proposed a Redlich-Kister model expressed as follows:

$$G^{ex} = (1-X)\ X\ [A + B(1-2X) + C(1-2X)^2] \qquad (3.24)$$

where, X is the mole-fraction of muscovite in the muscovite-paragonite solution and the constants are a function of temperature and pressure given by:

$$A = 11222 + 1.389xT + 0.2359xP$$

$$B = -1134 + 6.806xT - 0.0840xP$$

$$C = -7305 + 9.043xT$$

where, the units for temperature; pressure; and excess free-energy, and the Redlich-Kister constants are kelvin, bar and J/mol respectively.

xviii) Phlogopite - Annite

Wones and Eugster (1965) considered biotite a ternary solution with phlogopite, annite and "oxybiotite" ($KFe^{3+}_3AlSi_3O_{12}(H_{-1})$) as the end-members. Oxybiotite is present in natural biotites in significant amounts. They also calculated the activity of annite in the phlogopite-annite solution from the reaction

$$Ann = San + Mag + H_2 \qquad (3.vv)$$

They used the fugacity of hydrogen determined by Eugster and Wones (1962) and Shaw and Wones (1964). They calculated a symmetric

interaction parameter of -4211 J/mol. Wones (1972) later revised their work and concluded that the phlogopite-annite solution is ideal (see Hewitt and Wones, 1984). However, the fugacity of hydrogen has been revised many times since then (Saxena and Fei, 1988a). Thus, their calculations need to be revised.

In this work, the interaction parameters for this binary are determined in conjunction with the free energy of annite. This is discussed in the section under "annite and the phlogopite-annite solution".

xix) Cordierite - Ferrocordierite

This is discussed above under "ferrocordierite and the cordierite-ferrocordierite solution".

xx) Cordierite - Hydrous cordierite and Ferrocordierite - Hydrous cordierite

The cordierite - hydrous cordierite solution is considered ideal. The ferrocordierite - hydrous cordierite solution is approximated as the same as the ferrocordierite - cordierite solution.

xxi) Anorthite - Albite, Anorthite - Sanidine and Albite - Sanidine

The interaction parameters on these solutions are as evaluated by Nekvasil (1986) on the albite-anorthite-orthoclase solution.

TABLE 3.2. RECOMMENDED THERMOCHEMICAL DATA ON PHASES

Name, Formula	H°_f (J/mol)	$S^{\circ}(1,298)$ (J/K.mol)	N		
	a	bxE3	cxE-6	exE-8	gxE-4
1. Steam	H_2O				
	-241814.0	188.83	1		
	46.461	5.966	6.32	-7.957	-1.663
2. Calcium Oxide	CaO				
	-635089.0	38.21	1		
	51.409	3.812	-0.6824	-0.02538	-0.0785
3. Ferrous Oxide	FeO				
	-261780.0	63.44	1		
	56.61	0.37	0.4185	-0.259	-0.3185
4. Periclase	MgO				
	-601490.0	26.94	1		
	49.654	3.841	-1.3898	1.272	-0.0792
5. Corundum	Al_2O_3				
	-1675711.0	50.917	1		
	141.81	2.051	1.484	-3.408	-2.005
6. α-Quartz	SiO_2				
	-910700.0	41.46	2		
	101.49	2.782	4.353	-1.913	-2.961
	848.0	0.0			
	62.684	21.039	-2.5826	52.92	-0.48031
7. β-Quartz	SiO_2				
	-909340.0	40.003	1		
	78.812	1.205	1.731	1.202	-1.213
8. Andalusite	Al_2SiO_5				
	-2591900.0	91.39	1		
	221.69	2.581	-2.559	4.899	-2.669
9. Kyanite	Al_2SiO_5				
	-2596010.0	82.3	1		
	223.54	2.645	-4.149	7.601	-2.524
10. Sillimanite	Al_2SiO_5				
	-2587770.0	95.79	1		
	230.12	4.404	6.616	-7.813	-4.56

11. Wollastonite $CaSiO_3$

-1634766.0	81.028	1		
140.21	1.813	1.405	-1.354	-1.908

12. Gehlenite $Ca_2Al_2SiO_7$

-3980763.0	204.35	1		
341.54	3.795	-0.7663	4.074	-4.037

13. Akermanite $Ca_2MgSi_2O_7$

-3865440.0	209.33	1		
265.913	39.411	-4.7161	-0.6799	-0.52324

14. Spinel $MgAl_2O_4$

-2307160.0	81.5	1		
210.01	3.737	5.958	-7.165	-4.028

15. Hercynite $FeAl_2O_4$

-1961300.0	106.27	1		
232.08	5.465	8.015	5.302	-5.571

16. Forsterite $MgSi_{0.5}O_2$

-1087180.0	47.06	1		
96.731	1.278	1.89	-4.312	-1.309

17. Fayalite $FeSi_{0.5}O_2$

-739085.0	75.5	1		
109.57	1.852	2.963	-1.862	-2.001

18. Monticellite $(CaMgSi)_{0.5}O_2$

-1123300.0	55.229	1		
76.977	11.188	-1.6916	0.02279	0.00468

19. Enstatite $MgSiO_3$

-1546290.0	66.27	1		
144.45	1.882	-1.35	4.612	-1.938

20. Ferrosilite $FeSiO_3$

-1195200.0	94.56	1		
131.89	0.06214	-4.947	0.1425	0.02319

21. Orthodiopside $(CaMg)_{0.5}SiO_3$

-1591040.0	71.54	1		
110.605	16.4	-3.293	0.0	0.0

22. Orthohedenbergite $(CaFe)_{0.5}SiO_3$

-1416780.0	84.879	1		
114.665	17.1	-0.0314	0.0	0.0

23. Al_2O_3-opx Al_2O_3

-1641000.0	62.4	1		
80.36	37.0	0.0	0.0	0.0

24. Clinoenstatite $MgSiO_3$

-1544010.0	67.225	1		
144.45	1.882	-1.35	4.612	-1.938

25. Clinoferrosilite $FeSiO_3$

-1193590.0	95.4	1		
133.0	0.0	-4.847	0.0	0.0

26. Diopside $(CaMg)_{0.5}SiO_3$

-1600910.0	71.55	1		
110.605	16.4	-3.293	0.0	0.0

27. Hedenbergite $(CaFe)_{0.5}SiO_3$

-1419410.0	85.145	1		
114.665	17.1	-0.0314	0.0	0.0

28. Al_2O_3-cpx Al_2O_3

-1644900.0	58.0	1		
80.36	37.0	0.0	0.0	0.0

29. Ca-Tschermak $CaAl_2SiO_6$

-3306000.0	139.3	1		
280.08	2.685	-5.344	9.611	-2.711

30. Jadeite $1/2(NaAlSi_2O_6)$

-1514935.0	67.385	1		
132.83	6.93	1.647	-2.465	-1.913

31. Pyrope $MgAl_{2/3}SiO_4$

-2097180.0	88.757	1		
184.01	2.741	4.03	-7.376	-2.8

32. Almandine $FeAl_{2/3}SiO_4$

-1758790.0	112.1	1		
171.64	0.8644	0.5278	-11.98	-0.86

33. Grossular $CaAl_{2/3}SiO_4$

-2211436.0	86.706	1		
187.59	2.814	4.049	-7.39	-2.833

34. Spessartine $MnAl_{2/3}SiO_4$

-1854493.5	106.857	1		
221.286	-22.6216	5.6297	-5.1974	-4.2595

35. Rutile TiO_2

-945900.0 50.46 1
84.599 1.335 2.078 -1.471 -1.416

36. Ilmenite $FeTiO_3$

-1234800.0 108.9 1
154.56 2.292 3.385 -4.066 -2.348

37. Anorthite $CaAl_2Si_2O_8$

-4236000.0 199.6 1
372.23 6.568 9.787 -12.12 -6.768

38. Albite $NaAlSi_3O_8$

-3929560.0 220.3 1
343.45 4.415 -11.195 21.46 -2.578

39. Sanidine $KAlSi_3O_8$

-3959560.0 239.99 1
357.19 0.4692 -5.446 12.93 -4.182

40. Muscovite $KAl_2AlSi_3O_{10}(OH)_2$

-5976300.0 306.4 1
72.494 -57.11 25.93 -18.74 -17.97

41. Paragonite $NaAl_2AlSi_3O_{10}(OH)_2$

-5949100.0 277.1 1
56.806 10.44 7.199 -5.51 -8.966

42. Phlogopite $KMg_3AlSi_3O_{10}(OH)_2$

-6203900.0 334.6 1
56.917 3.931 -20.83 33.41 -3.19

43. Annite $KFe_3AlSi_3O_{10}(OH)_2$

-5125500.0 440.91 1
626.55 62.631 13.276 -7.9467 -11.675

44. Brucite $Mg(OH)_2$

-924620.0 64.082 1
103.01 16.533 -2.7462 0.0 -0.0114

45. Chrysotile $Mg_3Si_2O_5(OH)_4$

-4363000.0 219.82 1
507.68 28.294 10.798 -8.4309 -9.7731

46. Antigorite $Mg_{48}Si_{34}O_{85}(OH)_{62}$

-71376000.0 3672.8 1
7701.4 209.1 -38.256 114.4 -99.281

47. Talc	$Mg_3Si_4O_{10}(OH)_2$				
	-5898800.0	261.18	1		
	558.48	20.072	8.122	-13.24	-8.489
48. Anthophyllite	$Mg_7Si_8O_{22}(OH)_2$				
	-12071000.0	534.31	1		
	1128.7	38.86	5.043	-7.642	-15.1
49. Grunerite	$Fe_7Si_8O_{22}(OH)_2$				
	-9631500.0	714.6	1		
	763.704	356.55	-17.827	2.8902	0.55255
50. Cordierite	$Mg_2Al_4Si_5O_{18}$				
	-9164869.0	411.0	1		
	732.869	53.135	4.432	-10.903	-9.1068
51. Ferrocordierite	$Fe_2Al_4Si_5O_{18}$				
	-8446904.0	471.121	1		
	797.988	14.411	14.581	-32.3007	-11.9284
52. Hydrous cordierite	$Mg_2Al_4Si_5O_{18}.H_2O$				
	-9435890.0	276.024	1		
	732.869	53.135	4.432	-10.903	-9.1068

$C_p = a + bT + cT^{-2} + eT^{-3} + gT^{-1}$

* N = no. of C_p equations. When N>1, the first C_p equation is followed by the temperature and enthalpy of transition, which in turn is followed by the next C_p equation.

Sources of data

1-5) Steam, Calcium Oxide, Ferrous Oxide, Periclase, and Corundum: Robie et al. (1978).
6) α-Quartz: Enthalpy and entropy, Robie et al. (1978). Heat Capacity, Robie et al. (1978) (298-848 K) and this study (>848 K).
7) β-Quartz: Enthalpy and entropy, this study. Heat Capacity, Robie et al. (1978) (>848 K).
8-10) Andalusite, Kyanite and Sillimanite: Robie & Hemingway (1984b).
11) Wollastonite: Haas et al. (1981).
12) Gehlenite: Enthalpy and Heat Capacity, Saxena & Chatterjee (1986). Entropy, Woodhead (1977).
13) Akermanite: Enthalpy, Saxena & Chatterjee (1986) (adjusted from Yoder's (1968) experimental phase equilibrium data). Entropy and heat capacity, Robie et al. (1978).
14) Spinel: Enthalpy and entropy, Chatterjee (1987). Heat Capacity, Robie et al. (1978).

15) Hercynite: Enthalpy, Chatterjee (1987) (adjusted within the error limits of Robie et al., 1978). Entropy, Robie et al. (1978). Heat Capacity, Chatterjee (1987) (adjusted from Saxena & Eriksson, 1983b).
16) Forsterite: Enthalpy, Saxena & Chatterjee (1986). Entropy, Robie et al. (1982b), Heat Capacity, Watanabe (1982).
17) Fayalite: Robie et al. (1982a).
18) Monticellite: Enthalpy, Saxena & Chatterjee (1986) (adjusted to Yoder's (1968) experimental phase equilibrium data). Entropy, Robie et al. (1978). Heat capacity, Helgeson et al. (1978).
19) Enstatite: Enthalpy, Brousse et al. (1984). Entropy and Heat Capacity, Haselton (1979).
20) Ferrosilite: Enthalpy (adjusted slightly in Chatterjee, 1987) and entropy, Bohlen & Boettcher (1981). Heat Capacity, Chatterjee (1987).
21) Orthodiopside: Enthalpy and entropy, Saxena et al. (1986) (estimated by using the experimental data of Lindsley et al., 1981). Heat capacity, as in diopside.
22,27) Orthohedenbergite and Hedenbergite: Enthalpy and entropy, Saxena et al. (1986) (estimated by using the experimental data of Lindsley et al., 1981). Heat Capacity, Saxena et al. (1986) and Haselton et al. (1987) (heat capacity of orthohedenbergite assumed same as that of hedenbergite).
23) Al_2O_3-Orthopyroxene: Saxena & Chatterjee (1986) (entropy adjusted in this study).
24) Clinoenstatite: Enthalpy and entropy, Kiseleva et al. (1979) and Saxena & Chatterjee (1986) (estimated by using the data of Lindsley et al., 1981). Heat capacity, as in enstatite.
25) Clinoferrosilite: Saxena et al. (1986) (estimated by using the experimental data of Lindsley et al., 1981).
26) Diopside: Robie et al. (1978).
28) Al_2O_3-Clinopyroxene: Saxena & Chatterjee (1986).
29) Ca-Tschermak: Enthalpy and entropy, Chatterjee (1989). Heat Capacity, Saxena & Chatterjee (1986) (evaluated from the experimental data of Gasparik, 1984b).
30) Jadeite: Enthalpy, Hemingway et al. (1981). Entropy and Heat Capacity, Robie et al. (1978).
31) Pyrope: Enthalpy, Charlu et al. (1975). Entropy from Haselton & Westrum (1980). Heat capacity from Haselton (1979).
32) Almandine: Chatterjee (1987).
33) Grossular: Enthalpy, Charlu et al. (1978). Entropy, Haselton & Westrum (1980). Heat Capacity, Haselton (1979).
34) Spessartine: Bokreta (1989).
35) Rutile: Enthalpy and entropy, Chatterjee (1987) (adjusted within the error limits of Robie et al., 1978). Heat Capacity, Robie et al. (1978).
36) Ilmenite: Enthalpy, Chatterjee (1987) (adjusted within the error limits of Robie et al., 1978). Entropy and Heat Capacity, Anovitz et al. (1985).
37) Anorthite: Enthalpy, Chatterjee (1987). Entropy, Chatterjee (1987) (adjusted within the error limits of Robie et al., 1978). Heat Capacity, Chatterjee (1987) and Holland (1981).
38) Albite: Hemingway et al. (1981).
39) Sanidine: Enthalpy, Robie et al. (1978). Entropy, this study. Heat Capacity, Hemingway et al. (1981).

40) Muscovite: Enthalpy, this study. Entropy, Robie et al. (1978). Heat Capacity, Krupka et al. (1979).
41) Paragonite: Enthalpy and Heat Capacity, this study. Entropy, Robie & Hemingway (1984a).
42) Phlogopite: Robie & Hemingway (1984a).
43) Annite: This study.
44) Brucite: Enthalpy and entropy, Fei & Chatterjee (1988). Heat capacity (300-700 K), King et al. (1975).
45) Chrysotile: Enthalpy and entropy, this study. Heat capacity, King et al. (1967) (298 K) and this study.
46) Antigorite: Enthalpy and entropy, this study. Heat capacity (300-850 K), King et al. (1967).
47) Talc: Enthalpy and entropy, this study. Heat capacity (300-650 K), Krupka et al. (1985a,b).
48) Anthophyllite: Enthalpy and entropy, this study. Heat capacity (300-700 K), Krupka et al. (1985a,b).
49) Grunerite: Enthalpy and entropy, This study. Heat capacity, Miyano & Klein (1983).
50) Cordierite: Enthalpy and entropy, adjusted within the error limits of Robie et al. (1978). Heat capacity, Robie et al. (1978).
51) Ferrocordierite: This study
52) Hydrous cordierite: Enthalpy and entropy, Bhattacharya and Sen (1985) and this study. Heat capacity, same as in cordierite.

TABLE 3.3. RECOMMENDED THERMOPHYSICAL DATA ON PHASES

	V	α_0xE4	α_1xE8	α_2	K_0	K_0'
	cc/mol				Mbar	
2) Calcium Oxide	16.764	-	-	-	-	-
3) Ferrous Oxide	12.040	-	-	-	-	-
4) Periclase	11.250	0.36810	0.92830	-0.74450	1.603	4.13
5) Corundum	25.575	0.18714	0.91660	0.00227	2.496	4.20
6) α-Quartz	22.690	0.31000	2.67800	0.00000	0.374	6.40
7) β-Quartz	23.700	-0.03000	0.00000	0.00000	0.684	6.40
8) Andalusite	51.520	0.14739	2.87429	0.00259	1.492	4.00
9) Kyanite	44.150	0.17626	1.31316	0.00302	1.429	4.00
10) Sillimanite	49.860	0.04305	2.03178	-0.00025	1.539	4.00
11) Wollastonite	39.930	-	-	-	-	-
12) Gehlenite	90.060	0.25500	0.00000	0.00000	-	-
13) Akermanite	92.810	-	-	-	-	-
14) Spinel	39.710	0.18873	0.97736	0.00025	1.957	4.89
15) Hercynite	40.750	0.10038	1.93934	-0.00214	2.089	4.00
16) Forsterite	21.835	0.30520	0.85040	-0.58240	1.279	4.88
17) Fayalite	23.140	0.26600	0.87360	-0.24870	1.366	5.16
18) Monticellite	25.735	0.31100	0.80134	-0.00038	-	-
19) Enstatite	31.276	0.20303	1.28049	0.00100	1.160	4.20
20) Ferrosilite	32.950	0.22160	0.00000	0.00000	1.010	4.20
21) Orthodiopside	33.499	0.20303	1.28049	0.00100	1.080	4.20
22) Orthohedenbergite	34.61	0.18314	1.41273	0.00110	-	4.20
23) Al_2O_3-opx	26.780	0.20303	1.28049	0.00100	1.160	4.20
24) Clinoenstatite	31.453	0.20303	1.28049	0.00100	1.100	4.20
25) Clinoferrosilite	33.14	0.22160	0.00000	0.00000	1.000	4.20
26) Diopside	33.050	0.18314	1.41273	0.00110	1.000	4.20
27) Hedenbergite	34.130	0.18314	1.41273	0.00110	-	4.20
28) Al_2O_3-cpx	26.200	0.20303	1.28049	0.00100	1.160	4.20
29) Ca-Tschermak	63.560	0.24700	0.00000	0.00000	1.200	4.20
30) Jadeite	30.200	0.13096	2.23308	0.17442	1.333	4.20
31) Pyrope	37.760	0.22581	0.63182	-0.37841	1.754	4.80
32) Almandine	38.428	0.17378	1.24429	-0.45243	1.750	5.60
33) Grossular	41.770	0.18992	0.80873	-0.42877	1.486	4.30
34) Spessartine	39.387	0.20000	0.00000	0.00000	1.707	5.00
35) Rutile	18.820	-0.55100	2.39200	0.33800	2.112	6.91
36) Ilmenite	31.690	0.47030	0.00000	0.00000	1.786	4.00
37) Anorthite	100.200	0.14462	1.00454	-0.00299	0.909	4.00
38) Albite	100.430	0.20467	1.21847	-0.68600	0.500	4.00
39) Sanidine	109.050	0.23752	1.35680	-2.83695	0.550	4.00
40) Muscovite	140.820	0.56337	1.94990	-0.99049	0.830	4.00
41) Paragonite	131.880	0.12179	1.19080	-0.05094	0.830	4.10
42) Phlogopite	149.660	-	-	-	0.430	4.00
43) Annite	154.320	-	-	-	0.430	4.00
44) Brucite	24.630	0.10020	1.46810	1.86060	0.572	4.70
45) Chrysotile	108.500	0.00000	1.00540	-1.90900	0.585	4.57
46) Antigorite	1749.130	0.31243	2.12040	0.45093	0.254	3.70
47) Talc	136.250	0.03129	3.64800	0.04418	0.532	3.27
48) Anthophyllite	265.440	0.39859	1.79690	-2.37670	0.338	5.00
49) Grunerite	278.730	-	-	-	-	-

50) Cordierite	233.220	-	-	-	-	-
51) Ferrocordierite	234.42	-	-	-	-	-
52) Hydrous cordierite	223.98	1.5278	-	-	-	-

$$\alpha(T) = \alpha_0 + \alpha_1 T + \alpha_2 T^{-2}$$

For chemical formula, please refer to Table 3.2.

Sources of data

Molar volumes:

Robie et al. (1978): Calcium Oxide, Ferrous oxide, Periclase, Corundum, α-Quartz, Rutile, Ilmenite, Wollastonite, Spinel, Hercynite, Akermanite, Forsterite, Fayalite, Monticellite, Enstatite, Ferrosilite, Orthodiopside, Clinoenstatite, Diopside, Jadeite, Pyrope, Albite, Sanidine, Phlogopite, Brucite, Talc, Chrysotile, Cordierite

Robie et al. (1978) and Carmichael (1982): β-Quartz

Robie & Hemingway (1984b): Andalusite, Kyanite, Sillimanite

Charlu et al. (1981): Gehlenite

Syono et al. (1971): Clinoferrosilite

Saxena et al. (1986): Orthohedenbergite, Hedenbergite

Saxena & Chatterjee (1986): Al_2O_3-opx, Al_2O_3-cpx

Gasparik (1981): Ca-Tschermak

Skinner (1956): Almandine

Newton et al. (1977): Grossular

Bokreta (1989): Spessartine

Czank & Schultz (1971): Anorthite

Flux & Chatterjee (1986): Muscovite, Paragonite

Robie & Bethke (1963): Annite

Kunze (1961): Antigorite

Chernosky et al. (1985): Anthophyllite

Klein & Waldbaum (1967): Grunerite

This study: Ferrocordierite

This study and Bhattacharya and Sen (1985): Hydrous cordierite

Thermal expansion coefficients:

Saxena & Eriksson (1983a): Corundum, Andalusite, Kyanite, Sillimanite, Rutile, Spinel, Hercynite, Monticellite, Enstatite, Ferrosilite, Orthodiopside, Orthohedenbergite, Al_2O_3-opx, Clinoenstatite, Diopside, Hedenbergite, Al_2O_3-cpx, Anorthite

Fei & Saxena (1987): Periclase

Skinner (1966): α-Quartz, Gehlenite, Clinoferrosilite, Jadeite, Albite, Sanidine

Carmichael (1982): β-Quartz, Spessartine

Suzuki (1975): Forsterite

Suzuki et al. (1981): Fayalite

Haselton et al. (1984): Ca-Tschermak

Skinner (1956): Pyrope, Almandine, Grossular

This study: Muscovite, Paragonite, Ilmenite

Fei & Chatterjee (1988): Brucite, Chrysotile, Antigorite, Talc, Anthophyllite

This study and Bhattacharya and Sen (1985): Hydrous cordierite

Isothermal bulk modulus:

Saxena & Eriksson (1983a): Orthodiopside, Al_2O_3-opx, Clinoenstatite,

Diopside, Al_2O_3-cpx, Ca-Tschermak, Grossular

Fei & Saxena (1987): Periclase
Hankey & Schuele (1970): Corundum
Soga (1968): α-Quartz
Carmichael (1982): β-Quartz, Spessartine
Brace et al. (1969): Andalusite, Kyanite, Sillimanite
Wang & Simmons (1972): Spinel, Hercynite
Sumino et al. (1977): Forsterite
Sumino (1979): Fayalite
Liebermann (1974): Enstatite
Bass & Weidner (1984): Ferrosilite
Akimoto (1972): Clinoferrosilite
Birch (1966): Jadeite, Almandine, Albite, Sanidine, Muscovite, Phlogopite
Leitner et al. (1980): Pyrope
Grimsditch & Ramdas (1976): Rutile
Liebermann & Ringwood (1976): Anorthite
This study: Paragonite, Annite, Ilmenite
Fei & Chatterjee (1988): Brucite, Chrysotile, Antigorite, Talc, Anthophyllite

Pressure derivative of isothermal bulk modulus:
Fei & Saxena (1987): Periclase
Hankey & Schuele (1970): Corundum
Soga (1968): α-Quartz (value for β-Quartz assumed to be the same)
Chang & Barsch (1973): Spinel
Sumino et al. (1977): Fayalite
Weidner (1986): Enstatite, Ferrosilite
Bonzcar et al. (1977): Pyrope ($Pyr_{61}Alm_{36}Gr_2$)
Soga (1967): Almandine ($Alm_{75}Pyr_{20}Spess_3Gr_3$)
Halleck (1973): Grossular ($Gr_{98}Alm_1Spess_1$)
Fritz (1974): Rutile
Fei & Chatterjee (1988): Brucite, Chrysotile, Antigorite, Talc, Anthophyllite

Sources of K'_0 values not in the above list are the same as for bulk modulus. K'_0 values of phases not available are assigned an average value of 4.0 (4.2 for pyroxenes and 5.0 for spessartine).

TABLE 3.4. RECOMMENDED INTERACTION PARAMETERS FOR SOLUTIONS (J/mol)

MELILITE

Gehlenite-Akermanite $Ca_2Al_2SiO_7$-$Ca_2MgSi_2O_7$

W_{12} = 24288.1

W_{21} = 502.1

Charlu et al. (1981) (calorimetric determination)

SPINEL

Spinel-Hercynite $MgAl_2O_4$-$FeAl_2O_4$

W_{12} = 9124.0

W_{21} = 0.0

Chatterjee (1987) (evaluated from Engi, 1983 and valid in range 923-1176 K and XMg(Sp)=0.4-0.9)

OLIVINE

Forsterite-Fayalite $1/2(Mg_2SiO_4$-$Fe_2SiO_4)$

W = 4500.0

Chatterjee (1987) (evaluated from Bohlen & Boettcher, 1981)

Forsterite-Monticellite $1/2(Mg_2SiO_4$-$CaMgSiO_4)$

W_{12} = 21550.0 - 3.005xT

W_{21} = 30600.0 - 7.6xT

Adams & Bishop (1985) (phase equilibrium experiment)

Fayalite-Monticellite $1/2(Fe_2SiO_4$-$CaMgSiO_4)$

W = 7716.5

estimated

ORTHOPYROXENE

Enstatite-Ferrosilite $MgSiO_3$-$FeSiO_3$

W_{12} = 13100.0 - 15.0xT (T <= 873 K)

= 0.0 (> 873 K)

W_{21} = 3370.0 - 5.0xT (T <= 673 K)

= 0.0 (> 673 K)

Saxena et al. (1986) (when nonideal) and Chatterjee (1987) (when ideal : approximately equal to the calorimetric values of Chatillon-Colinet et al., 1983b)

Enstatite-Orthodiopside $MgSiO_3$-$1/2(CaMgSi_2O_6)$

W = 25000.0

Lindsley et al. (1981) (evaluated from phase equilibria)

Enstatite-Orthohedenbergite $MgSiO_3$-1/2($CaFeSi_2O_6$)

W_{12} = 60000.0

W_{21} = 30000.0 - 8.34xT

Saxena et al. (1986) (evaluated from Lindsley, 1983)

Enstatite-Al_2O_3-opx $MgSiO_3$-Al_2O_3

W = 0.0

Saxena & Chatterjee (1986) (assumed)

Ferrosilite-Orthodiopside $FeSiO_3$-1/2($CaMgSi_2O_6$)

W_{12} = 16000.0

W_{21} = 20000.0

Saxena et al. (1986) (evaluated from Lindsley, 1983)

Ferrosilite-Orthohedenbergite $FeSiO_3$-1/2($CaFeSi_2O_6$)

W = 15000.0

Saxena et al. (1986) (evaluated from Lindsley, 1983)

Ferrosilite-Al_2O_3-opx $FeSiO_3$-Al_2O_3

W = 0.0

(assumed)

Orthodiopside-Orthohedenbergite 1/2($CaMgSi_2O_6$-$CaFeSi_2O_6$)

W_{12} = 5000.0

W_{21} = 7000.0

Saxena et al. (1986) (evaluated from Lindsley, 1983)

Orthodiopside-Al_2O_3-opx 1/2($CaMgSi_2O_6$)-Al_2O_3

W = 30000.0

Saxena & Chatterjee (1986) (evaluated from phase equilibria)

Orthohedenbergite-Al_2O_3-opx 1/2($CaFeSi_2O_6$)-Al_2O_3

W = 30000.0

same as Orthodiopside-Al_2O_3-opx

CLINOPYROXENE

Clinoenstatite-Clinoferrosilite $MgSiO_3$-$FeSiO_3$

W = 0.0

Saxena et al. (1986) (evaluated from Lindsley, 1983)

Clinoenstatite-Diopside $MgSiO_3$-1/2($CaMgSi_2O_6$)

W_{12} = 25484.0 + 0.0812xP

W_{21} = 31216.0 - 0.0061xP

Lindsley et al. (1981) (evaluated from phase equilibria)

Clinoenstatite-Hedenbergite $MgSiO_3$-1/2($CaFeSi_2O_6$)

W_{12} = 93300.0 - 45.0xT

W_{21} = -20000.0 + 28.0xT

Saxena et al. (1986) (evaluated from Lindsley, 1983)

Clinoenstatite-Al_2O_3-cpx $MgSiO_3$-Al_2O_3

W = 0.0

Saxena & Chatterjee (1986) (assumed)

Clinoenstatite-Jadeite $MgSiO_3$-1/2($NaAlSi_2O_6$)

W = 30000.0

estimated from Windom & Boettcher (1981)

Clinoferrosilite-Diopside $FeSiO_3$-1/2($CaMgSi_2O_6$)

W_{12} = 15000.0

W_{21} = 24000.0

Saxena et al. (1986) (evaluated from Lindsley, 1983)

Clinoferrosilite-Hedenbergite $FeSiO_3$-1/2($CaFeSi_2O_6$)

W_{12} = 16941.0 + 0.00592xP

W_{21} = 20697.0 - 0.00235xP

Saxena et al. (1986) (evaluated from Lindsley, 1983)

Clinoferrosilite-Al_2O_3-cpx $FeSiO_3$-Al_2O_3

W = 0.0

(assumed)

Clinoferrosilite-Jadeite $FeSiO_3$-1/2($NaAlSi_2O_6$)

W = 30000.0

same as Clinoenstatite-Jadeite

Diopside-Hedenbergite 1/2($CaMgSi_2O_6$-$CaFeSi_2O_6$)

W = 12000.0

Saxena et al. (1986) (evaluated from Lindsley, 1983)

Diopside-Al_2O_3-cpx 1/2($CaMgSi_2O_6$)-Al_2O_3

W = 10000.0

Saxena & Chatterjee (1986) (evaluated from phase equilibria)

Diopside-Jadeite 1/2($CaMgSi_2O_6$-$NaAlSi_2O_6$)

A = 6300 - 4.725xT

B = 6300 - 3.8xT

C = -10700 + 8.1xT

Gasparik (1985) (phase equilibrium experiment)

Hedenbergite-Al_2O_3-cpx 1/2($CaFeSi_2O_6$)-Al_2O_3

W = 10000.0

same as Diopside-Al_2O_3-cpx

Hedenbergite-Jadeite $1/2(CaFeSi_2O_6\text{-}NaAlSi_2O_6)$

A = 6300 - 4.725xT
B = 6300 - 3.8xT
C = -10700 + 8.1xT
same as Diopside-Jadeite

Al_2O_3-cpx-Jadeite $Al_2O_3\text{-}1/2(NaAlSi_2O_6)$

W = 0.0
(assumed)

GARNET

Pyrope-Almandine $1/3(Mg_3Al_2Si_3O_{12}\text{-}Fe_3Al_2Si_3O_{12})$

W_{12} = 12050.0 - (11.76 - 0.0016xT)xT + 0.02xP
W_{21} = -5258.0 - (-10.146 + 0.0037xT)xT - 0.003xP
Newton et al. (1986) (WH: calorimetric and WV: unit cell measurement), Chatterjee (1987) (WS: evaluated)

Pyrope-Grossular $1/3(Mg_3Al_2Si_3O_{12}\text{-}Ca_3Al_2Si_3O_{12})$

W_{12} = 4184.0 - 15.61xT + 0.1xP
W_{21} = 16932.0
Ganguly & Saxena (1984) (WH: evaluated), Newton et al. (1986) (WS: evaluated, WV: unit cell measurement)

Pyrope-Spessartine $1/3(Mg_3Al_2Si_3O_{12}\text{-}Mn_3Al_2Si_3O_{12})$

W_{12} = 12050.0 - (11.76 - 0.0016xT)xT + 0.02xP
W_{21} = -5258.0 - (-10.146 + 0.0037xT)xT - 0.003xP
Same as Pyrope-Almandine

Almandine-Grossular $1/3(Fe_3Al_2Si_3O_{12}\text{-}Ca_3Al_2Si_3O_{12})$

W_{12} = 4560.0 - (-16.07 + 0.0126xT)xT + 0.1xP
W_{21} = -3026.4 - (-16.07 + 0.0126xT)xT
Newton et al. (1986) (WH: calorimetric, WV: unit cell measurement), Chatterjee (1987) (WS: evaluated and valid in range 1023-1323 K and XCa(Gar) = 0.33)

Almandine-Spessartine $1/3(Fe_3Al_2Si_3O_{12}\text{-}Mn_3Al_2Si_3O_{12})$

W = 0.0
(assumed)

Grossular-Spessartine $1/3(Ca_3Al_2Si_3O_{12}\text{-}Mn_3Al_2Si_3O_{12})$

W_{12} = -3026.4 - (-16.07 + 0.0126xT)xT
W_{21} = 4560.0 - (-16.07 + 0.0126xT)xT + 0.1xP
Same as Grossular-Almandine

MUSCOVITE

Muscovite-Paragonite* $KAl_2AlSi_3O_{10}(OH)_2$-$NaAl_2AlSi_3O_{10}(OH)_2$

$A = 11222 + 1.389xT + 0.2359xP$
$B = -1134 + 6.806xT - 0.0840xP$
$C = -7305 + 9.043xT$
Flux & Chatterjee (1986) (calorimetric determination)

BIOTITE

Phlogopite-Annite $KMg_3AlSi_3O_{10}(OH)_2$-$KFe_3AlSi_3O_{10}(OH)_2$

$W_{12} = 5540.7$
$W_{21} = 5068.5$
This study (evaluated from experimental data of Perchuk & Lavrent'eva, 1983)

CORDIERITE

Cordierite-Ferrocordierite $Mg_2Al_4Si_5O_{18}$-$Fe_2Al_4Si_5O_{18}$

$W = 1830.6$
This study (evaluated from experimental data referred in Perchuk & Lavrent'eva, 1983)

Cordierite-Hydrous cordierite $Mg_2Al_4Si_5O_{18}$-$Mg_2Al_4Si_5O_{18}.H_2O$

$W = 0.0$
(assumed)

Ferrocordierite-Hydrous cordierite $Fe_2Al_4Si_5O_{18}$-$Mg_2Al_4Si_5O_{18}.H_2O$

$W = 1830.6$
same as Cordierite-Ferrocordierite

FELDSPAR

Anorthite-Albite $CaAl_2Si_2O_8$-$NaAlSi_3O_8$

$W_{12} = 11221.5 - 7.891xT$
$W_{21} = 14129.4 - 6.18xT$
Nekvasil (1986) (evaluated)

Anorthite-Sanidine $CaAl_2Si_2O_8$-$KAlSi_3O_8$

$W_{12} = 25020.3 + 10.795xT$
$W_{21} = 75023.3 - 23xT$
Nekvasil (1986) (evaluated)

Albite-Sanidine $NaAlSi_3O_8$-$KAlSi_3O_8$

$W_{12} = 30978.3 - 21.422xT$
$W_{21} = 17062.35$
Nekvasil (1986) (evaluated)

Unless otherwise stated the excess free energy is given by:

$G^{ex} = (1-X)\ X\ [W_{12}X + W_{21}(1-X)]$

where, X is the mole-fraction of the second end-member.

* $G^{ex} = (1-X)\ X\ [A + B(1-2X) + C(1-2X)^2]$

where, X is the mole-fraction of the first end-member.

III. MANAGEMENT OF THE DATA BASE

A summary of the data base is given in Tables 3.2, 3.3 and 3.4. The thermodynamic properties of the pure phases and the end-members of solid solutions are stored in a file called MASTER. Table 3.5, which shows an entry for the mineral α-quartz, shows the format in which the values are printed when the inspection part of the program RETR (described below) is run. In addition to the thermodynamic data itself, the uncertainties and the references for the data are also stored. The entire data base is more extensive and contains data on many other elements and compounds. The properties of the solid solutions are stored in another file called SOLNMAS. The interaction parameters in both the Margules and the Redlich-Kister form for each binary solution, which in many cases is a part of a multicomponent solid solution, are stored in this file.

In order to inspect and retrieve data only on the relevant phases to be used in a certain calculation, the program RETR is used. The program is written in FORTRAN and serves two major purposes.

The first part of the program serves to inspect data on any of the phases present in the data base. If desired, a list of the available phases can be seen on the screen. In order to inspect the data the name of the phase is entered. The data can be inspected at standard conditions (298 K and 1 bar) or at any other conditions of pressure and temperature. The subroutine INSP serves this purpose. It is called by the main program RETR. Two other subroutines, REED and WRIT, are called

by the subroutine INSP. Data on a phase are read through REED and is printed through WRIT.

The solution properties of a particular binary solution can also be inspected through this procedure. Table 3.6 shows an example of an output when data on a solution are inspected.

The second part of the program is used to retrieve data on the phases necessary in the calculation. The subroutine SYST is used to prepare a file, to be used with programs SOLGASMIX and REAC (described in Chapter 6), containing thermodynamic properties of the desired phases. The user is instructed to define a system using elements in which he wants to do his calculation. For example, in a calculation involving enstatite, ferrosilite, forsterite and fayalite, the system will be defined as Mg-Fe-Si-O. A list of all phases available in the system is seen on the screen. The user then selects from this list the relevant phases. The data are then written on a file in a form acceptable to the applications programs. An example of a data file created in this way is shown in Table 3.7. The program also has a provision to create a data file in a different format, which includes the free energy expression instead of the enthalpy, entropy and heat capacity and the interaction parameters of the solution phases. A visual inspection of the solution properties can also be made at the same time. This format of the data file is not used in this study. The subroutine SYST is called by the main program.Subroutine REED is again used in SYST to read data from the data base.

TABLE 3.5. Output from program RETR using subroutine INSP. It shows the thermodynamic properties of α-quartz as stored in file MASTER

```
--------------------------------------------------------------------------
SIO2
A-QUARTZ                    Formula wt. (gm) =    60.09
--------------------------------------------------------------------------

Enthalpy (J/mol)  =    -910700.000          +-1000.0  Robie et al. (1978)

Entropy (J/mol.K) =         41.460          +-0.2     Robie et al. (1978)

Heat Capacity (a,bT,cT-2,dT2,eT-3,fT-.5,gT-1):
No. of Cp ranges  =  2     Robie (298-848K), Chatterjee (1989) (848-1673K)
  1.0149000E+02  2.7820E-03  4.3530E+06  0.0000E+00
 -1.9130E+08  0.0000E+00 -2.9610E+04
Temp. and enthalpy of transition:
     848.00                0.00
  6.2684000E+01  2.1039E-02 -2.5826E+06  0.0000E+00
  5.2920E+09  0.0000E+00 -4.8031E+03

Volume  (cc/mol)  =         22.688          Robie et al. (1978)

Thermal expn. (a0*1E4,a1*1E8,a2):
   0.31000    2.67800    0.00000   Skinner (1966)

Isot. bulk mod. (Mbar), P deriv., T deriv.(Kbar/K):
   0.37400    6.40000       -      Soga (1968)

Melting pt.  and enthalpy of melting:
      -          -

NOTE:
     All the values were determined through calorimetry except the heat
capacity expression of a-quartz above 848 K and the enthalpy and entropy
of b-quartz, which are determined through optimization of the phase
equilibrium data on the transformation:
                              a-quartz  =  b-quartz
The experimental data on this transformation are from Fenner (1913),
Cohen and Klement (1967) and Mirwald and Massonne (1980).
```

The heat capacity constants, as indicated by the entry within parentheses, are related as follows:

$$C_p(T) = a + bT + cT^{-2} + dT^{2} + eT^{-3} + fT^{-0.5} + gT^{-1}$$

The thermal expansion coefficients are related as follows:

$$\alpha(T) = \alpha_0 x1E4 + \alpha_1 x1E8\ T + \alpha_2\ T^{-2}$$

Other abbreviations are as follows:

Isot. bulk mod.: Isothermal bulk modulus
P deriv.: Pressure derivative
T deriv.: Temperature derivative

TABLE 3.6. Output from program RETR using subroutine INSP.
It shows the solution properties of the pyrope-almandine solution.

Interaction parameters of the selected binary (J/mol)

GARNET
Pyrope-Almandine 1/3(Mg3Al2Si3O12-Fe3Al2Si3O12)

	H	S	V
Margules constants:			
W12	12050.0	11.76-.0016*T	0.02
W21	-5258.0	-10.146+.0037*T	-0.003
Redlich-Kister constants:			
A0	3396.0	.807-.00105*T	0.0085
A1	-8654.0	-10.953+.00265*T	-0.0115

REF.: WH and WV, Newton et al. (1986); WS, Chatterjee (1987)
NOTE: WH: calorimetric, WV: unit cell measurement, WS: evaluated

The interaction parameter, W, is given by:

$$W = W^H - TW^S + PW^V$$

Thus in the above table, $W_{Mg\text{-}Fe}$ of the pyrope-almandine solution is given by:

$$W_{12} = (12050.0) - T\,(11.76\text{-}0.0016xT) + P\,(0.02)$$

In the third line, H, S and V represent W^H, W^S and W^V respectively.

TABLE 3.6. Example of a data file created through program RETR using subroutine SYST

```
SYSTEM Fe-Mg-Si-O
15    1    0    4
'FORSTERITE '       0.500    0.000    0.000    0.000    0.000    1.000    0.000
    0.000    0.000    0.000    2.000    0.000    0.000    0.000    0.000
'FAYALITE   '       0.500    0.000    0.000    0.000    1.000    0.000    0.000
    0.000    0.000    0.000    2.000    0.000    0.000    0.000    0.000
'ORTHOENSTA '       1.000    0.000    0.000    0.000    0.000    1.000    0.000
    0.000    0.000    0.000    3.000    0.000    0.000    0.000    0.000
'ORTHOFERRO '       1.000    0.000    0.000    0.000    1.000    0.000    0.000
    0.000    0.000    0.000    3.000    0.000    0.000    0.000    0.000
-3
 21.835    0.30520    0.85040   -0.58240    1.27930    4.88000
 23.140    0.26600    0.87360   -0.24870    1.36570    5.16000
 31.276    0.20303    1.28049    0.00100    1.16000    4.20000
 32.950    0.23326   -0.10413   -0.00059    1.01000    4.20000
1173
-1087180.00    47.060    1
   9.6731000E+01   1.278000E-03   1.890000E+06   0.000000E+00
 -4.312000E+08   0.000000E+00  -1.309000E+04
 -739085.00    75.500    1
   1.0957000E+02   1.852000E-03   2.963000E+06   0.000000E+00
 -1.862000E+08   0.000000E+00  -2.001000E+04
-1546290.00    66.270    1
   1.4445000E+02   1.882000E-03  -1.350000E+06   0.000000E+00
  4.612000E+08   0.000000E+00  -1.938000E+04
-1195200.00    94.560    1
   1.3189000E+02   6.214000E-05  -4.947000E+06   0.000000E+00
  1.425000E+07   0.000000E+00   2.319000E+02
  2   1   2
  7
 20000.00
  2
  1
  2   2
 10.000
 10.000
  10
```

The first line is the title indicating that the phases contained in this file made out of the elements Fe, Mg, Si and O. The second line contains four numbers indicating the number of elements the phases are composed of, number of solutions in the list, number of end-members in the first solution and the number of pure phases in the list. The next segment of the file contains names of the phases and the number of atoms of elements contained in the chemical formula of each phase. Since the phases are made out of only four elements, all but four columns in the composition matrix have zero as their elements. The first, sixth, seventh and eleventh columns give the number Si, Fe, Mg and O atoms in the chemical formula of each phase. The number -3 is an instuction for the applications program. The next four lines contain the molar volume, the thermal expansion coefficients α_0x1E4, α_1x1E8, α_2,

the bulk modulus and the pressure derivative of the bulk modulus of each phase in the same order. The number 1173, which is changeable is the temperature in K for the calculation. The next section gives the thermochemical data for each phase in the same order in groups of three lines. The numbers in a group of three lines are the enthalpy, entropy, number of heat capacity expressions (in the first line) and the seven constants (a, b, c, d, e, f and g) of the heat capacity expression (in the last two lines). The last nine lines are numbered instructions identifiable by the applications program. For phases with transitions (not in this example) there will be three additional lines to the original three giving the temperature and enthalpy of transition and the seven constants for the second heat capacity expression valid above the transition temperature.

CHAPTER 4

COMPARISON WITH OTHER STUDIES

In 1978, Helgeson et al. published an extensive set of thermodynamic data that reproduced all experimentally determined phase equilibria at that time. In the subsequent period of ten years, many more experiments have been done and the data set of Helgeson et al. can not reproduce many of them. One of the purposes of this study is to create a data base that would reproduce all experimental equilibria observed to date. Many researchers have attempted to create such a data base. However, most of them worked on small chemical systems. Recently, Berman (1988) has published an extensive data base which includes important igneous and metamorphic minerals. It should be noted, however, that neither Helgeson et al. nor Berman attempted to systematize the properties of solid solutions. In this study, the thermodynamic properties are not only consistent among the pure and end-member phases, but they are also consistent with the different solution properties.

In the first part of this chapter, a comparison is given of phase equilibria in particular systems calculated from the data presented in this study and those calculated from purely calorimetric data or from some other data base. The fit of the experimental data with the phase diagrams calculated from this study is discussed in Chapter 3. In this chapter, the experimental data are not shown separately, but it is clear from Chapter 3 that the equilibria calculated from this study represent the best fit of the experiments. As will be seen, in most cases the

unsystematized calorimetric data do not reproduce the equilibrium data. This further corroborates the importance of this study.

In the second and third parts of this chapter, details of how the data in this study and data from other sources compare are given.

I. Comparison of phase equilibria

The $CaO-Al_2O_3-SiO_2$ system

In Figure 4.1, calculated equilibria for reactions (3.c), (3.d), (3.e), (3.i) and (3.k) are shown. The curves shown in dotted lines are calculated directly from the data quoted in Robie et al. (1978). Except for reactions 1 and 2, the curves calculated using the two data sets are very inconsistent. This is specially true for the reactions involving corundum. Gehlenite, anorthite and Ca-Tschermak all show progressive disorder with increasing temperature. The systematized data presented here may be assumed to include an excess energy associated with factors such as disorder.

The $MgO-SiO_2-H_2O$ system

In this system, equilibrium curves for seven reactions (3.cc) through (3.ii) calculated using the data in this study are shown in Figure 3.8 through 3.10. Curves calculated using the calorimetric data of Krupka et al. (1985a,b) and Robie et al. (1978) lie far outside the pressure and temperature ranges of the diagrams.

The $Na_2O-Al_2O_3-SiO_2-H_2O$ system

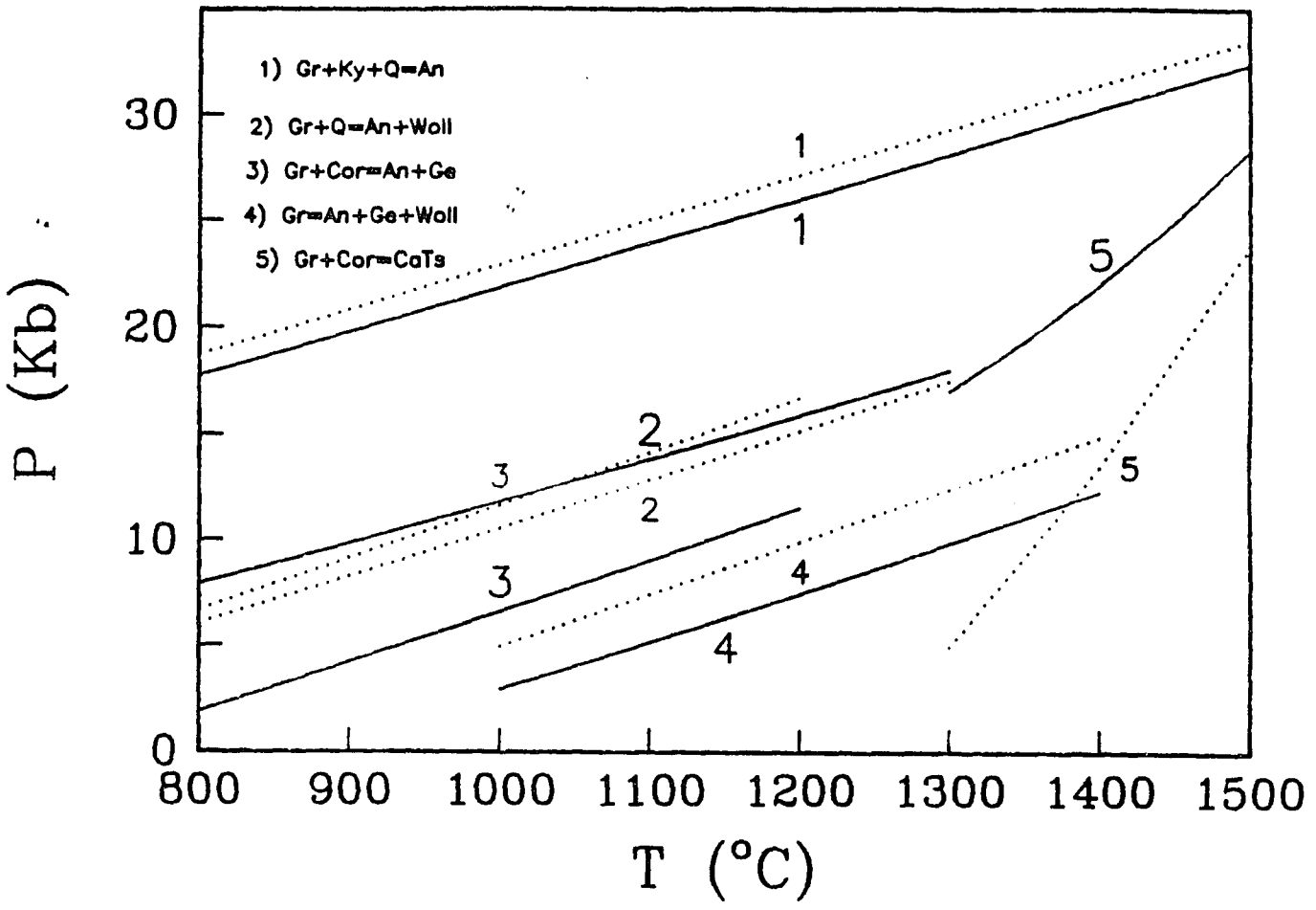

Figure 4.1: Calculated equilibria in the CaO-Al_2O_3-SiO_2 system for the following reactions:

1) Gr + Ky + Q = An
2) Gr + Q = An + Woll
3) Gr + Cor = An + Ge
4) Gr = An + Ge + Woll
5) Gr + Cor = CaTs

The dotted curves are calculated using thermochemical data from calorimetric sources (Robie et al., 1978).

In Figure 4.2, calculated equilibria for reactions (3.v), (3.w), (3.x) (for kyanite and andalusite) and (3.y) are shown. are shown. The curves shown in dotted lines are calculated directly from the data quoted in Robie et al. (1978) and Robie and Hemingway (1984a). The dotted lines show considerable inconsistency with the experimental data which are consistent with the calculated curves shown by solid lines. Paragonite is known to disorder with increasing temperature. Again, the systematized data here are considered to include energies associated with factors such as disorder.

The K_2O-Al_2O_3-SiO_2-H_2O system

Figure 4.3 shows calculated boundaries for reactions (3.t) and (3.u) (for andalusite and sillimanite). The curves in dotted lines are calculated from the calorimetric data of Hemingway et al. (1981), Robie and Hemingway (1984a) and in Robie et al. (1978). The discrepancies are removed by adding a disorder term in the entropy of sanidine.

II. Comparison of pure-phase properties with calorimetric data and data from other sources

In Table 4.1, a comparison between the calorimetric values and the values presented in this study of enthalpy and entropy of selected phases is given. Figures 4.4 and 4.5 show the differences in enthalpies and entropies respectively in this study from their calorimetric mean values. The sources of the calorimetric values are given at the end of the table. Details for each mineral is given below. Minerals whose

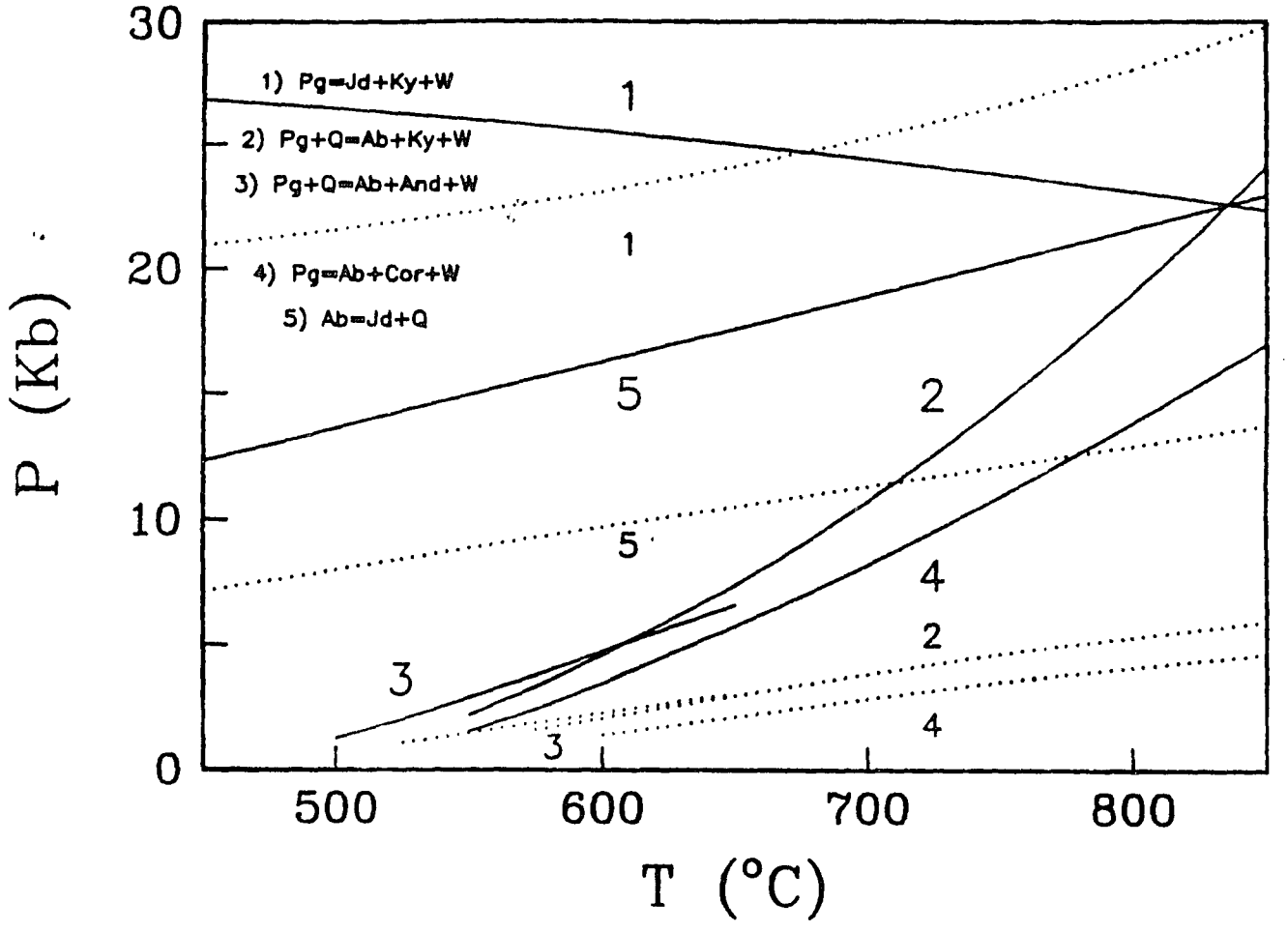

Figure 4.2: Calculated equilibria in the Na_2O-Al_2O_3-SiO_2-H_2O system for the following reactions:

1) $Pg = Jd + Ky + H_2O$ 2) $Pg + Q = Ab + Ky + H_2O$

3) $Pg + Q = Ab + And + H_2O$ 4) $Pg = Ab + Cor + H_2O$

5) $Ab = Jd + Q$

The dotted curves are calculated using thermochemical data from calorimetric sources (Robie et al., 1978 and Robie and Hemingway, 1984a).

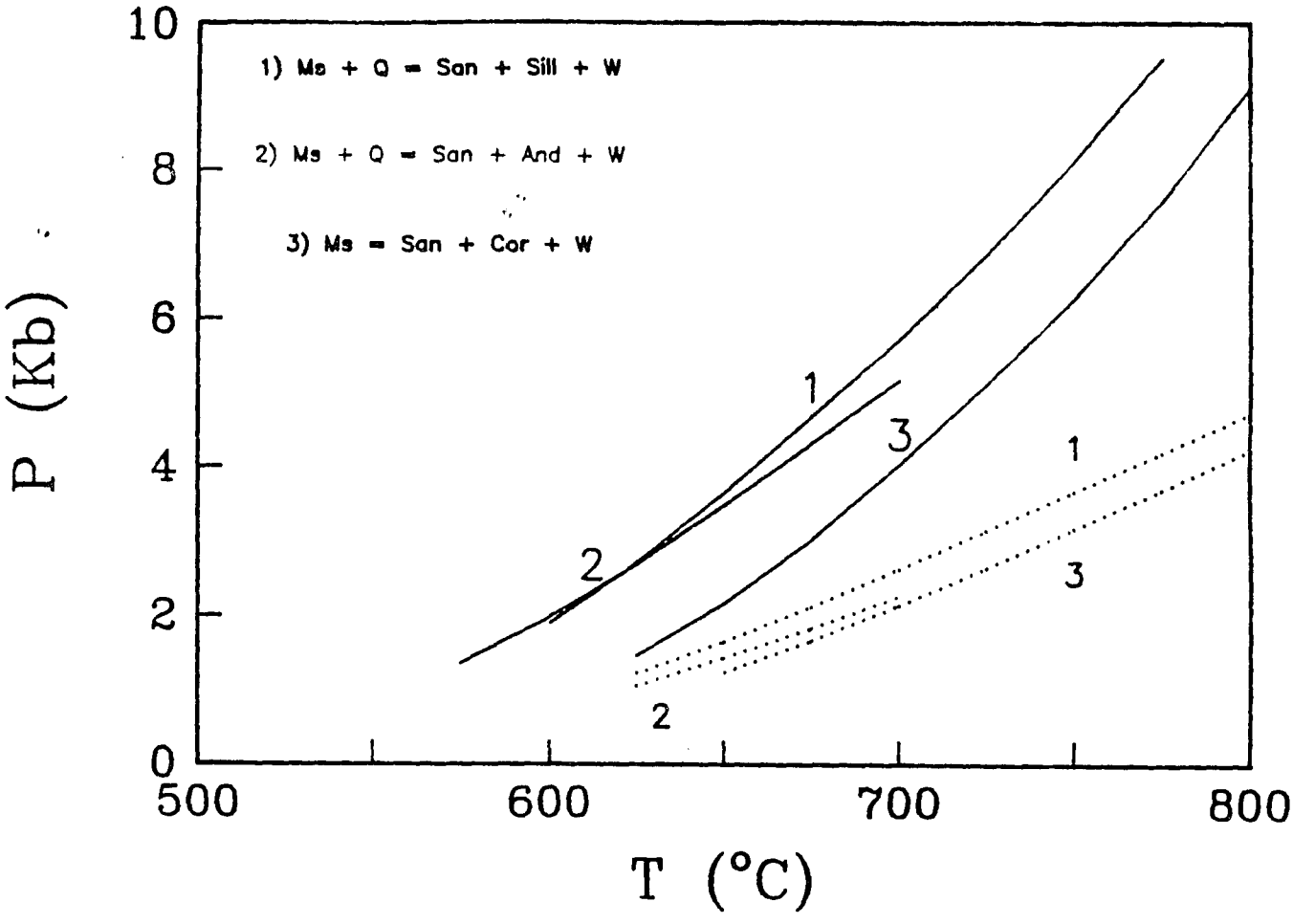

Figure 4.3: Calculated equilibria in the K_2O-Al_2O_3-SiO_2-H_2O system for the following reactions:
1) Ms + Q = San + Sill + H_2O 2) Ms + Q = San + And + H_2O
3) Ms = San + Cor + H_2O
The dotted curves are calculated using thermochemical data from calorimetric sources (Robie et al., 1978; Hemingway et al., 1981 and Robie and Hemingway, 1984a).

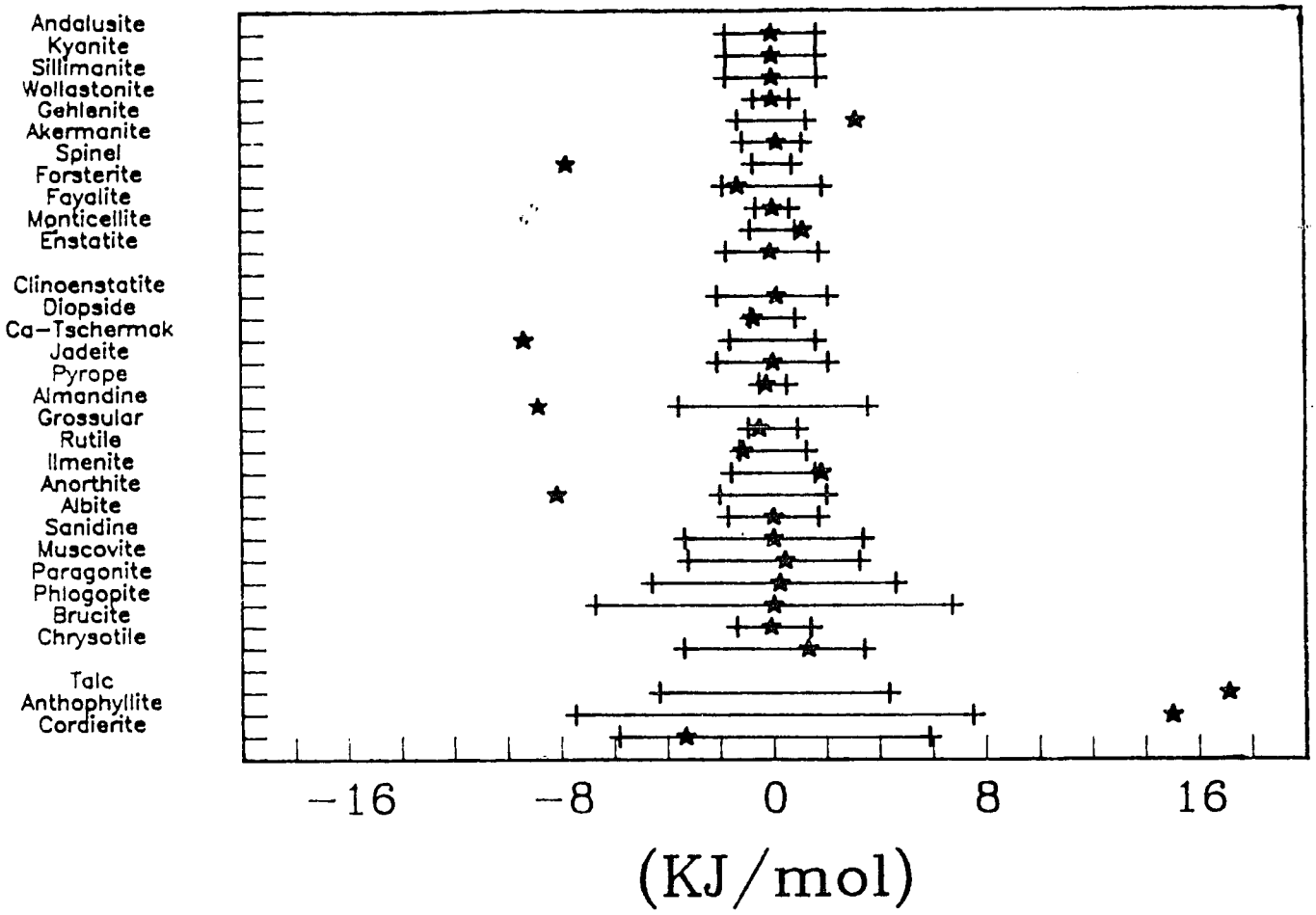

Figure 4.4: Difference between the enthalpies of minerals in this study (stars) and enthalpies from calorimetric sources (for references, see footnote of Table 4.1) given by bars. The zero point represents the mid-point of the calorimetric value.

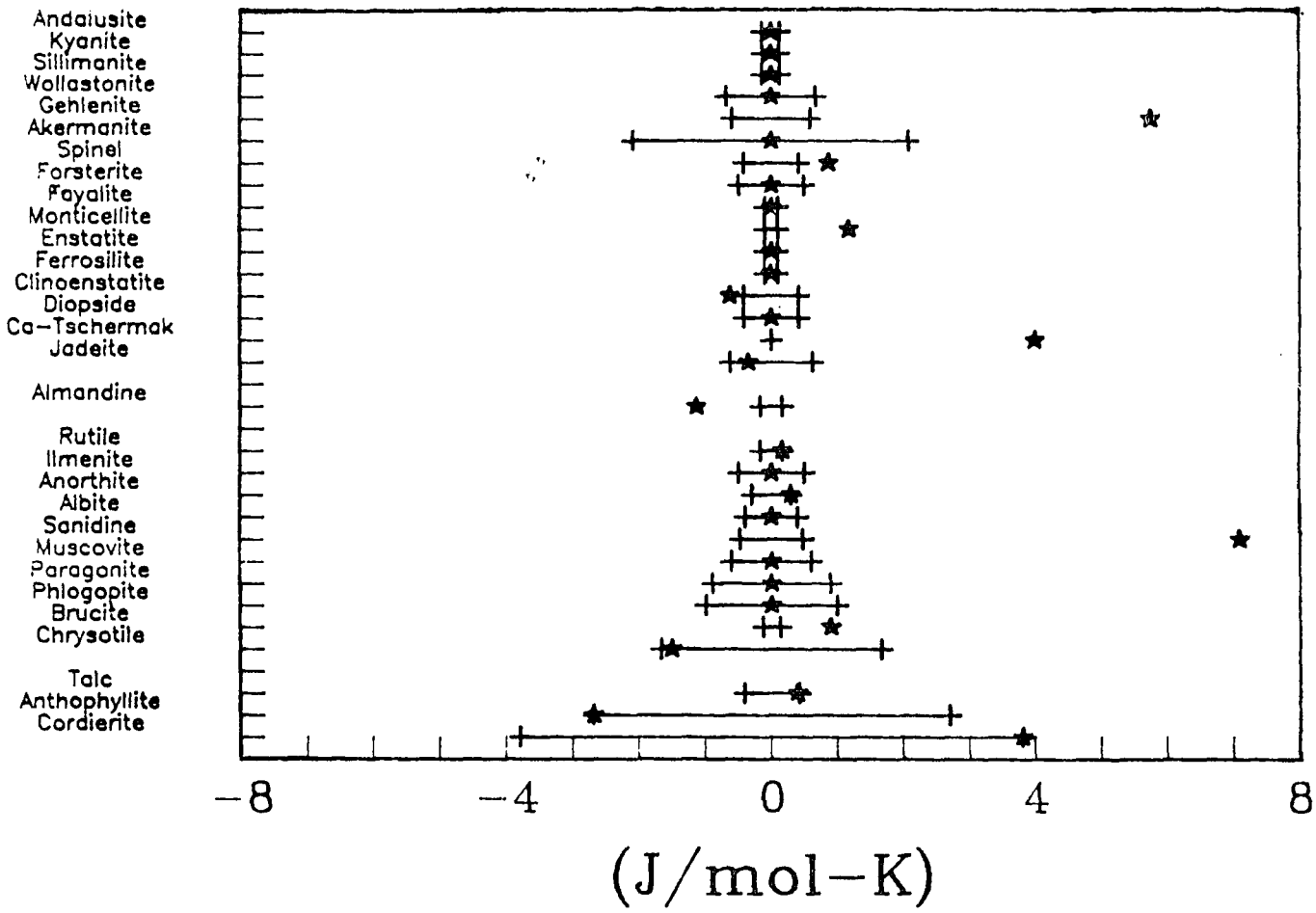

Figure 4.5: Difference between the entropies of minerals in this study (stars) and entropies from calorimetric sources (for references, see footnote of Table 4.1) given by bars. The zero point represents the mid-point of the calorimetric value.

thermochemical properties are unknown or unavailable are not dicussed here.

Corundum: Helgeson et al. (1978) recommend an enthalpy value for corundum different from the value presented in this study. His value was derived from phase equilibrium analysis. In this work, the calorimetric value for the enthalpy is retained. All calculated equilibria involving corundum and other phases are internally consistent and no adjustment in the enthalpy of corundum is necessary.

Quartz: Various workers (e.g., Halbach and Chatterjee, 1984) have tried to adjust the calorimetric data on quartz to fit different phase equilibrium data. In this work no such adjustment is found to be necessary.

Wollastonite: The present values, adopted from Haas et al. (1981), are different from the values in the data bases of Halbach and Chatterjee (1984) (82.13 J/mol-K for entropy) and Berman and Brown (1984) (-1632.17 KJ/mol and 83.53 J/mol-K for enthalpy and entropy respectively). Berman's (1988) value of enthalpy (-1631.5 KJ/mol), which is consistent with the calorimetric value of Kiseleva et al. (1979), is different from this study.

Gehlenite: The present values are different from those of Gasparik (1984b). Gasparik considered a different entropy (210.19 J/mol-K) from

Hemingway and Robie (1984) which does not include the effect of intracrystalline disorder. This choice of entropy by Gasparik is consistent with different values of enthalpy and heat capacity as seen from phase equilibrium analysis. The value of entropy selected here includes disorder (Woodhead, 1977). Also, the heat capacity equation is modified to include energies which are not characterized in this study. Thus it is different from heat capacity recommended by Berman (1988).

Akermanite and Monticellite: The values for akermanite presented here are consistent with the enthalpy of Charlu et al. (1981) and the entropy in Robie et al. (1978) The entropy of akermanite presented by Berman (1988) is different. His value (212 J/mol-K) is consistent with that of Hemingway et al. (1986). The heat capacities of akermanite and monticellite are also different from Berman (1988). The same approach is followed here to modify the heat capacities as in the case of gehlenite.

Spinel: Wood and Holloway's (1984) values on spinel are based on a model dealing with its intracrystalline disorder. Also, their data are consistent with the data on forsterite, pyrope and enstatite different from those recommended in this study. The values recommended in this study are different from those of Wood and Holloway, but the conclusion reached regarding the intercrystalline disorder is similar. Berman (1988) present a different value of entropy of spinel (84.54 J/mol-K) which is very different from the calorimetric value.

Forsterite: Wood and Holloway (1984) recommended a slightly different enthalpy of forsterite. The enthalpy recommended here are within the error limits of Haselton (1979) and Brousse et al. (1984). Also, the values here are related to the distribution data of Mg and Fe between olivine and orthopyroxene and between olivine and garnet (Figures 3.15, 3.16, 3.19 and 3.20). The heat capacity in this study is consistent with both Robie et al. (1982b) and Watanabe (1982), who measured it upto a temperature of 700 K. The heat capacity recommended by Berman (1988) is not consistent with the measurements of Watanabe.

Enstatite: The recommended enthalpy of enstatite, from Brousse et al. (1984), is consistent with the distribution data of Mg and Fe between orthopyroxene and garnet and between orthopyroxene and olivine (Figures 3.15, 3.16, 3.17 and 3.18).

Ferrosilite: The entropy value given by Berman (1988), 95.88 J/mol-K, is different from the value obtained by Bohlen and Boettcher (1981) which is similar to the conclusion in this study. The estimated heat capacity is also quite different from that of Berman (1988).

Diopside: The heat capacity in this study deviates significantly from Berman's (1988) values above 1273 K. This is because Berman derived the heat capacity expression of diopside by considering some very old high temperature measurements (White, 1919 in the range 373-1523 K and Wagner, 1932 in the range 573-1573 K). These data are of poor quality and are not used in this study.

Ca-Tschermak: The values in this study on Ca-Tschermak are different from the calorimetric data of Charlu et al. (1978) and the values in the data bases of Gasparik (1984b) and Wood and Holloway (1984). Details about the values are discussed in Chapter 3. The enthalpy and the entropy lie outside the error limits of calorimetry. Berman (1988), in his analysis, also reached a similar conclusion.

Pyrope and Grossular: Wood and Holloway (1984) and Gasparik (1984b) used slightly adjusted values of enthalpy of these two garnets. In this study the calorimetric data are retained. The enthalpy values recommended by Halbach and Chatterjee (1984) and Berman and Brown (1984) for grossular are quite different (by approximately 2.7 KJ and 1.7 KJ per cation respectively). The heat capacity of grossular given by Berman (1988) disagrees with that recommended in this study which is from Haselton (1979).

Almandine: Bohlen et al. (1986) recommended a different set of values for almandine. They cited the heat capacity equation of Metz et al.. However, they did not attempt to reproduce the distribution data of Mg and Fe between garnet and orthopyroxene and between garnet and olivine. The heat capacity recommended in this study along with data on enthalpy and entropy (closely similar to the calorimetric data) is consistent with the distribution data and the experimental data on reactions (3.o) through (3.s) (Figure 3.3). The enthalpy value given by

Berman (1988) (-1755.17 KJ/mol) is similar to the value presented here. The heat capacity estimated here is different from that of Berman (1988).

Rutile and Ilmenite: Anovitz et al. (1985) systematized the data on phases in the $FeO-TiO_2$ sub-system. Their data set incorporates the heat capacity of ilmenite determined by them and is adopted here. Berman's (1988) heat capacties of ilmenite and rutile differ significantly from the calorimetric values of Anovitz et al. (1985) and Robie et al. (1978). Although the enthalpy and entropy values of Anovitz et al. (1985) are consistent within the sub-system $FeO-TiO_2$, they made no attempt to reproduce reactions (3.r) and (3.s). The present data are consistent with these two reactions (Figure 3.3). Appropriate adjustments should be made in the enthalpy and entropy of the other phases in the $FeO-TiO_2$ sub-system in order to make them consistent with the present data base. The value of enthalpy of ilmenite given by Berman (1988) (-1231.95 KJ/mol) is outside the error limits of the value quoted in Robie et al. (1978).

Anorthite: The enthalpy of anorthite in this study is outside the error limits of the calorimetric value of Charlu et al. (1978). It is calculated from the phase equilibrium relation of reaction (3.k) given by Goldsmith (1980). Goldsmith's experiments are preferred because their results represent an average of all other experiments. There could be a range of values for the enthalpy of anorthite depending upon the experimental data on reaction (3.k) considered (see Gasparik, 1984a;

Wood and Holloway, 1984; Halbach and Chatterjee, 1984 and Berman and Brown, 1984). Wood and Holloway's enthalpy value is closer to the calorimetric value. However, the value recommended here is consistent not only with reaction (3.k), but also with reactions (3.c), (3.d), (3.e), (3.m), (3.n), (3.p) and (3.s).

Albite: As discussed earlier, the values recommended by Hemingway et al. (1981) are preferred over those recommended by Holland (1979) as the former authors derived the data from not only reaction (3.v), but also from the low-albite -> albite transition. The enthalpy value given by Berman (1988) (-3921.62 KJ/mol) is not consistent with the conclusion of Hemingway et al. (1981). Their entropy value (224.41 J/mol-K) also lies outside the errors of calorimetry.

Sanidine: The entropy of sanidine in this study is different from the calorimetric value since a disorder term is added to the original value. This is discussed in Chapter 3. Berman's (1988) entropy value of sanidine is closer to the calorimetric value since they have adopted a different approach to deal with the disorder.

Muscovite: The enthalpy value recommended here is from Robie et al. (1978) with minor adjustment. This is also within the error limits of the value given by Krupka et al. (1979) (-5971.6±5.2 KJ/mol for a disordered muscovite) who adopted a similar approach. The value here is derived using the water fugacity equation of Saxena and Fei (1987a,b) and is optimized along with the thermal expansion of muscovite. The

entropy presented by Berman (1988) (293.16 J/mol-K) is different because they adopted a different approach to deal with the disorder.

Paragonite: The values recommended here are different from those recommended by Holland (1980) who followed a similar approach to derive the data using phase equilibrium relations of reactions (3.w) through (3.y). However, they used different data for albite. In this work, in addition to the free energy data, the thermal expansion and the bulk modulus of paragonite are also optimized. The present enthalpy and entropy are from the ordered model of Robie and Hemingway (1984a). The heat capacity is different from calorimetry as it is modified to reproduce the phase equilibria. The value of enthalpy given by Berman (1988) (-5944.21 KJ/mol) is different from the value of Robie and Hemingway (1984a).

Talc, Anthophyllite, Chrysotile and Antigorite: The data for these phases presented here are similar to those of Day et al. (1985) and Berman (1988) except the entropy of antigorite. A little difference is due to their consideration of different values of enstatite and forsterite than presented in this study. Also, in this work the thermal expansion and the bulk modulus of these phases are optimized along with their enthalpies and entropies. Compared to the calorimetric values the enthalpies of talc and anthophyllite are about 10 KJ outside the error limits. However, these molecules are very large and the differences are not significant when the values are considered on a one-cation basis. The heat capacities of chrysotile and antigorite are significantly

different from those optimized by Berman (1988).

Grunerite: As noted earlier, Miyano and Klein (1983) derived the free energy of grunerite from reaction (3.nn) using a different set of values for fayalite and quartz. Hence, the values presented here are different from their values. Recently, Anovitz et al. (1988) determined the heat capacity of natural grunerite by calorimetry. The entropy of natural grunerite at 298 K calculated by them is 706.88 J/mol-K which, upon correction to the end-member composition, became 744.2 J/mol-K. In this study, the recommended entropy at 298 K is 714.6 J/mol-K.

Cordierite: The values presented here are closely similar to the calorimetric values. The entropy value of Berman (1988) (417.97 J/mol-K) is outside the error limits of calorimetry.

III. Comparison of solid-solution properties with calorimetric data and data from other sources

Spinel - Hercynite

Engi (1983) presented a derivation of the solution properties of Mg and Fe aluminate and chrome spinels. They adopted the distribution-of-species model and compared it with the classical reciprocal salt model adopted by Wood and Nicholls (1978) and extended by Sack (1982). In this study only the aluminate spinels are considered. The results obtained are somewhat different since the data for forsterite and fayalite are

Table 4.1. Comparison between calorimetric values and values presented in this study of enthalpy and entropy

Phase	Calorimetric value		This study	
	$H^{o}_{f}(298)$ KJ/mol	$S^{o}(298)$ J/mol.K	$H^{o}_{f}(298)$ KJ/mol	$S^{o}(298)$ J/mol.K
Andalusite	-2591.9 ±1.72	91.39±0.14	-2591.9	91.39
Kyanite	-2596.01±1.7	82.3 ±0.13	-2596.01	82.3
Sillimanite	-2587.77±1.73	95.79±0.14	-2587.77	95.79
Wollastonite	-1634.77±0.7	81.03±0.68	-1634.77	81.03
Gehlenite	-3983.93±1.3	198.6 ±0.6	-3980.76	204.35
Akermanite	-3865.6 ±1.13	209.33±2.09	-3865.44	209.33
Spinel	-2299.38±0.75	80.63±0.42	-2307.16	81.5
Forsterite	-1085.86±1.88	47.06±0.5	-1087.18	47.06
Fayalite	-739.09±0.65	75.5 ±0.1	-739.09	75.5
Monticellite	-1124.45±0.86	54.05±0.1	-1123.3	55.23
Enstatite	-1546.19±1.76	66.27±0.1	-1546.29	66.27
Ferrosilite	-	94.6 ±0.1*	-1195.2	94.56
Clinoenstatite	-1544.15±2.09	67.86±0.42	-1544.01	67.23
Diopside	-1600.15±0.86	71.55±0.42	-1600.91	71.55
Ca-Tschermak	-3296.62±1.63	135.3	-3306.0	139.3
Jadeite	-1514.94±2.1 *	66.74±0.63	-1514.94	66.39
Pyrope	-2096.92±0.53	88.76	-2097.18	88.76
Almandine	-1749.94±3.57	113.23±0.17	-1758.79	112.1
Grossular	-2210.92±0.93	86.71	-2211.44	86.71
Rutile	-944.75±1.26	50.29±0.17	-945.9	50.46
Ilmenite	-1236.62±1.59	108.9 ±0.5	-1234.8	108.9
Anorthite	-4227.83±2.01	199.3 ±0.3	-4236.0	199.6
Albite	-3929.56±1.71*	220.3 ±0.4	-3929.56	220.3
Sanidine	-3959.56±3.37	232.9 ±0.48	-3959.56	239.99

Muscovite	-5976.74±3.24	306.4 ±0.61	-5976.3	306.4
Paragonite	-5949.33±4.6 *	277.1 ±0.9	-5949.1	277.1
Phlogopite	-6203.9 ±6.73*	334.6 ±1.0	-6203.9	334.6
Brucite	-924.5 ±1.4	63.18±0.13	-924.62	64.08
Chrysotile	-4364.3 ±3.4	221.33±1.67	-4363.0	219.82
Antigorite	-	3598.53±26.78	-71376.0	3672.8
Talc	-5915.9 ±4.33	260.79±0.42	-5898.8	261.18
Anthophyllite	-12086.0 ±7.5	537.0 ±2.7	-12071.0	534.31
Cordierite	-9161.52±5.85	407.2 ±3.8	-9164.87	411.0

Sources of calorimetric values (* derived indirectly from other measurements, H and S stand for enthalpy and entropy):
Andalusite, Kyanite, Sillimanite: Robie and Hemingway (1984b).
Wollastonite: Haas et al. (1981).
Gehlenite: H, Charlu et al. (1981); S, Hemingway and Robie (1984). S in this study includes disorder from Woodhead (1977).
Akermanite: H, Charlu et al. (1981); S, Robie et al. (1978).
Spinel: H, Charlu et al. (1975); S, Robie et al. (1978). H in this study includes disorder.
Forsterite: H, Brousse et al. (1984) (-1087.07 from Haselton, 1979); S, Robie et al. (1982b).
Fayalite: Robie et al. (1982a).
Monticellite: H, Brousse et al. (1984); S, Sharp et al. (1986).
Enstatite: H, Brousse et al. (1984); S, Krupka et al. (1985a).
Ferrosilite: S, Bohlen and Boettcher (1981).
Clinoenstatite: Kiseleva et al. (1979).
Diopside: Robie et al. (1978).
Ca-tschermak: H, Charlu et al. (1978); S, Haselton et al. (1984).
Jadeite: H, Hemingway et al. (1981); S, Robie et al. (1978). S in this study follows Hemingway et al. (1981).
Pyrope: H, Charlu et al. (1975); S, Haselton and Westrum (1980).
Almandine: H, Chatillon-Colinet et al.(1983a); S, Metz et al.(1983).
Grossular: H, Charlu et al. (1978); S, Haselton and Westrum (1980).
Rutile: Robie et al. (1978).
Ilmenite: H, Robie et al. (1978); S, Anovitz et al. (1985).
Anorthite: H, Charlu et al. (1978); S, Robie et al. (1978).
Albite: aluminum avoidance model from Hemingway et al. (1981).
Sanidine: as listed in Robie et al. (1978). S in this study includes disorder.
Muscovite: as listed in Robie et al. (1978).
Paragonite: ordered model from Robie and Hemingway (1984a).
Phlogopite: H, Clemens et al.(1987); S, Robie and Hemingway (1984a).
Brucite: Robie et al. (1978).
Chrysotile, Antigorite: King et al. (1967).
Talc: H, Robie et al. (1978); S, Robie and Stout (1963).

Anthophyllite: H, Weeks (1955); S, Krupka et al. (1985a).
Cordierite: Robie et al. (1978).

---

different in this study. Also, Engi found some excess entropy and ΔW_{Cp} (Engi, 1980) in their calculation. The present model also differs from that suggested by Jamieson and Roeder (1984) because their experimental data are not consistent with the experimental data of Engi (1983). This is discussed in detail in Chapter 3.

Forsterite - Fayalite

The model derived here is very close to that determined through calorimetry by Wood and Kleppa (1981).

Pyroxenes

Interaction parameters of all binaries in the multicomponent orthopyroxene and clinopyroxene solutions are based on phase equilibrium data of Lindsley (1983) except the enstatite-ferrosilite binary above 873 K. Chatillon-Colinet et al. (1983b) determined this binary through calorimetry and found a positive deviation from ideality (W = 4 KJ/cation). Analysis of site-occupancy data (e.g. Saxena and Ghose, 1971) indicate a slight excess entropy. This cancels out the excess enthalpy at metamorphic temperatures. Thus, the enstatite-ferrosilite solution is considered ideal above 873 K. Below 873 K, however, Saxena et al. (1986) found a considerable positive deviation and their model is adopted in this study below the stated temperature. According to their model the enstatite-ferrosilite and the ferrosilite-enstatite solutions become ideal at 873 K and 674 K respectively. From Lindsley's (1983) phase equilibrium data on quadrilateral pyroxenes many workers have

attempted to calculate the binary interaction parameters of the pyroxenes. Nickel & Brey (1984) proposed a symmetric model for the clinoenstatite-diopside join. However, the model of Lindsley et al. (1981) for this join is retained here. The difference between the two models is not significant in calculations. The other parameters are adopted from Saxena et al. (1986), who based their calculations on the Bertrand-Kohler model for multicomponent solutions. The Al_2O_3 solution in pyroxenes are modeled also on the basis of phase equilibrium data dealing with aluminous enstatite and pyrope. This is discussed in Chapter 3.

Pyrope - Almandine

The result obtained here is significantly different from the analysis of Ganguly and Saxena (1984). According to Ganguly and Saxena, at 1000°C, W_{Mg-Fe} = 10.46 KJ/cation and W_{Fe-Mg} = 0.837 KJ/cation. At the same temperature, from the data recommended here, W_{Mg-Fe} = -0.328 KJ/cation and W_{Fe-Mg} = 1.662 KJ/cation. Thus, in this study, the solution is closer to ideality. Recently, Hackler and Wood (1988) calculated the excess enthalpy of this solution based on their distribution data of Fe, Mg and Mn between garnet and olivine. According to them the W^H parameters are W_{Mg-Fe} = 1.8 KJ/cation and W_{Fe-Mg} = 0.167 KJ/cation assuming a symmetric interaction parameter of 4.184 KJ/cation of olivine. Their result agrees well with the result in this study.

Pyrope - Grossular

Ganguly & Saxena (1984) recommended a symmetric parameter of 6.276 J/mol for the excess entropy of this binary. However, from phase equilibrium analysis it is concluded that the asymmetric model as recommended here is more consistent with the experiments (Chatterjee, 1987).

Almandine - Grossular

The present model for excess enthalpy determined calorimetrically by Newton et al. (1986) differs considerably from the conclusions of Ganguly and Saxena (1984) who recommended an asymmetric model with W^{H}_{Ca-Fe} = -2636 J/cation and W^{H}_{Fe-Ca} = 19330 J/cation. Also, the conclusion regarding the excess entropy reached here is different from that of Ganguly and Saxena (1984). Recently, based on phase equilibrium data, Koziol and Newton (1988b), calculated the excess enthalpy of this solution. The interaction parameters calculated by them are W^{H}_{Ca-Fe} = -2185 J/cation and W^{H}_{Fe-Ca} = 3133 J/cation. At 1033 K, according to this study, the interaction parameters are as W_{Ca-Fe} = 128.6 J/cation and W_{Fe-Ca} = 7715.1 J/cation.

Phlogopite - Annite

As noted earlier Wones and Eugster (1965) calculated a symmetric interaction parameter of -4211 J/mol. Wones (1972) later revised their work and concluded that the phlogopite-annite solution is ideal. In this work a slight positive deviation from ideality of this solution is detected.

CHAPTER 5

APPLICATIONS

I. CALCULATION OF PHASE DIAGRAMS

The thermodynamic data presented in this study have a variety of applications. An advantage of having an internally consistent data base is to be able to store a large amount of physical and chemical information regarding a system in a concise way. Experimental results can be calculated back from the data base whenever they are required. A computer is a useful tool in both storage of the data base and calculations. In the following two examples, the method of minimization of free energy is implemented through the program SOLGASMIX (discussed later) to calculate phase diagrams.

The data base can not only be used to reproduce experimental results, but it can also be used in interpolations and extrapolations. In cases such as the heat capacity, the extrapolations are based on good theoretical models. Predictions of thermodynamic properties of phases for which experiments have not been conducted are also possible. The principle behind these calculations are discussed in Chapter 2. In the first example (Figure 5.1), the stability fields of the assemblages spinel + enstatite and pyrope + forsterite in the MgO-Al_2O_3-SiO_2 system are calculated in a pressure-temperature field. The calculated

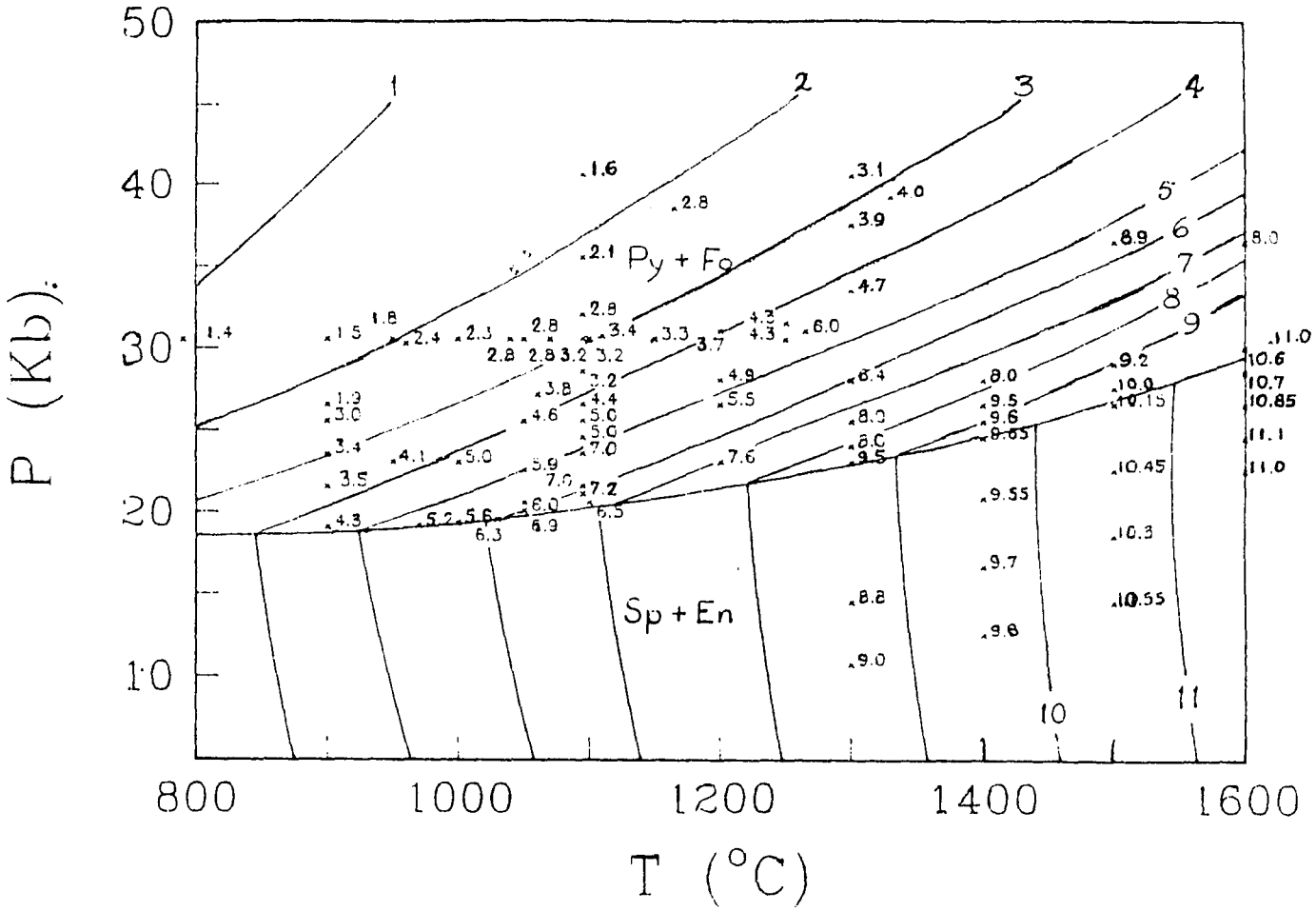

Figure 5.1: Calculated equilibrium phase relations in the MgO-Al_2O_3-SiO_2 system. The numbered lines are isopleths of Al_2O_3 mole % in orthopyroxene. The experimental data are from Danckwerth & Newton (1978), Gasparik & Newton (1984), Haselton (1979), Lane & Ganguly (1980), and Perkins et al. (1981).

mole-percents of Al_2O_3-orthopyroxene in solution with enstatite are also shown. In some cases, the calculated value of Al_2O_3 content of orthopyroxene does not match with the experimental data. This is because there is a considerable scatter in the experimental data. However, extrapolations based on the best fit are made at conditions under which experimental data are not available. Also, while calculating this diagram, the enthalpy of spinel and the free energy of the fictitious phase Al_2O_3-orthopyroxene are optimized. The optimized enthalpy of spinel is less than the calorimetric value. This is explained in a previous chapter and is accounted for the disorder in spinel.

The system used to construct the phase diagram in the previous example is further extended by adding Ca in the next example. Figure 5.2 shows the stability fields of typical lherzolite assemblages plagioclase + opx + cpx + olivine, spinel + opx + cpx + olivine and garnet + opx + cpx + olivine in the CaO-MgO-Al_2O_3-SiO_2 system. The Al_2O_3 content of orthopyroxene is also calculated and is shown as isopleths in the diagram.

II. BAROMETRY AND THERMOMETRY

A major application of the data base is to predict temperature or pressure or both of equilibration of natural assemblages using their chemical analyses. Following is a general description of an exchange reaction, in which the exchange of two cations such as Fe and Mg between two coexisting phases, such as garnet and biotite, is considered.

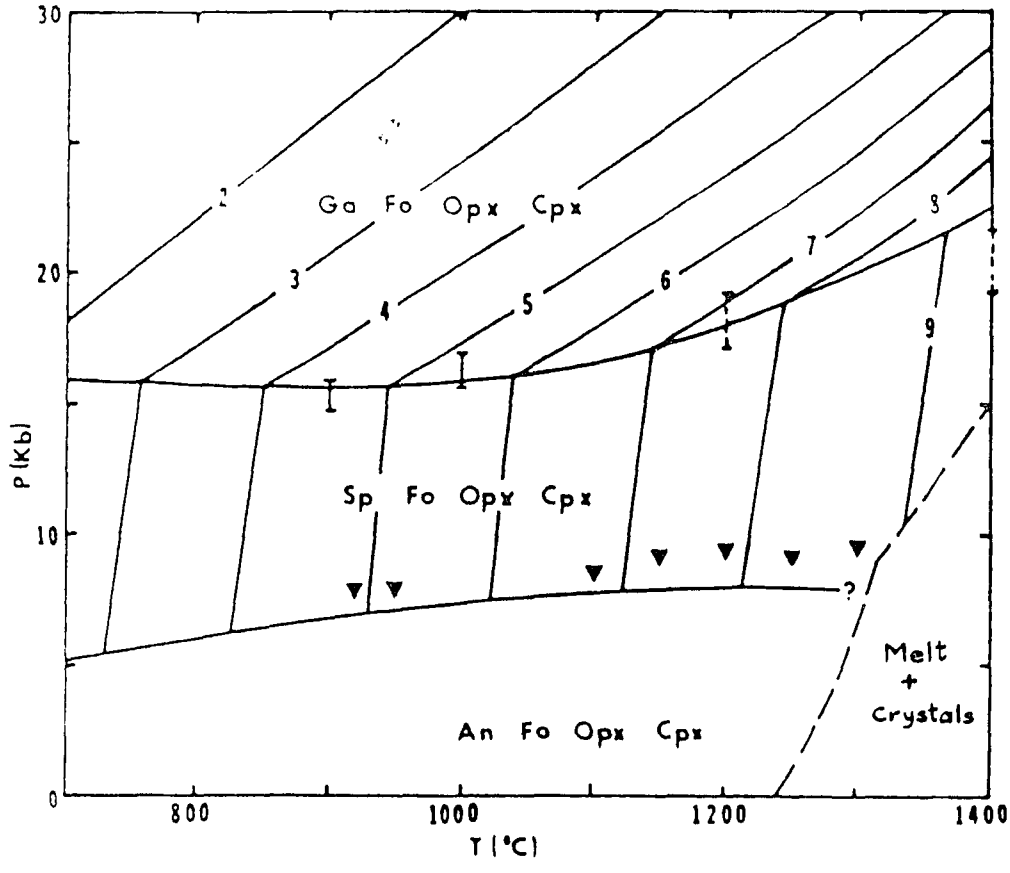

Figure 5.2: Calculated phase equilibrium in the silica undersaturated CaO-MgO-Al_2O_3-SiO_2 system. Solid bars are from Jenkins and Newton (1979). Broken bars are from Patera (1982) and Gasparik (1984a). Inverted triangles are from Kushiro and Yoder (1966) and Yoder (1968). The dashed lines (not calculated) are from Presnall (1976) and Dixon (1980). The numbered lines are isopleths of Al_2O_3 mole % in orthopyroxene.

Although the discussion is for an exchange reaction, the same principle can be applied to any reaction.

$$M1\text{-}\alpha + M2\text{-}\beta = M2\text{-}\alpha + M1\text{-}\beta \qquad (5.a)$$

where, α and β are the coexisting phases and M1 and M2 are the exchanging cations. At equilibrium,

$$\Delta G^{\circ}_{(5.a)}(1,T) + \int_1^P \Delta V^{\circ}_{(5.a)}(1,T)dP = -RT\ln K_{(5.a)} \qquad (5.1)$$

where, $K_{(5.a)} = K_D.K_\gamma$ The above equation can be solved for pressure or temperature using the chemical analyses of α and β if one of the two variables is known. K_γ depends on the activity coefficients of the four end-member phases described by solution models in Chapter 2 and whose interaction parameters are given in the Table 4.4. Thus, equation (5.1) becomes

$$\begin{aligned}
&\Delta H^{\circ}_{(5.a)}(1,298) + \int_{298}^{T} \Delta C_{p(5.a)}dT \\
&- T\Delta S^{\circ}_{(5.a)}(1,298) - T\int_{298}^{T} \Delta C_{p(5.a)}/TdT \\
&+ \int_1^P \Delta V^{\circ}_{(5.a)}(1,T)dP + RT\ln[\{X_{M2}^{\alpha}(1-X_{M2}^{\beta})\}/\{X_{M2}^{\beta}(1-X_{M2}^{\alpha})\}] \\
&+ \{3(X_{M2}^{\beta})^2-2X_{M2}^{\beta}\}W_{M1\text{-}M2}^{\beta} - \{3(X_{M2}^{\beta})^2-4X_{M2}^{\beta}+1\}W_{M2\text{-}M1}^{\beta} \\
&- \{3(X_{M2}^{\alpha})^2-2X_{M2}^{\alpha}\}W_{M1\text{-}M2}^{\alpha} + \{3(X_{M2}^{\alpha})^2-4X_{M2}^{\alpha}+1\}W_{M2\text{-}M1}^{\alpha} \\
&\qquad = 0 \qquad (5.2)
\end{aligned}$$

The enthalpy, entropy and heat capacity differences are calculated from Table 4.2, the molar volumes are calculated from Table 4.3 and using the Murnaghan equation (2.6) and the interaction parameters are given in Table 4.4. At lower pressures it is not necessary to use the Murnaghan equation and it is sufficient to take only the molar volume difference of the reaction. If all the solutions were ideal in reaction (5.a), the

last four terms on the left hand side of equation (5.2) would become zero.

This is a formulation valid for binary solid solutions. Addition of other cations in α or β will introduce other terms in equation (5.2) arising from the multicomponent solution model (Kohler formulation). This is more conveniently done through the programs discussed below in a separate section which also consider the effects of molar volume, thermal expansion and bulk modulus of each reactant and thus, minimizes the error in the resulting temperature or pressure.

For barometry, the equilibrium constant of the reaction should vary sensitively with pressure rather than with temperature. An example of a good barometer is reaction (3.k). Al_2SiO_5 (kyanite) and SiO_2 (quartz) are pure phases. So, their activities are unity. But anorthite and grossular go into the plagioclase and garnet solid solutions respectively. Their activities will depend on their mole fractions and activity coefficients given by the models described in Chapter 2. Thus, K_D, the distribution coefficient, is given by

$$K_D = X_{Gr}^{gar}/(X_{An}^{plag})^3 \qquad (5.3)$$

where, X_{Gr}^{gar} and X_{An}^{plag} are the mole fractions of grossular in garnet and of anorthite in plagioclase respectively. And K_γ is given by

$$K_\gamma = \gamma_{Gr}^{gar}/(\gamma_{An}^{plag})^3 \qquad (5.4)$$

where, γ_{Gr}^{gar} and γ_{An}^{plag} are the activity coefficients of grossular in

garnet and of anorthite in plagioclase respectively. Thus, if the temperature is known, the pressure can be calculated from equation (5.1) using the chemical analyses of plagioclase and garnet.

For thermometry, a reaction should be chosen such that its equilibrium constant varies sensitively with temperature, but not with pressure. Several exchange thermometers are described below:

i) The Spinel - Olivine thermometer

$MgAl_2O_4 + FeSi_{0.5}O_2 = FeAl_2O_4 + MgSi_{0.5}O_2$
spinel fayalite hercynite forsterite

ii) The Olivine - Orthopyroxene thermometer

$MgSi_{0.5}O_2 + FeSiO_3 = FeSi_{0.5}O_2 + MgSiO_3$
forsterite ferrosilite fayalite enstatite

iii) The Olivine - Clinopyroxene thermometer

$MgSi_{0.5}O_2 + FeSiO_3 = FeSi_{0.5}O_2 + MgSiO_3$
forsterite clinoferrosilite fayalite clinoenstatite

iv) The Olivine - Garnet thermometer

$MgSi_{0.5}O_2 + FeAl_{2/3}SiO_4 = FeSi_{0.5}O_2 + MgAl_{2/3}SiO_4$
forsterite almandine fayalite pyrope

v) The Olivine - Grunerite thermometer

$MgSi_{0.5}O_2 + 1/7Fe_7Si_8O_{22}(OH)_2 = FeSi_{0.5}O_2 + 1/7Mg_7Si_8O_{22}(OH)_2$
forsterite grunerite fayalite cummingtonite

vi) The Orthopyroxene - Clinopyroxene thermometer

$MgSiO_3 + FeSiO_3 = FeSiO_3 + MgSiO_3$
enstatite clinoferrosilite ferrosilite clinoenstatite

vii) The Orthopyroxene - Garnet thermometer

$MgSiO_3 + FeAl_{2/3}SiO_4 = FeSiO_3 + MgAl_{2/3}SiO_4$
enstatite almandine ferrosilite pyrope

viii) The Clinopyroxene - Garnet thermometer

$MgSiO_3 + FeAl_{2/3}SiO_4 = FeSiO_3 + MgAl_{2/3}SiO_4$
clinoenstatite almandine clinoferrosilite pyrope

ix) The Garnet - Biotite thermometer

$MgAl_{2/3}SiO_4 + 1/3KFe_3AlSi_3O_{10}(OH)_2 = FeAl_{2/3}SiO_4 + 1/3KMg_3AlSi_3O_{10}(OH)_2$
pyrope annite almandine phlogopite

x) The Garnet - Cordierite thermometer

$MgAl_{2/3}SiO_4 + 1/2Fe_2Al_4Si_5O_{18} = FeAl_{2/3}SiO_4 + 1/2Mg_2Al_4Si_5O_{18}$
pyrope ferrocordierite almandine cordierite

xi) The Biotite - Cordierite thermometer

$$1/3KMg_3AlSi_3O_{10}(OH)_2 + 1/2Fe_2Al_4Si_5O_{18} = 1/3KFe_3AlSi_3O_{10}(OH)_2 + 1/2Mg_2Al_4Si_5O_{18}$$

phlogopite — ferrocordierite — annite — cordierite

In addition to the above exchange thermometer, the following thermometers based on the polymorphic transformation of enstatite and the Al content of enstatite are also considered:

xii) The Enstatite thermometer

$$MgSiO_3 = MgSiO_3$$

enstatite — clinoenstatite

xiii) The Al-enstatite - Garnet thermometer

$$3MgSiO_3 + Al_2O_3 = 3MgAl_{2/3}SiO_4$$

enstatite — Al-opx — pyrope

III. SOME EXAMPLES

Thermobarometric calculations can be done manually using equation (5.1) and the thermodynamic data presented in this study. However, this is very cumbersome and sometimes inaccurate because of the various assumptions that have to be made. An easier way to calculate temperature or pressure is by using graphical thermometers, some of which are presented here. These diagrams are calculated using the free energy

minimization program (SOLGASMIX) described in the next section. However, there are several limitations of these diagrams as discussed below. In the second part of this section, the program THERMO (described in the next section) is used to calculate temperatures of various equilibria in a rock. The approach here is more direct and does not depend on free energy minimization. There are disadvantages of this method as will be discussed at the end of this section and under the description of the program.

The major limitation of a graphical thermometer is that only three or at the most four variables can be represented in a diagram. In a multicomponent system, it is sometimes necessary to deal with five or six or more variables. For example, in the garnet-orthopyroxene system, besides a K_D (defined for the Fe-Mg exchange) and the pressure and temperature, mole-fractions of Al, Ca, Mn and Na components in orthopyroxene and of Ca, Mn, Cr and Fe^{3+} components in garnet are some of the other variables to be considered. In this work, Cr and Fe^{3+} are not considered. Mn is considered in the examples discussed here with with certain limitations.

In reactions involving ideal solutions, the distribution coefficient is constant at a certain pressure and temperature and fixed compositions of other elements not directly participating in the reaction. For these reactions, the following relation is true:

$$K_D = \exp(-\Delta G^{\circ}(P,T)/RT) \qquad (5.5)$$

If non-ideal solutions are involved, however, relation (5.5) takes the following form:

$$K_D = [\exp(-\Delta G^{\circ}(P,T)/RT)] \; / \; K_{\gamma} \qquad (5.6)$$

In this case, K_D itself becomes a function of the mole-fractions of the solution phases involved in the reaction because of the K_{γ} term. Thus K_D is not a constant at a fixed pressure and temperature. This phenomenon is very hard to represent graphically, considering all the other variables to be represented. The graphical thermometers presented here are for reactions involving ideal or close to ideal solutions or such that the K_{γ} term is close to unity.

The thermometers chosen to be represented graphically are orthopyroxene-garnet, garnet-biotite and garnet-cordierite. All calculations were made using the program SOLGASMIX described below. In Figures (5.3a) through (5.3d), which represent the orthopyroxene-garnet thermometer, variation of K_D (defined as $(X_{Fe}/X_{Mg})^{opx}/(X_{Fe}/X_{Mg})^{gar}$) with temperature at different values of X_{Ca}^{gar} is shown. Figures (5.3a), (5.3b) and (5.3c) are calculated at 6 Kb, 10 Kb and 20 Kb respectively. Al is excluded from orthopyroxene in these three cases. In Figure (5.3d) Al is allowed to vary in orthopyroxene. However, it has no effect on the distribution coefficient as seen by comparing Figures (5.3c and d) which are identical. These four diagrams also suggest that addition of Ca in garnet increases the temperature specially at higher temperatures. The curves are not calculated below 873 K since orthopyroxene behaves non-ideally below that temperature and as a result K_D does not remain constant.

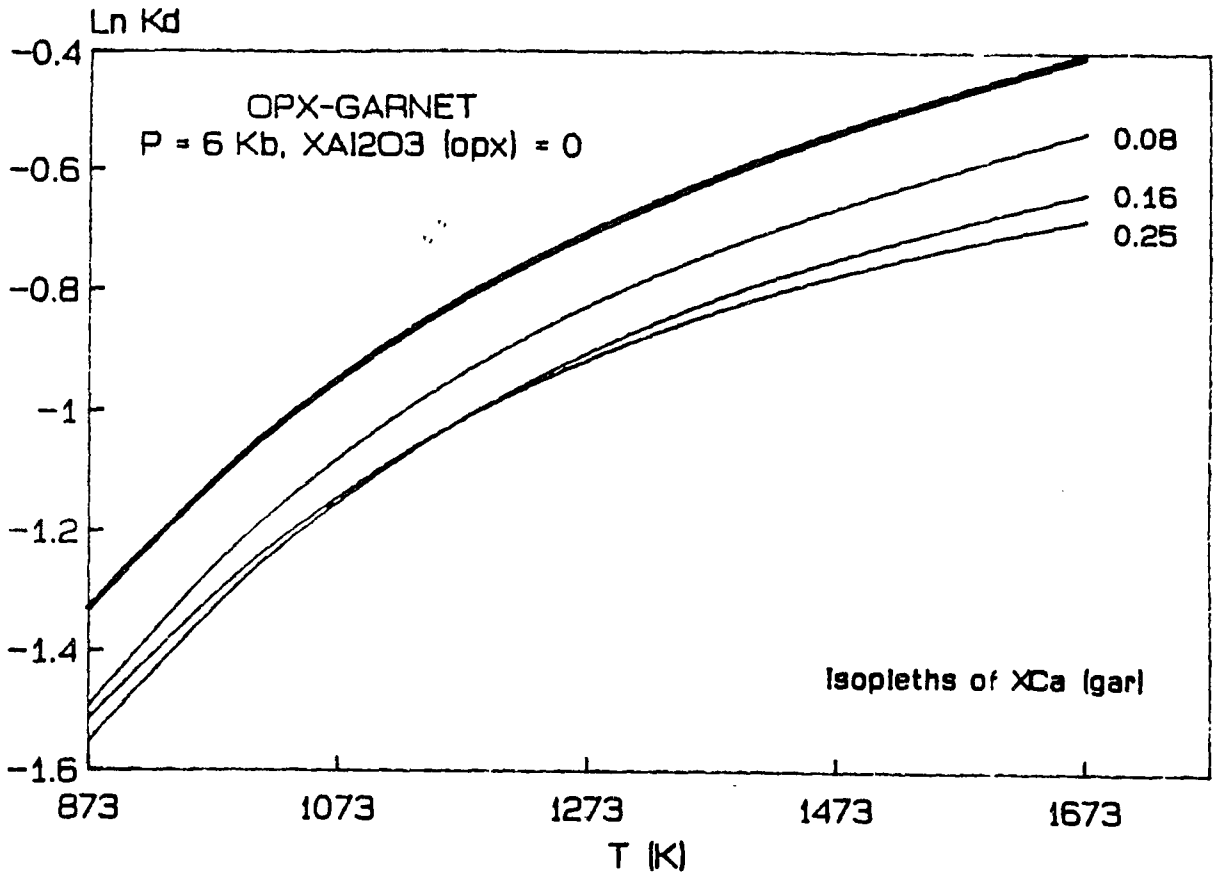

Figure 5.3a: Variation of Ln K_D [$K_D = (X_{Fe}/X_{Mg})^{opx}/(X_{Fe}/X_{Mg})^{gar}$] with temperature at different values of mole-fraction of Ca in garnet, 6 Kbar and $X_{Al_2O_3}^{opx} = 0$. The thick line represents $X_{Ca}^{gar} = 0$.

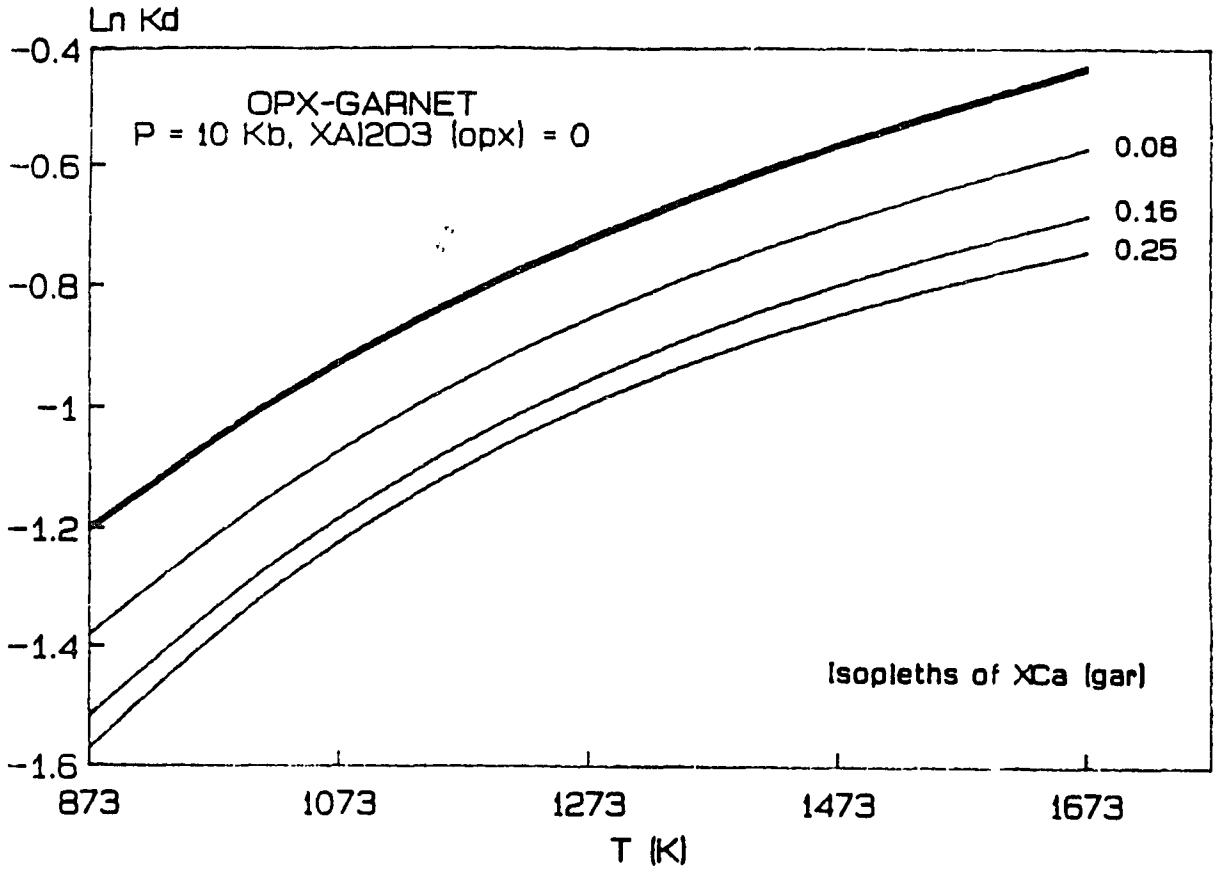

Figure 5.3b: Variation of Ln K_D [$K_D = (X_{Fe}/X_{Mg})^{opx}/(X_{Fe}/X_{Mg})^{gar}$] with temperature at different values of mole-fraction of Ca in garnet, 10 Kbar and $X_{Al_2O_3}^{opx} = 0$. The thick line represents $X_{Ca}^{gar} = 0$.

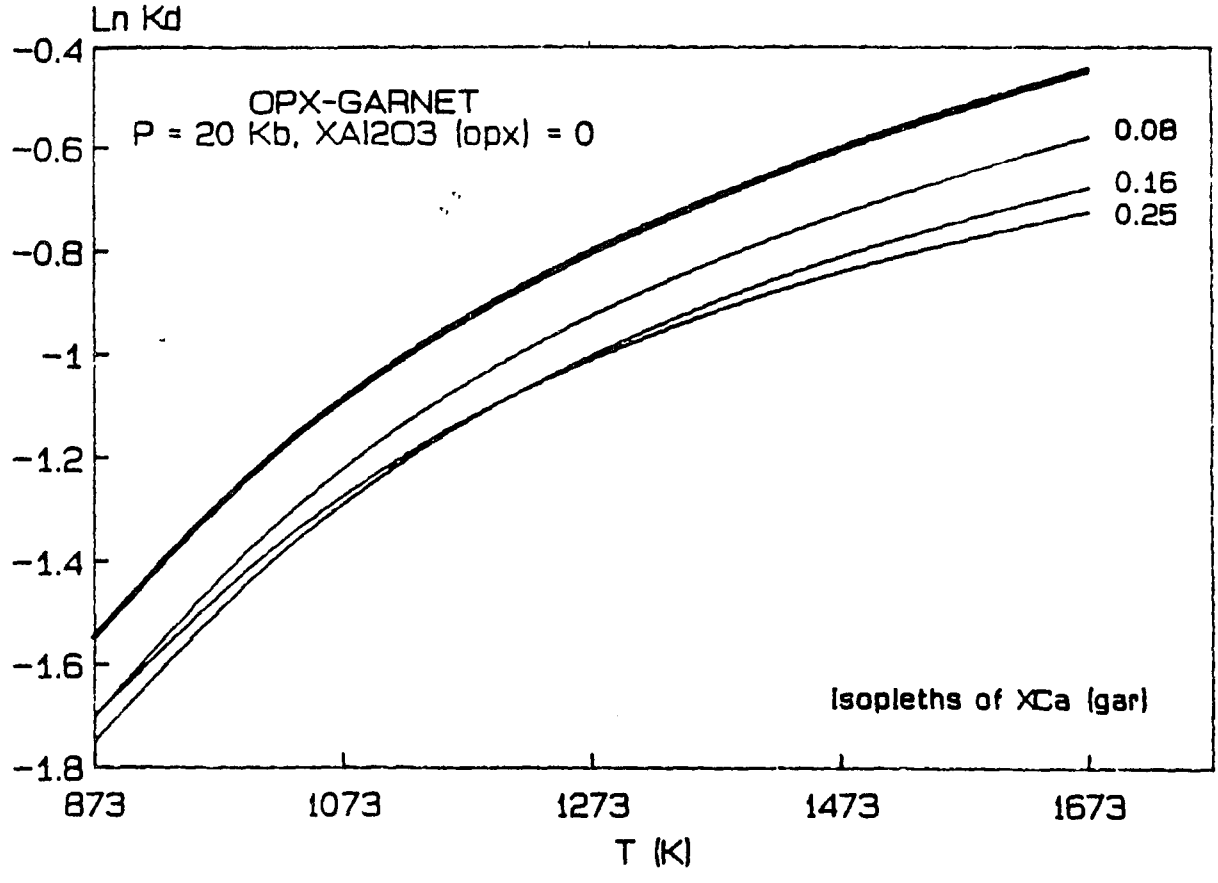

Figure 5.3c: Variation of Ln K_D [$K_D = (X_{Fe}/X_{Mg})^{opx}/(X_{Fe}/X_{Mg})^{gar}$] with temperature at different values of mole-fraction of Ca in garnet, 20 Kbar and $X_{Al_2O_3}^{opx} = 0$. The thick line represents $X_{Ca}^{gar} = 0$.

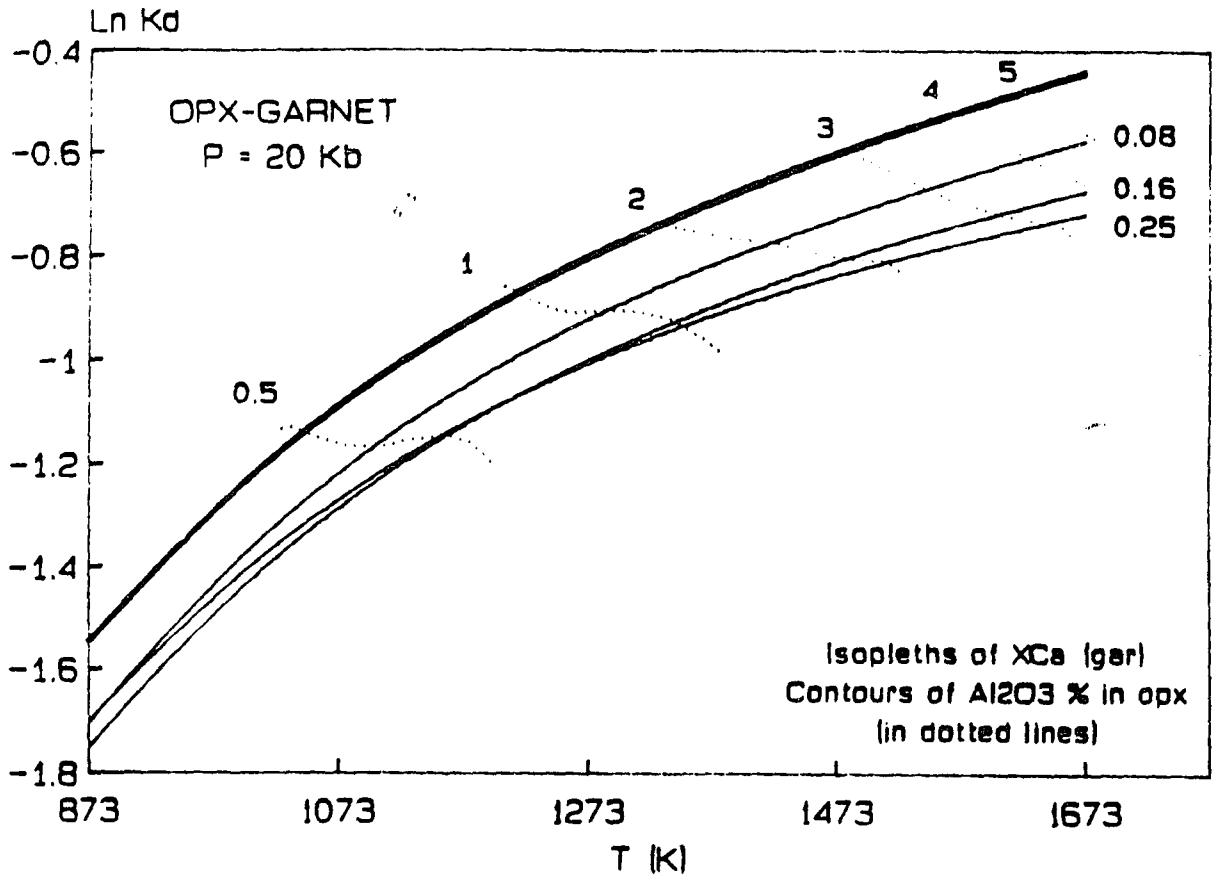

Figure 5.3d: Variation of Ln K_D [$K_D = (X_{Fe}/X_{Mg})^{opx}/(X_{Fe}/X_{Mg})^{gar}$] with temperature at different values of mole-fraction of Ca in garnet and 20 Kb. $X_{Al_2O_3}^{opx}$ is variable and is shown by dotted lines representing contours. The thick line represents $X_{Ca}^{gar} = 0$. No difference is observed between this figure and Figure 5.3c and therefore, Al_2O_3 in orthopyroxene does not affect the K_D.

The garnet-biotite thermometer is represented in Figures (5.4a, b and c) and (5.5a, b and c). Here, the variation of K_D (defined as $(X_{Fe}/X_{Mg})^{gar}/(X_{Fe}/X_{Mg})^{bio}$) with X_{Ca}^{gar} at different temperatures is shown. Figures (5.4a) through (5.4c) are calculated at 6, 10 and 20 Kb respectively. In Figures (5.5a) through (5.5c), varying amounts of X_{Mn}^{gar} are introduced while the pressure is kept constant at 6 Kb. Again, temperatures are raised by the addition Ca upto a X_{Ca}^{gar} of about 0.2. Above that, the temperature decreases. Addition of Mn is found to lower the temperature.

Figures (5.6a) through (5.6d) represent the garnet-cordierite thermometer. The variation of K_D (defined as $(X_{Fe}/X_{Mg})^{gar}/(X_{Fe}/X_{Mg})^{cord}$) with X_{Ca}^{gar} at different temperatures is shown in these four diagrams. The different diagrams are calculated at different concentrations of Mn in garnet and at a fixed pressure (6 Kb). In Figure (5.6d) solution of H_2O in cordierite is considered. However, it has no effect on the distribution coefficient as seen by comparing Figures (5.6c and d) which are identical. Addition of Ca in garnet raises the temperature except when the garnet is rich in Mn in which case the temperature decreases.

In the next example, a rock analysis (ultrabasic nodule from Letseng-la-terae area, Lesotho; Boyd, 1973) is used to determine the temperatures (at different pressures) of various equilibria in the rock. This is done through the program THERMO, which was originally used by

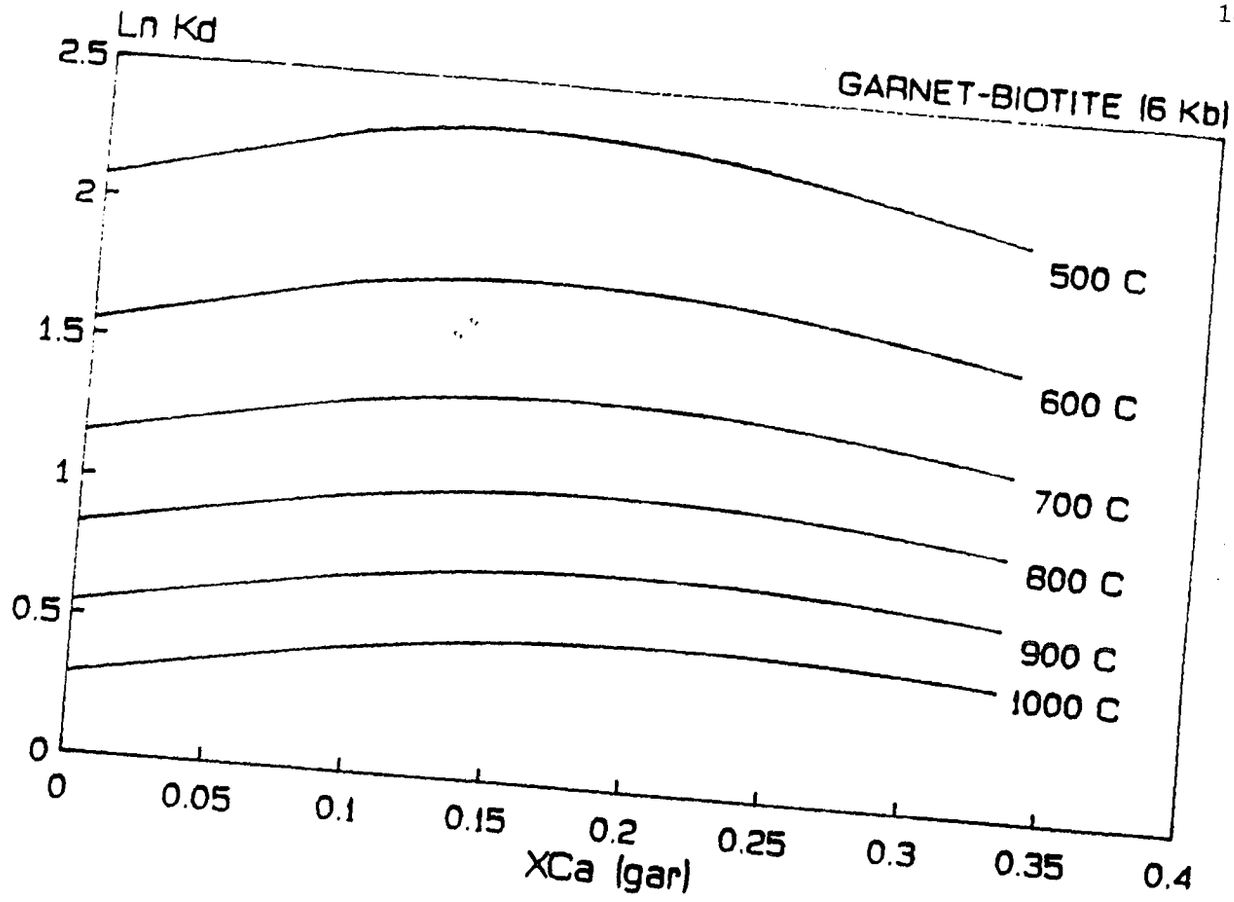

Figure 5.4a: Variation of Ln K_D [$K_D = (X_{Fe}/X_{Mg})^{gar}/(X_{Fe}/X_{Mg})^{bio}$] with mole-fraction of Ca in garnet at 6 Kb and different values of temperature.

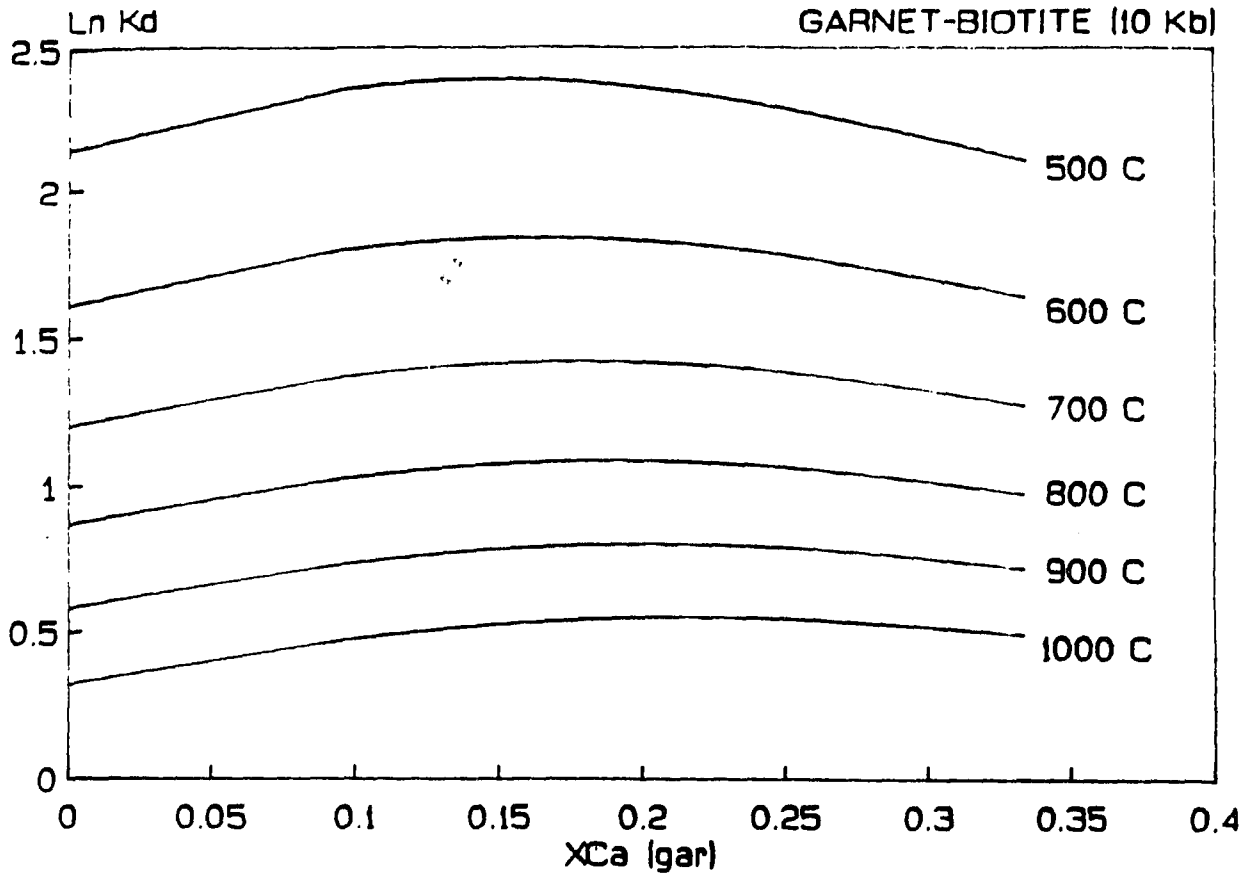

Figure 5.4b: Variation of Ln K_D [$K_D = (X_{Fe}/X_{Mg})^{gar}/(X_{Fe}/X_{Mg})^{bio}$] with mole-fraction of Ca in garnet at 10 Kb and different values of temperature.

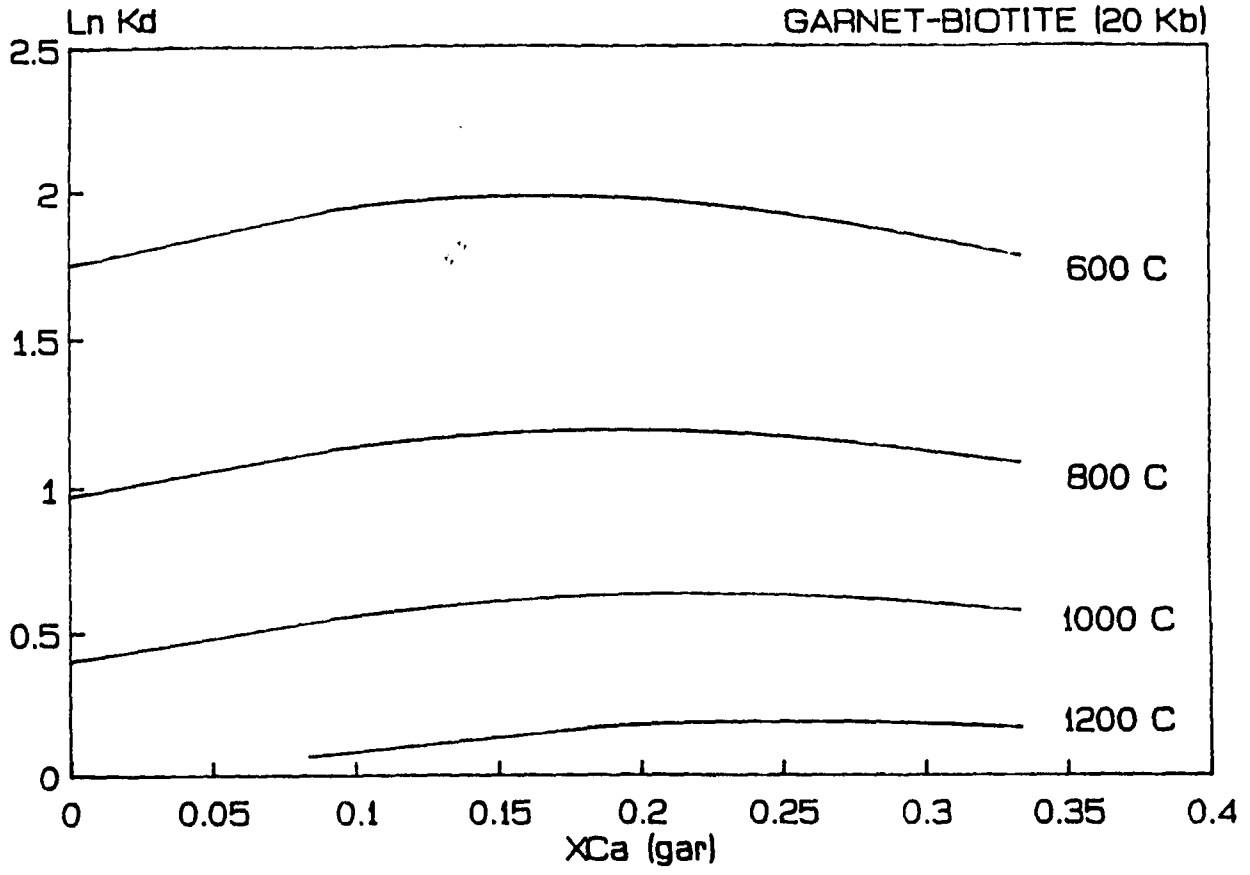

Figure 5.4c: Variation of Ln K_D [$K_D = (X_{Fe}/X_{Mg})^{gar}/(X_{Fe}/X_{Mg})^{bio}$] with mole-fraction of Ca in garnet at 20 Kb and different values of temperature.

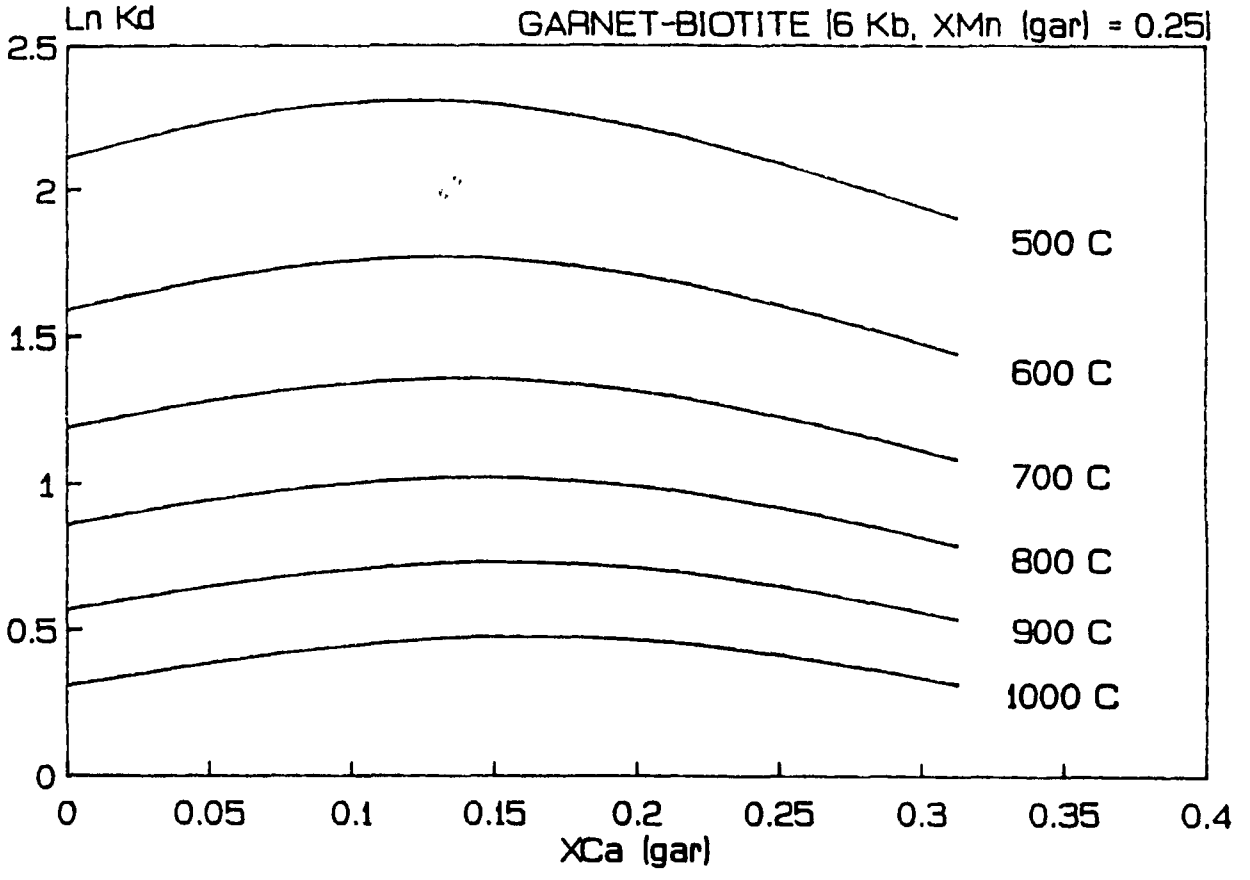

Figure 5.5a: Variation of Ln K_D [$K_D = (X_{Fe}/X_{Mg})^{gar}/(X_{Fe}/X_{Mg})^{bio}$] with mole-fraction of Ca in garnet at 6 Kb, $X_{Mn}^{gar} = 0.25$ and different values of temperature.

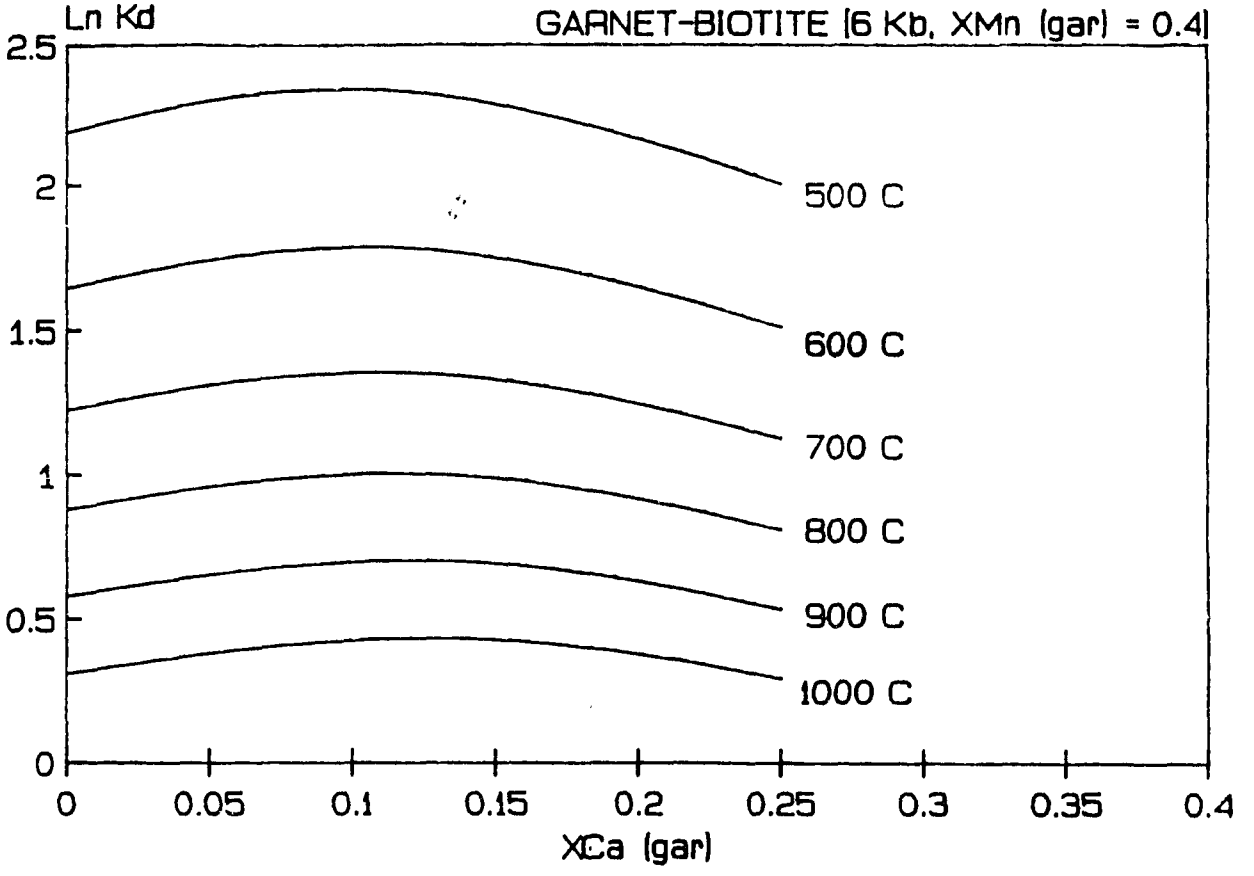

Figure 5.5b: Variation of Ln K_D [$K_D = (X_{Fe}/X_{Mg})^{gar}/(X_{Fe}/X_{Mg})^{bio}$] with mole-fraction of Ca in garnet at 6 Kb, $X_{Mn}^{gar} = 0.4$ and different values of temperature.

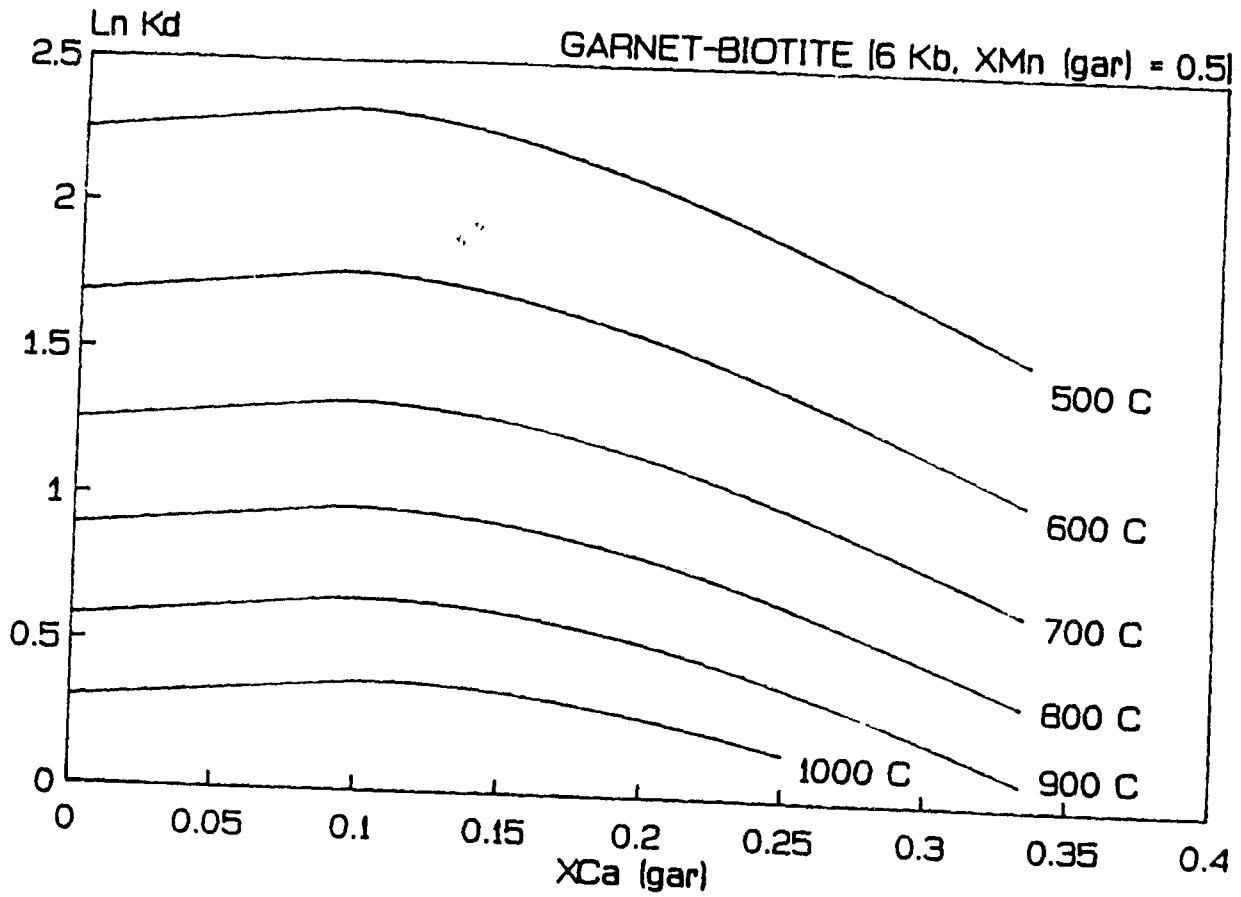

Figure 5.5c: Variation of Ln K_D [$K_D = (X_{Fe}/X_{Mg})^{gar}/(X_{Fe}/X_{Mg})^{bio}$] with mole-fraction of Ca in garnet at 6 Kb, $X_{Mn}^{gar} = 0.5$ and different values of temperature.

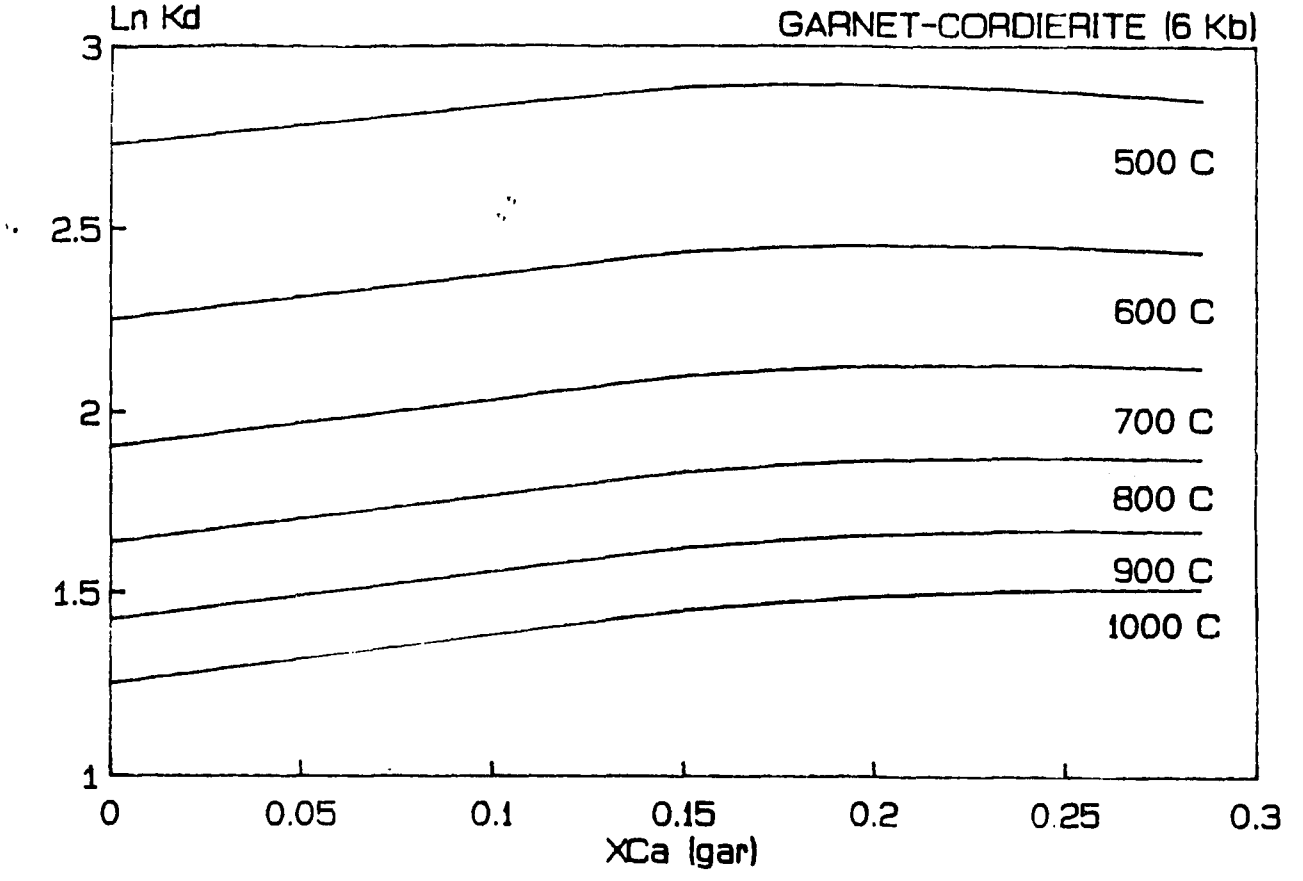

Figure 5.6a: Variation of Ln K_D [$K_D = (X_{Fe}/X_{Mg})^{gar}/(X_{Fe}/X_{Mg})^{cord}$] with mole-fraction of Ca in garnet at 6 Kb and different values of temperature.

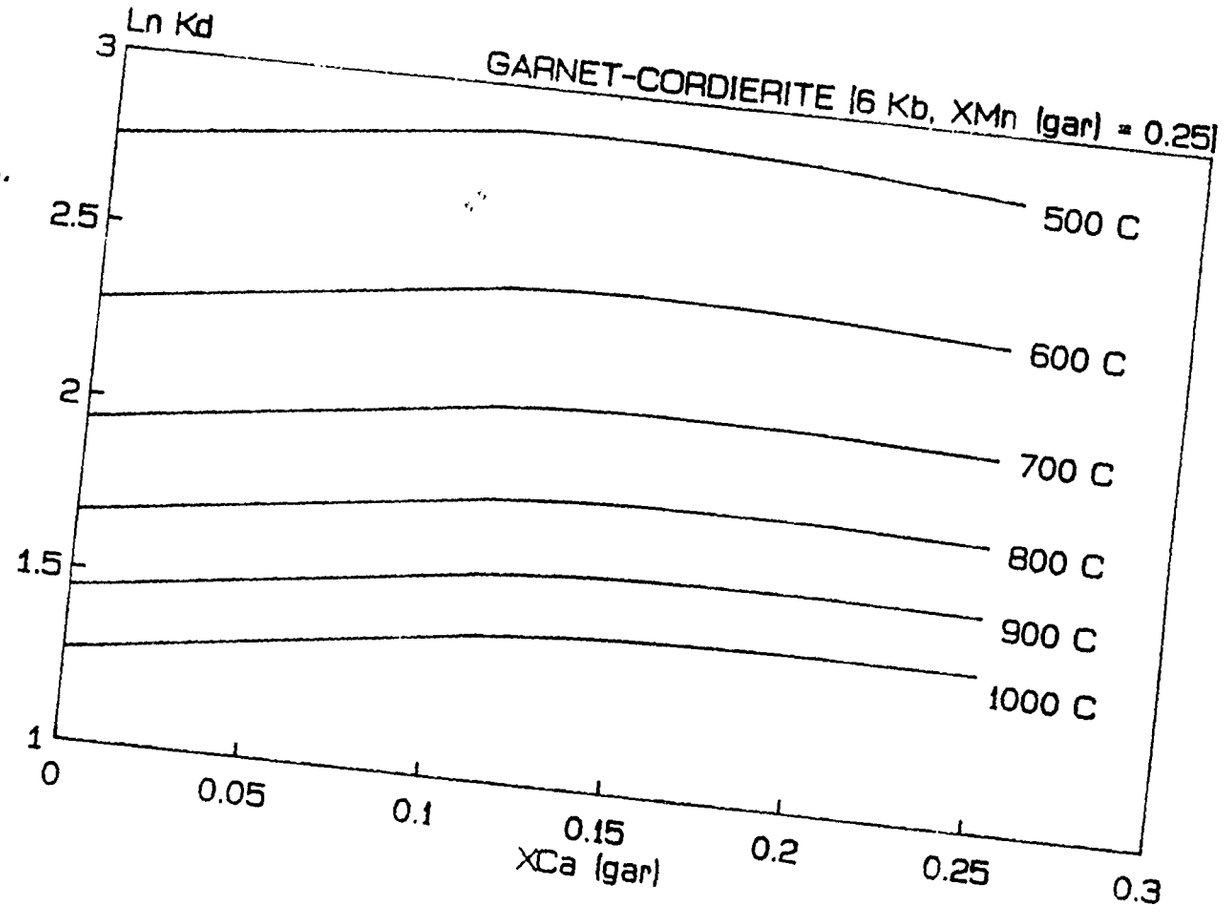

Figure 5.6b: Variation of Ln K_D [$K_D = (X_{Fe}/X_{Mg})^{gar}/(X_{Fe}/X_{Mg})^{cord}$] with mole-fraction of Ca in garnet at 6 Kb, $X_{Mn}^{gar} = 0.25$ and different values of temperature.

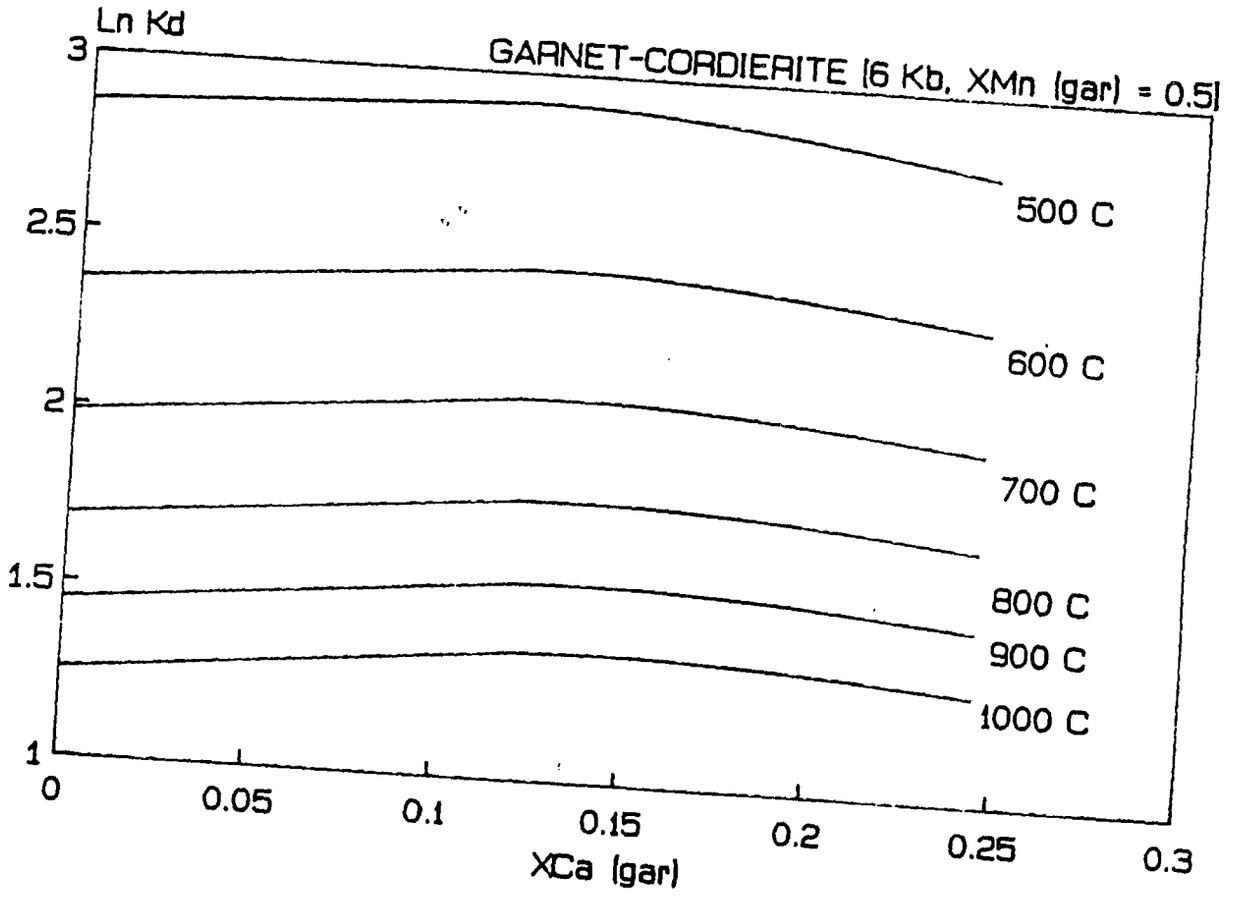

Figure 5.6c: Variation of Ln K_D [$K_D = (X_{Fe}/X_{Mg})^{gar}/(X_{Fe}/X_{Mg})^{cord}$] with mole-fraction of Ca in garnet at 6 Kb, $X_{Mn}^{gar} = 0.5$ and different values of temperature.

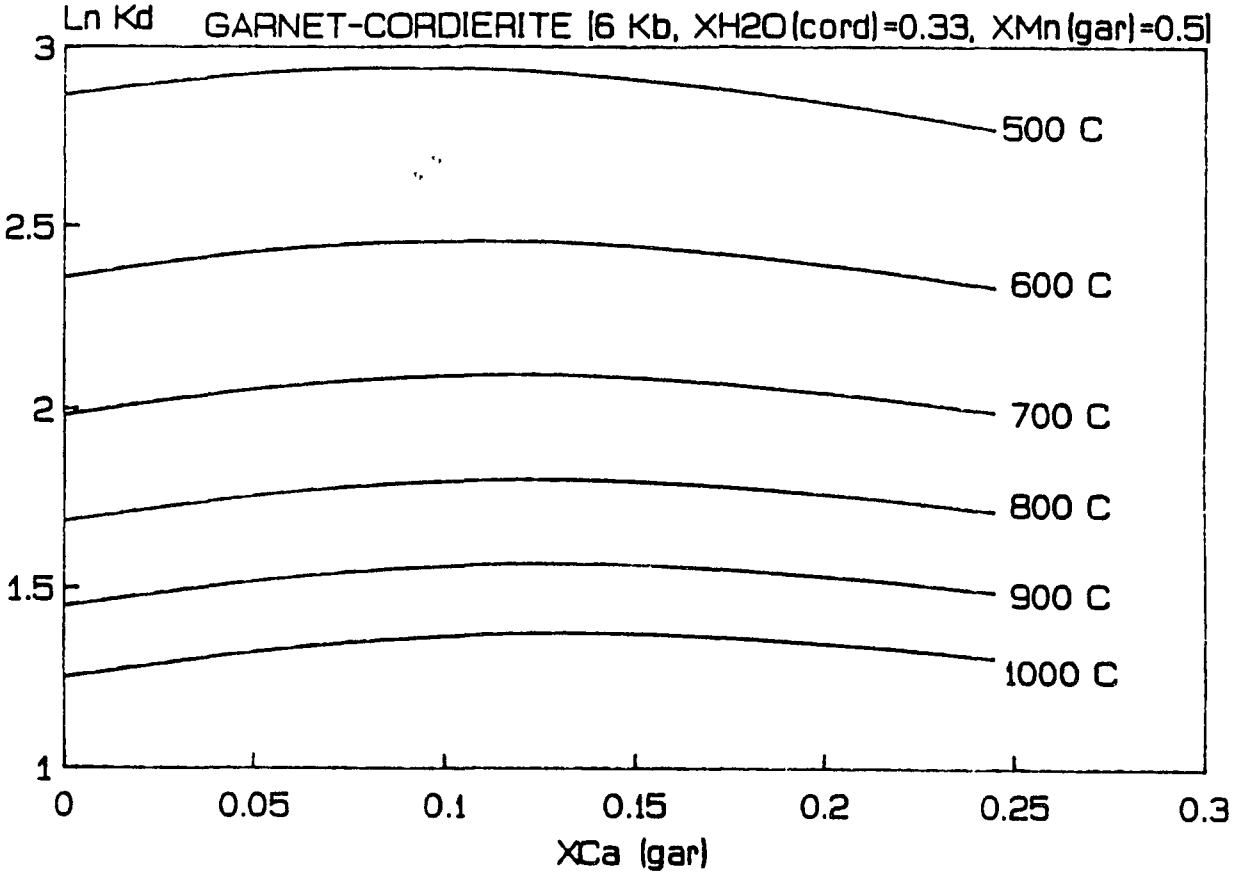

Figure 5.6d: Variation of Ln K_D [$K_D = (X_{Fe}/X_{Mg})^{gar}/(X_{Fe}/X_{Mg})^{cord}$] with mole-fraction of Ca in garnet at 6 Kb, $X_{Mn}^{gar} = 0.5$, $X_{H_2O}^{cord} = 0.33$ and different values of temperature. No difference is observed between this figure and Figure 5.6c and therefore, H_2O in cordierite does not affect the K_D.

Saxena and Eriksson (1985). This program directly uses equation (5.1) to calculate the pressure and temperature of an observed equilibrium. Details of the input and output are dicussed in the following section. A graph (Figure 5.7) is plotted for the different reactions in a pressure-temperature field. In an ideal case, there will be a pressure at which the temperatures obtained from different reactions will be the same. This temperature and the corresponding pressure will represent the conditions under which the rock formed. However, this in not the case in reality because different reactions have different kinetic rates and hence, different pairs of minerals equilibrate at different temperatures. Also, these reactions are temperature sensors and a little change in temperature produces a large change in pressure. Hence, the error associated with the temperature translates into a large pressure difference. In the present example, The Al-orthopyroxene-garnet curve (thermometer (xiii) in the above section), which also acts as a geobarometer, intersects three other curves between 39 and 44.5 Kb. Hence, the pressure could be given as 41.75 ± 2.75 Kb. At this pressure, the temperatures given by thermometers (ii), (viii), (iv), (vii) and (xii) are 587 ± 10, 887 ± 15, 1227 ± 10, 1317 ± 10 and 1332 ± 5^{o}C respectively. The conclusion may be that the pairs olivine-opx and cpx-garnet equilibrated at a much lower temperature than the pairs olivine-garnet, opx-garnet and ortho-clino enstatite. However, it is also possible that the coexisting minerals in the pairs olivine-opx and cpx-garnet are not in equilibrium. In such a case, the pairs olivine-opx and cpx-garnet do not give the equilibrium temperature.

IV. APPLICATIONS PROGRAMS

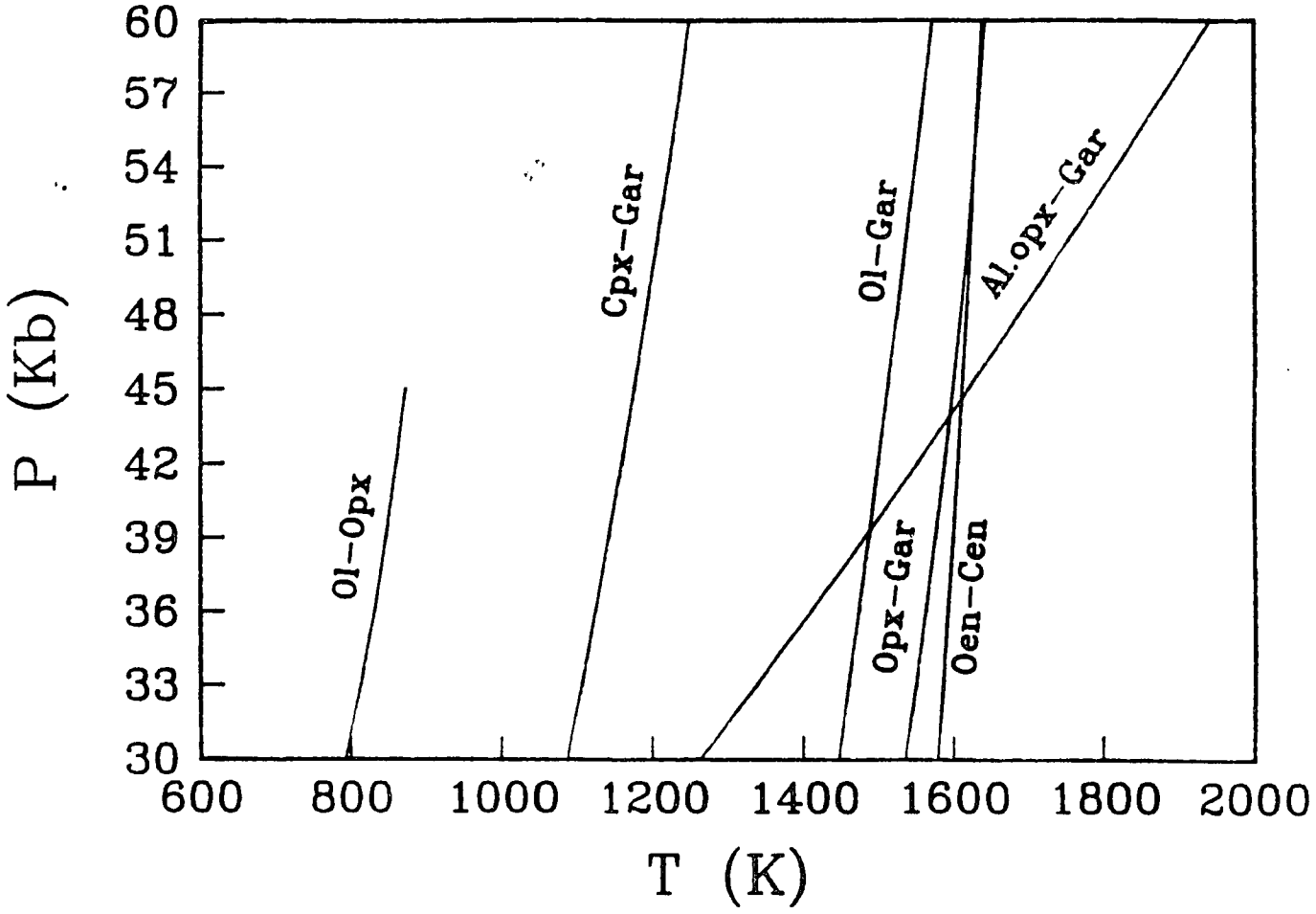

Figure 5.7: Calculated equilibria for Fe-Mg exchange reactions olivine-orthopyroxene, olivine-garnet, clinopyroxene-garnet and orthopyroxene-garnet, the polymorphic transition enstatite-clinoenstatite and the Al_2O_3-enstatite-pyrope equilibria at given chemical compositions of olivine, orthopyroxene, clinopyroxene and garnet (ultrabasic nodule sample 2573, Letseng-la-terae area, Lesotho; Boyd 1973).

i) SOLGASMIX

This is a versatile program which uses the principle of minimization of free energy of a system (Smith and Missen, 1982) discussed in Chapter 2. The program is written in FORTRAN by Eriksson (1975). The program is used not only to calculate the equilibrium assemblage under a given set of conditions which include pressure, temperature and bulk chemical composition, but also to calculate equilibrium amounts, mole-fractions, activities and the density of the assemblage. The program was modified by Fei (1988) to include the fluid phase in calculations using fugacities and mixing models of Saxena and Fei (1987a,b, 1988b). Thus, the fugacities and the composition of the fluid phase can also be calculated. A major advantage of using this program is that it tests for a global consistency of the data base in every calculation. Every possible phase combination that can form from the supplied bulk composition is tried until the combination that has the minimum free energy under the given pressure and temperature condition is selected. Thus, the phases which do not participate in the reaction equilibrium relating the assemblage are also considered in the calculation.

Thermodynamic data on the phases are supplied to the program in an external data file. Such a file is created through the program RETR which is described in Chapter 3. The solution parameters are supplied in a subroutine called FACTOR. Another subroutine called GAMMA1, which is called by FACTOR, is used to calculate activities of the end-members of the solid solution. This is done using the Bertrand-Kohler model described in Chapter 2. The fugacity expressions are programmed into the

main body of the program. Densities of each phase and the average density of the assemblage are calculated through the subroutine SPEQUA. This subroutine can also be modified to calculate distribution coefficients and other informations needed for specific calculations.

ii) THERMO

This program, written in FORTRAN, is designed to calculate equilibrium temperatures of assemblages at given pressures from chemical analyses of coexisting minerals. The program was originally written by Eriksson and Saxena (1984) and is modified in this study as described in the following paragraph. The program is available from the author upon request. Different reactions involving equilibrium phases present in the assemblage are considered. Most of these reactions are cation exchange reactions. Reactions involving fluids are not considered in this program. A list of the reactions that can be considered by the program is as follows:

Spinel + Fayalite = Hercynite + Forsterite

Forsterite + Orthoferrosilite = Fayalite + Orthoenstatite

Forsterite + Clinoferrosilite = Fayalite + Clinoenstatite

Forsterite + Almandine = Fayalite + Pyrope

Forsterite + 1/7 Grunerite = Fayalite + 1/7 Cummingtonite

Orthoenstatite + Clinoferrosilite = Orthoferrosilite + Clinoenstatite

Orthoenstatite + Almandine = Orthoferrosilite + Pyrope

Clinoenstatite + Almandine = Clinoferrosilite + Pyrope

Pyrope + 1/3 Annite = Almandine + 1/3 Phlogopite

Pyrope + 1/2 Ferrocordierite = Almandine + 1/2 Cordierite

1/3 Phlogopite + 1/2 Ferrocordierite = 1/3 Annite + 1/2 Cordierite

Clinoenstatite = Orthoenstatite

3 Orthoenstatite + Al_2O_3-Orthopyroxene = 3 Pyrope

Thermodynamic parameters of the phases and the solution parameters are incorporated in the program. Activity coefficients of the phases participating in the calculation are calculated using the Bertrand-Kohler model. This is done through the subroutine GAM1 written by the present author. The VdP integrals for solids are calculated using the Murnaghan equation of state and the heat capacity equation is from Fei and Saxena (1986). This part of the program is also written by the present author. Temperatures at eleven different pressures are calculated. This is done by taking trial values of temperatures until the total free energies of phases on either side of the reaction under consideration are equal. Depending on the presence or absence of certain elements in the minerals, certain reactions are not considered.

The compositions of the mineral phases are supplied in an external input file. An example of an input file is given in Table 5.1. The compositions should be in terms of the constituent oxides. The program can be slightly changed to accept compositions in terms of constituent

elements. When the program is run, the user is asked to enter an initial pressure and a pressure interval. Temperatures at eleven different pressures including the initial pressure and at the pressure interval entered are calculated.

An example of an output from the program is shown in Table 5.2. It shows the mole-fractions of end-members of the solution phases calculated from the mineral analysis. It also shows a list of the reactions considered and a table containing the temperatures calculated at each pressure for each reaction. Only temperatures in the range 600-2000 K are printed.

There are several limitations of this program. Amounts of certain major elements present in small amounts such as Cr, Mn, etc. are added to the amounts of the elements of similar affinity. For example, the amount of MnO is added to the amount of FeO in garnet. A major problem faced in the method followed in this program is in calculating end-member compositions of multicomponent-multisite solutions such as the pyroxenes. Certain assumptions are made while doing this. Accurate end-member compositions can only be calculated by considering the site-occupancy data of these minerals. This involves modeling of the solutions through ionic models. Moreover, site-occupancy data are not available in most cases. Another way to approach this problem is by using the principle of minimization of free energy of the solution. The stable composition of the mineral will have the least free energy of all compositions possible from the chemical analysis of the mineral. This is

the method followed in the program SOLGASMIX and is implemented here. In spite of the above limitations, this program is very useful for single site solutions.

iii) REAC

This program, also written in FORTRAN, is used to calculate pressures at given temperatures from given mole-fractions of phases participating in a reaction defined by the user. Some or all of the phases could be pure in the reaction. Reactions involving H_2O can also be used. With slight modifications in the program, other fluid phases can also be considered. However, unlike in the program THERMO, only one reaction can be considered at a time. The program is available from the author upon request.

Thermodynamic parameters of phases are read from an external file whose name is given as an input. Such a file is created through the program RETR. If the reaction involves phases with solid solutions, the interaction parameters are supplied in another external file. An example of a file containing the interaction parameters is given in Table 5.3.

When the program is run, the file containing the thermodynamic data is read by the program and the phases are listed. The user then defines the reaction by supplying the numbers of the phases appearing in the list and their stoichiometric coefficients in the balanced reaction. If the reaction contains fluid phases, the stoichiometric coefficients of the fluid phases are reentered. Then, if the reaction contains solution

phases, the user is asked to supply the name of the file containing the interaction parameters. The mole fractions of the solid solution phases are then entered. The user is finally asked to supply appropriate ranges of pressure and temperature and a temperature interval.

The pressures are calculated at each temperature by a process of iteration. An equilibrium is obtained when the two sides of the reaction under consideration have equal free energy. If equilibrium is not obtained in the pressure range specified, the user is asked to enter a new range of pressure. On the other hand, if equilibium is obtained, the pressures calculated at different temperatures are printed. This is also shown graphically in a pressure-temperature plot. An example of a typical run of the program is given in Table 5.4.

If desired, instead of calculating the equilibrium pressures, the free energy change and the equilibrium constant of the reaction at the given pressures and temperatures can be listed. This gives the user an idea of the ranges of pressure and temperature under which the equilibria occur.

This program has the same limitations as the program THERMO. In this case, the mole-fractions of the end-members are supplied by the user. But the problem of calculating the mole-fractions from the chemical analysis of the mineral remains. Nevertheless, the program is useful. The advantage of this program over THERMO is that any reaction can be defined by the user whereas, in THERMO a set of reactions is predefined

in the program. The disadvantage is that only reaction can be considered during a single run of the program.

TABLE 5.1 Sample input file for program THERMO
Sample 2573 (Boyd, 1973)

```
'2573 Nixon (p. 34)'
'Spinel'
      '  FEO'  0.0
      '  MNO'  0.0
      '  MGO'  0.0
'Olivine'
      '  FEO'  9.38
      '  MNO'  0.1
      '  MGO' 50.23
      '  CAO'  0.0
      '  NIO'  0.0
'Opx'
      ' TIO2'  0.0
      'AL2O3'  1.45
      'CR2O3'  0.24
      '  FEO'  5.56
      '  MNO'  0.13
      '  MGO' 34.45
      '  CAO'  1.42
      ' NA2O'  0.0
'Cpx'
      ' TIO2'  0.0
      'AL2O3'  2.75
      'CR2O3'  0.68
      '  FEO'  4.04
      '  MNO'  0.14
      '  MGO' 21.16
      '  CAO' 15.03
      ' NA2O'  1.59
'Garnet'
      '  FEO'  7.14
      '  MNO'  0.26
      '  MGO' 22.5
      '  CAO'  4.42
      ' NA2O'  0.0
'Biotite'
      '  FEO'  0.0
      '  MNO'  0.0
      '  MGO'  0.0
      '  CAO'  0.0
'Grunerite'
      '  FEO'  0.0
      '  MNO'  0.0
      '  MGO'  0.0
      '  CAO'  0.0
      ' NA2O'  0.0
```

```
'Cordierite'
      '  FEO'  0.0
      '  MNO'  0.0
      '  MGO'  0.0
'END'
```

The first line represents the sample number. The apostrophies and the last line are important and must not be deleted. Mineral names and the order also must not be changed. However, If a mineral is not present, it can be deleted. In the above example, spinel, biotite, grunerite and cordierite can be deleted.

TABLE 5.2 Sample output from program THERMO
Sample 2573 (Boyd, 1973)

```
 NAME OF INPUT FILE: Z2573
 SAMPLE & ANALYSIS NO.:  2573 Nixon (p. 34)

 FOR  0.9043   FAY  0.0957
 OEN  0.8756   OFE  0.0811   ODI  0.0244   OHE  0.0023   OAL  0.0166
 CEN  0.4616   CFE  0.0512   CDI  0.3925   CHE  0.0435   CAL  0.0094 JAD  0.0417
 PYR  0.7543   ALM  0.1392   GRO  0.1065

 REACTIONS CONSIDERED
  2  1/2MG-OL + FESIO3-OPX = 1/2FE-OL + MGSIO3-OPX
  3  1/2MG-OL + FESIO3-CPX = 1/2FE-OL + MGSIO3-CPX
  4  1/2MG-OL + 1/3FE-GAR = 1/2FE-OL + 1/3MG-GAR
  6  MGSIO3-OPX + FESIO3-CPX = FESIO3-OPX + MGSIO3-CPX
  7  MGSIO3-OPX + 1/3FE-GAR = FESIO3-OPX + 1/3MG-GAR
  8  MGSIO3-CPX + 1/3FE-GAR = FESIO3-CPX + 1/3MG-GAR
 12  MGSIO3-OPX = MGSIO3-CPX
 13  3MGSIO3-OPX + AL2O3-OPX = MG-GAR
                                    TEMPERATURE OF FORMATION
 REACTION                             PTOT/KBAR
             30    33    36    39    42    45    48    51    54    57    60
      2     793   814   832   847   861   874
      3
      4    1448  1461  1475  1488  1500  1513  1526  1538  1550  1562  1574
      6
      7    1536  1551  1564  1577  1589  1600  1610  1620  1628  1636  1643
      8    1086  1106  1124  1142  1160  1176  1192  1208  1223  1237  1250
     12    1580  1587  1593  1600  1606  1612  1618  1624  1629  1634  1640
     13    1263  1338  1411  1482  1552  1620  1687  1752  1817  1880  1942
 TEMPERATURES OF FORMATION OUTSIDE THE RANGE 600-2000 K ARE NOT GIVEN
```

The first two lines print the name of the input file (given in Table 5.1) and the sample number. The next section gives the mole-fractions of end-members calculated from the oxide analysis. The abbreviations used are:
FOR: forsterite, FAY: fayalite, OEN: orthoenstatite,
OFE: orthoferrosilite, ODI: orthodiopside , OHE: orthohedenbergite,
OAL: Al_2O_3-orthopyroxene, CEN: clinoenstatite, CFE: clinoferrosilite,
CDI: clinodiopside, CHE: clinohedenbergite, CAL: Al_2O_3-clinopyroxene,
JAD: jadeite, PYR: pyrope, ALM: almandine, GRO: grossular
The next section gives the reactions considered in the calculation. The last section tabulates the temperatures at different pressures (left to right) for reactions identified by the numbers in the first column.

TABLE 5.3 Sample solution data file used as input in program REAC

	4						
	-1 3						
W12	12050.0	11.76	-0.0016133	0	0.02	1	0
W13	4184.0	15.61	0	0	0.1	0	0
W23	4560.6	-16.07	0.0126	0	0.1	1	0
W21	-5258.0	-10.146	0.0037	0	-0.003	1	0
W31	16931.25	0	0	0	0	0	0
W32	-3026.43	-16.07	0.0126	0	0	1	0
	-1 2						
W12	1689.5	0	0	0	0	0	0
W21	1846.9	0	0	0	0	0	0
	1 3						
W12	-5258.0	-10.146	0.0037	0	-0.003	1	0
W13	4560.6	-16.07	0.0126	0	0.1	1	0
W23	4184.0	15.61	0	0	0.1	0	0
W21	12050.0	11.76	-0.0016133	0	0.02	1	0
W31	-3026.43	-16.07	0.0126	0	0	1	0
W32	16931.25	0	0	0	0	0	0
	1 2						
W12	1846.9	0	0	0	0	0	0
W21	1689.5	0	0	0	0	0	0

This is a data file containing interaction parameters for the reaction:

pyrope + 1/3 annite = almandine + 1/3 phlogopite

The first column in only for explanation and should not be used in the actual data file. The first line indicates the number of solution phases in the reaction. The second line indicates the stoichiometric coefficient (negative for reactants and positive for product phases) of the first phase (pyrope) in the balanced reaction and the number of other end members associated with it in the solution (almandine and grossular). The following three lines give the interaction parameters W12, W13, W23, W21, W31, and W32. Each line represents a single W parameter broken down into WH, WS1, WS2, WS3, WV, b and c, where,

$$WS = WS1 + WS2*T^{b} + WS3*T^{c}.$$

The same order is then followed for the other solution phases (annite, almandine and phlogopite in this sequence).

TABLE 5.4 Sample output from program REAC

```
 Enter name of data file:                FIN
  1 STEAM            2 CARBON DIO       3 METHANE          4 CARBON MON
  5 OXYGEN           6 HYDROGEN         7 SPINEL           8 HERCYNITE
  9 FORSTERITE      10 FAYALITE        11 ORTHOENSTA      12 ORTHODIOPS
 13 ORTHOFERRO      14 ORTHOHEDEN      15 AL-ORTHOPY      16 PYROPE
 17 ALMANDINE       18 GROSSULAR       19 SPESSARTIN      20 PHLOGOPITE
 21 ANNITE          22 CORDIERITE      23 FERROCORDI      24 HYDR-CORD
 25 ALBITE          26 HIGH SANID      27 ANORTHITE       28 QUARTZ
 29 CORUNDUM        30 FEO             31 PERICLASE       32 CAO
 33 K2O             34 CARBON          35 IRON(BCC)       36 MAGNETITE
 37 ANDALUSITE      38 KYANITE         39 SILLIMANIT      40 WOLLASTONI

 Enter total no. of phases in the reaction  =    4
 Enter no. of moles of phases (+pr/-re) =   -1  -1   1   1
 Enter name of solution file (Enter "H" for help):  GTBT.SOL
 Enter mol. frac. of each participant member =   0.3350
 Enter mol. frac. of each additional member =   0.1000
 Enter mol. frac. of each participant member =   0.4700
 Enter mol. frac. of each participant member =   0.5650
 Enter mol. frac. of each additional member =   0.1000
 Enter mol. frac. of each participant member =   0.5300
       Enter nos. of phases from above list =   16  21  17  20
 Enter Tmin, Tmax & interval =   1223.0  1273.0    10.0
 Enter Pmin, Pmax =      1.0 20000.0
  P(kb)          T(K)                      PRESSURE, kbar
                        0         4         8        12        16        20
                        I---------I---------I--------I---------I---------I---
   1.99          1223.0 I    +
   4.72          1233.0 I         +
   7.51          1243.0 I                   +
  10.35          1253.0 I                            +
  13.24          1263.0 I                                    +
  16.18          1273.0 I                                              +
```

Output from REAC showing the calculated equilibria for the reaction

pyrope + 1/3 annite = almandine + 1/3 phlogopite

for a given composition of garnet ($Pyr_{.335}Alm_{.565}Gro_{.1}$) and biotite ($Phl_{.53}Ann_{.47}$). The first segment contains the name of the file containing the free energy data and a list of the phases read form that file. The second segment contains the definition of the reaction, the mole fractions of the participating phases and the pressure and temperature ranges of interest. It also contains the name of the data file containing the interaction parameters for the defined reaction (GTBT.SOL as shown in Table 5.3). The last segment shows tabulated values of equilibrium pressures and temperatures and a graphical representation of the result.

REFERENCES

Adams, G.E. and Bishop, F.C. (1985) An experimental investigation of thermodynamic mixing properties and unit-cell parameters of forsterite-monticellite solid solution. Amer. Mineral., 70, 714-722.

Akimoto, S. (1972) The system MgO-FeO-SiO_2 at high pressures and temperatures - Phase equilibria and elastic properties. Tectonophysics, 13, 167-187.

Althaus, E. (1967) The triple point andalusite-sillimanite-kyanite. Contr. Mineral. Petrol., 16, 29-44.

Althaus, E., Karotke, E., Nitsch, K.H. and Winkler, H.G.F. (1970) An experimental re-examination of the upper stability limit of muscovite plus quartz. N. Jahbr. Mineral. Monatsh., 325-336.

Anovitz, L.M., Essene, E.J., Hemingway, B.S., Komada, N.L. and Westrum, E.F. (1988) The heat-capacities of grunerite and deerite: phase equilibria in the system Fe-Si-C-O-H and implications for the metamorphism of banded iron formations. EOS Trans., AGU, 69, no. 16, pp. 515.

Anovitz, L.M., Treiman, A.H., Essene, E.J., Hemingway, B.S., Westrum, E.F., Wall, V.J., Burriel, R. and Bohlen, S.R. (1985) The heat capacity of ilmenite and phase equilibria in the system Fe-Ti-O. Geochim. Cosmochim. Acta 49, 2027-2040.

Barnes, H.L. and Ernst, W.G. (1963) Ideality and ionization in hydrothermal fluids: the system MgO-H_2O-$NaOH$. Amer. J. Sci., 261, 129-150.

Bass, J.D. and Weidner, D.J. (1984) Elasticity of single-crystal orthoferrosilite. J. Geophy. Res. 89, 4359-4371.

Berman, R.G., (1988) Internally consistent thermodynamic data for minerals in the system Na_2O-K_2O-CaO-MgO-FeO-Fe_2O_3-Al_2O_3 -SiO_2-TiO_2-H_2O-CO_2. J. Petrol., 29, 445-552.

Berman, R.G. and Brown, T.H. (1984) A thermodynamic model for multicomponent melts, with application to the system CaO-Al_2O_3-SiO_2. Geochim. Cosmochim. Acta, 48, 661-678.

Berman, R.G., Engi, M., Greenwood, H.J. and Brown, T.H. (1986) Derivation of internally-consistent thermodynamic data by the technique of mathematical programming: a review with application to the system MgO-SiO_2-H_2O. J. Petrol., 27,1331-1364.

Bertrand, G.L., Acree, W.E. and Burchfield, T. (1983) Thermochemical excess properties of multicomponent systems: representation and estimation from binary mixing data. J.Sol.Chem. 12, 327-340.

Bhattacharya, A. and Sen, S.K. (1985) Energetics of hydration of cordierite and water barometry in cordierite-granulites. Contr. Mineral. Petrol., 89, 370-378.

Birch, F. (1966) Compressibility; Elastic constants. In "Handbook of physical constants", Clark, S.P. (ed.). Geol. Soc. Am. Memoirs. 97, 77-173.

Boettcher, A.L. (1970) The system $CaO-Al_2O_3-SiO_2-H_2O$ at high pressures and temperatures. J. Petrol., 11, 337-379.

Bohlen, S.R. and Boettcher, A.L. (1981) Experimental investigations and geological applications of orthopyroxene geobarometry. Amer. Mineral. 66, 951-964.

Bohlen, S.R. and Liotta, J.J. (1986) A barometer for garnet amphibolites and garnet granulites. J. Petrol. 27, 1025-1034.

Bohlen, S.R., Dollase, W.A. and Wall, V.J. (1986) Calibration and applications of spinel equilibria in the system $FeO-Al_2O_3-SiO_2$. J. Petrol., 27, 1143-1156.

Bohlen, S.P., Essene, E.J. and Boettcher, A.L. (1980) Reinvestigation and application of olivine-quartz-orthopyroxene barometry. Earth Planet. Sci. Lett., 47, 1-10.

Bohlen, S.R., Wall, V.J. and Boettcher, A.L. (1983a) Experimental investigation and application of garnet granulite equilibria. Contr. Mineral. Petrol., 83, 52-61.

Bohlen, S.R., Wall, V.J. and Boettcher, A.L. (1983b) Experimental investigations and geological applications of equilibria in the system $FeO-TiO_2-Al_2O_3-SiO_2-H_2O$.. Amer. Mineral. 68, 1049-1058.

Bohlen, S.R., Boettcher, A.L., Wall, V.J. and Clemens, J.D. (1983c) Stability of phlogopite-quartz and sanidine-quartz: a model for melting in the lower crust. Contr. Mineral. Petrol., 83, 273-277.

Bokreta, M. (1989) Lattice energy calculations. Ph.D. thesis, Univ. Penn., Philadelphia.

Bonzcar, L.J., Graham, E.K. and Wang, H. (1977) The pressure and temperature dependence of the elastic constants of pyrope garnet. J. Geophy. Res. 82, 2529-2534.

Boyd, A.R. (1973) Appendix of mineral analyses. In 'Lesotho Kimberlites', (P.H. Nixon, ed.), Lesotho National Development Corporation, Maseru, (350 p), 33-36.

Brace, W.F., Scholz, C.H. and LaMori, P.N. (1969) Isothermal compressibility of kyanite, andalusite and sillimanite from synthetic aggregates. J. Geophys. Res., 74, 2089-2098.

Brousse, C., Newton, R.C. and Kleppa, O.J. (1984) Enthalpy of formation of forsterite, enstatite, akermanite, monticellite and merwinite at 1073 K determined by alkali borate solution calorimetry. Geochim. Cosmochim. Acta 48, 1081-1088.

Burnham, C.W., Holloway, J.R. and Davis, N.F. (1969) Thermodynamic properties of water to 1000°C and 10,000 bars. Geol. Soc. Amer. Special Paper 32.

Carlson, W.D. and Lindsley, D.H. (1988) Thermochemistry of pyroxenes on the join $Mg_2Si_2O_6$-$CaMgSi_2O_6$ Amer. Mineral., 73, 242-252.

Carmichael R.S. (1982) Handbook of physical properties of rocks. CRC Press.

Chang, Z.P. and Barsch, G.R. (1973) Pressure dependence of single-crystal elastic constants and anharmonic properties of spinel. J. Geophy. Res. 78, 2418.

Charlu, T.V., Newton, R.C. and Kleppa O.J. (1981) Thermochemistry of synthetic $Ca_2Al_2SiO_7$ (gehlenite) - $Ca_2MgSi_2O_7$ (akermanite) melilites. Geochim. Cosmochim. Acta 45, 1609-1617.

Charlu, T.V., Newton, R.C. and Kleppa O.J. (1978) Enthalpy of formation of lime silicates by high temperature calorimetry, with discussion of high pressure phase equilibrium. Geochim. Cosmochim. Acta 42, 367-375.

Charlu, T.V., Newton, R.C. and Kleppa, O.J. (1975) Enthalpies of formation in the system MgO-Al_2O_3-SiO_2 from high temperature solution calorimetry. Geochim. Cosmochim. Acta 39, 1487-1497,

Chatillon-Colinet, C., Kleppa, O.J., Newton, R.C. and Perkins D. (1983a) Enthalpy of formation of $Fe_3Al_2Si_3O_{12}$ (almandine) by high temperature alkali borate solution calorimetry. Geochim. Cosmochim. Acta, 47, 439-444.

Chatillon-Colinet, C., Newton, R.C., Perkins, D. and Kleppa, O.J.(1983b) Thermochemistry of $(Fe^{2+},Mg)SiO_3$ orthopyroxene. Geochim. Cosmochim. Acta 47, 1597-1603.

Chatterjee, N. (1987) Evaluation of thermochemical data on Fe-Mg olivine, orthopyroxene, spinel and Ca-Fe-Mg-Al garnet. Geochim. Cosmochim. Acta 51, 2515-2525.

Chatterjee, N.D. (1972) The upper stability limit of the assemblage paragonite + quartz and its natural occurances. Contr. Mineral. Petrol., 34, 288-303.

Chatterjee, N.D. (1970) Synthesis and upper stability of paragonite. Contr. Mineral. Petrol., 27, 244-257.

Chatterjee, N.D. and Flux, S. (1986) Thermodynamic mixing properties of muscovite-paragonite crystalline solutions at high

temperatures and pressures, and their geological applications. J. Petrol., 27, 677-693.

Chatterjee, N.D. and Froese, E. (1975) A thermodynamic study of the pseudobinary join muscovite-paragonite in the system $KAlSi_3O_8$-$NaAlSi_3O_8$-Al_2O_3-SiO_2-H_2O. Amer. Mineral., 60, 985-993.

Chatterjee N.D. and Johannes, W. (1974) Thermal stability and standard thermodynamic properties of synthetic $2M_1$ muscovite, $KAl_2[AlSi_3O_{10}](OH)_2$. Contr. Mineral. Petrol., 48, 89-114.

Chernosky, J.V. (1982) The stability of clinochrysotile. Can. Mineral., 20, 19-27.

Chernosky, J.V. (1976) The stability field of anthophyllite - A reevaluation based on new experimental data. Amer. Mineral., 61, 1145-1155.

Chernosky, J.V. and Autio, L.K. (1979) The stability of anthophyllite in the presence of quartz. Amer. Mineral., 64, 294-303.

Chernosky, J.V., Day, H.W. and Caruso, L.J. (1985) Equilibria in the system MgO-SiO_2-H_2O: experimental determination of the stability of Mg-anthophyllite. Amer. Mineral., 70, 223-236.

Clemens, J.D., Circone, S., Navrotsky, A., McMillan, P.F., Smith, B.K. and Wall, V.J. (1987) Phlogopite: High temperature solution calorimetry, thermodynamic properties, Al-Si and stacking disorder, and phase equilibria. Geochim. Cosmochim. Acta, 51, 2569-2578.

Cohen, L.H. and Klement, W. (1967) High-low quartz inversion: determination to 35 kilobars. J. Geophys. Res., 72, 4245-4251.

Czank, M. and Schultz, H. (1971) Thermal expansion of anorthite. Naturwiss, 58, 94.

Danckwerth, P.A. and Newton, R.C. (1978) Experimental determination of the spinel peridotite to garnet peridotite reaction in the system MgO-Al_2O_3-SiO_2 in the range 900-1100°C and Al_2O_3 isopleths of enstatite in the spinel field. Contr. Mineral. Petrol., 66, 189-201.

Day, H.W. (1973) The high temperature stability of muscovite plus quartz. Amer. Mineral., 58, 255-262.

Day, H.W. and Kumin, H.J. (1980) Thermodynamic analysis of the aluminum silicate triple point. Amer. J. Sci., 280, 265-287.

Day, H.W., Chernosky, J.V. and Kumin, H.J. (1985) Equilibria in the system MgO-SiO_2-H_2O; a thermodynamic analysis. Amer. Mineral., 70, 237-248.

Dixon, J.R. (1980) A spinel lherzolite barometer. Ph. D. thesis, Univ. of Texas, Dallas.

Engi, M. (1983) Equilibria involving Al-Cr spinel: Mg-Fe exchange with olivine. Experiments, thermodynamic analysis, and consequences for geothermometry. Amer. J. Sci. 283A, 29-71.

Engi, M. (1980) The solid solution behavior of olivine in the temperature range from 500 K - 1500 K. Geol. Soc. Amer. Abst. Prog., 12, 421.

Eriksson, G. (1975) Quantitative equilibrium calculations in multiphase systems at high temperatures, with special reference to the roasting of chalocopyrite (CuFeS2). Akademisk Avhandling, Umea Univesitet.

Eriksson, G. and Rosen, E. (1973) Thermodynamic studies of high temperature equilibria. VIII. General equations for the calculation of equilibria in multiphase systems. Chemica Scripta 4, 193-194.

Eriksson, G. and Saxena, S.K. (1984) Personal communication.

Eugster, H.P. and Wones, D.R. (1962) Stability relations of the ferruginous biotite, annite. J. Petrol., 3, 82-125.

Eugster, H.P., Albee, A.L., Bence, A.E., Thompson, J.B., Jr. Waldbaum, D.R. (1972) The two-phase region and excess mixing properties of paragonite-muscovite crystalline solutions. J. Petrol., 13, 147-179.

Evans, B.W. (1977) Metamorphism of alpine peridotite and serpentinite. Ann. Rev. Earth Planet. Sci., 5, 397-447.

Evans, B.W. (1965) Application of a reaction-rate method to the breakdown equilibria of muscovite and muscovite plus quartz. Amer. J. Sci., 263, 647-667.

Evans, B.W., Johannes, W., Oterdoom, W.H. and Trommsdorff, V. (1976) Stability of chrysotile and antigorite in the serpentinite multisystem. Schweiz. Mineral. Petrograph. Mitteilungen, 56, 79-93.

Fawcett, J.J. and Yoder, H.S. (1966) Phase relations of chlorites in the system MgO-Al_2O_3-SiO_2-H_2O at 2 kbar water pressure. Amer. Mineral., 51, 353-380.

Fei, Y. (1988) Personal communication.

Fei, Y. and Chatterjee, N. (1988) Optimized thermodynamic data on hydrous phases in the system MgO-SiO_2-H_2O. EOS Transactions, AGU. v. 69, p. 473.

Fei, Y. and Saxena, S.K. (1987) An equation for the heat capacity of solids. Geochim. Cosmochim. Acta, 51, 251-254.

Fei, Y. and Saxena, S.K. (1986) A thermochemical data base for phase equilibria in the system Fe-Mg-Si-O at high pressure and temperature. Phys. Chem. Minerals, 13, 311-324.

Fenner, C.L. (1913) The stability relations of the silica minerals. Amer. J. Sci., 36, 331-384.

Ferry, J.M. and Spear, F.S. (1978) Experimental calibration of the partitioning of Fe and Mg between biotite and garnet. Contr. Mineral. Petrol., 66, 113-117.

Fisher, J.R. and Zen, E-an (1971) Thermodynamic calculations from hydrothermal phase equilibrium data and the free energy of H_2O. Amer. J. Sci., 270, 297-314.

Flux, S. and Chatterjee, N.D. (1986) Experimental reversal of the Na-K exchange reaction between muscovite-paragonite crystalline solutions and a 2 molal aqueous (Na,K)Cl fluid. J. Petrol., 27, 665-676.

Fonarev, V.I., Korol'kov, G.Ya., and Dokina, T.N. (1979) Laboratory data on the stability field of the cummingtonite+olivine+quartz association. Geokhimiya, 7, 984-995.

Forbes, W.C. (1977) Stability relations of grunerite, $Fe_7Si_8O_{22}(OH)_2$. Amer. J. Sci., 277, 735-749.

Franz, G. (1982) The brucite-periclase equilibrium at reduced H_2O activities: some information about the system H_2O-NaCl. Amer. J. Sci., 282, 1325-1339.

Fritz, I.J. (1974) Pressure and temperature dependences of the elastic properties of rutile (TiO_2). J. Phys. Chem. Solids. 35, 817.

Fyfe, W.S. (1962) On the relative stabilities of talc, anthophyllite and enstatite. Amer. J. Sci., 270, 151-154.

Ganguly, J. and Ghose, S. (1979) Aluminous orthopyroxene, order-disorder, thermodynamic properties and petrological implications. Contr. Mineral. Petrol., 68, 375-385.

Ganguly, J. and Saxena, S.K. (1988) Mixtures and mineral reactions. Springer-Verlag, New York, 291 p.

Ganguly, J. and Saxena, S.K. (1984) Mixing properties of aluminosilicate garnets:constraints from natural and experimental data and application to geothermobarometry. Amer. Mineral. 69,88-97.

Gasparik, T. (1985) Experimentally determined compositions of diopside-jadeite pyroxene in equilibrium with albite and quartz at 1200-1350°C and 15-34 kbar. Geochim. Cosmochim. Acta, 49, 865-870.

Gasparik, T. (1984a) Two-pyroxene thermobarometry with new experimental data in the system CaO-MgO-Al_2O_3-SiO_2. Contr. Mineral. Petrol., 87, 87-97.

Gasparik, T. (1984b) Experimental study of subsolidus phase relations and mineral properties of pyroxene in the system CaO-Al_2O_3-SiO_2. Geochim. Cosmochim. Acta, 48, 2537-2545.

Gasparik, T. (1984c) Experimentally determined stability of clinopyroxene+garnet+corundum in the system CaO-MgO-Al_2O_3-SiO_2. Amer. Mineral., 69, 1025-1035.

Gasparik, T. (1981) Thermodynamic properties of pyroxenes in the NCMAS system saturated with silica. Ph.D. dissertation, State Univ. New York, Stony Brook.

Gasparik, T. and Newton, R.C. (1984) The reversed alumina contents of orthopyroxene in equilbrium with spinel and forsterite in the system MgO-Al_2O_3-SiO_2. Contr. Mineral. Petrol., 85, 186-196.

Goldsmith, J.R. (1980) The melting and breakdown reactions of anorthite at high pressures and temperatures. Amer. Mineral., 65, 272-284.

Gordon, T.M. (1973) Determination of internally consistent thermochemical data from phase equilibrium experiments. J. Geol., 81, 199-208.

Greenwood, H.J. (1963) The synthesis and stability of anthophyllite. J. Petrol., 4, 317-351.

Grimsditch, M.H. and Ramdas, A.K. (1976) Elastic and elasto-optic constants of rutile from a Brillouin scattering study. Phys. Rev. 14, 1670.

Haar, C., Gallagher, J.S. and Kell, G.S. (1984) NBS/NRC Steam Tables. Thermodynamic and transport properties and computer programs for vapor and liquid states of water in SI units. Hemisphere Publishing Co., Washington.

Haas, J.L. and Fisher, J.R. (1976) Simultaneous evaluation and correlation of thermochemical data. Amer. J. Sci. 276, 525-545.

Haas, J.L., Robinson, G.R.,Jr. and Hemingway, B.S. (1981) Thermodynamic tabulations for selected phases in the system CaO-Al_2O_3-SiO_2-H_2O at 101.325 KPa (1 atm) between 273.15 and 1800 K. J. Phys. Chem. Ref. Data, 10, 575-669.

Hackler, R.T. and Wood, B.J. (1988) Experimental determination of Fe, Mg, Mn exchange between garnet and olivine. EOS Trans., AGU, 69, no. 16, pp. 512.

Halbach, H. and Chatterjee, N.D. (1984) An internally consistent set of thermodynamic data for twenty-one CaO-Al_2O_3-SiO_2-H_2O phases by linear programming. Contr. Mineral. Petrol., 88, 14-23.

Halbach, H. and Chatterjee, N.D. (1982) The use of linear parametric programming for determination of internally consistent thermodynamic data for minerals. In: Schreyer, W. (ed.) High-Pressure Researches in Geoscience. E. Schweizerbartsche Verlagsbuchhandlung, 475-491.

Halleck, P.M. (1973) The compression and compressibility of grossular garnet, a comparison of X-ray and ultrasonic methods. Ph.D. thesis, Univ. of Chicago, Ill.

Hankey, R.E. and Schuele, D.E. (1970) Third order elastic constants of Al_2O_3. J. Acoust. Soc. Amer. 48, 190-202.

Hariya, Y. and Kennedy, G.C. (1968) Equilibrium study of anorthite under high pressure and high temperature. Amer. J. Sci., 266, 193-203.

Harley S.L. (1984) An experimental study of the partitioning of Fe and Mg between garnet and orthopyroxene. Contr. Mineral. Petrol., 86, 359-373.

Haselton, H.T. (1979) Calorimetry of simple synthetic pyrope-grossular garnets and calculated stability relations. Ph.D. thesis, Univ. of Chicago, Ill., 98 p.

Haselton, H.T. and Westrum, E.F. (1980) Low-temperature heat capacities of synthetic pyrope, grossular and $pyrope_{60}grossular_{40}$. Geochim. Cosmochim. Acta, 44, 701-710.

Haselton, H.T., Hemingway, B.S. and Robie, R.A. (1984) Low temperature heat capacities of $CaAl_2SiO_6$ pyroxene. Amer. Mineral., 69, 481-489.

Haselton, H.T., Robie, R.A. and Hemingway, B.S. (1987) Heat capacities of synthetic hedenbergite, ferrobustamite, and $CaFeSi_2O_6$ glass. Geochim. Cosmochim. Acta, 51, 2211-2218.

Hays, J.F. (1966) Lime-alumina-silica. Carnegie Instn. Wash. Yr. Book, 65, 234-239.

Helgeson, H.C., Delany, J.M., Nesbitt, H.W. and Bird, D.K. (1978) Summary and critique of the thermodynamic properties of rock forming minerals. Amer. J. Sci., 278 A, 229.

Hemingway, B.S. and Robie, R.A. (1984) Heat capacity and thermodynamic functions for gehlenite and staurolite: with comments on the Schottky anomaly in the heat capacity of staurolite. Amer. Mineral., 69, 307-318.

Hemingway, B.S., Evans, H.T., Nord, G.L.Jr., Haselton, H.T., Robie, R.A. and McGee, J.J. (1986) Akermanite: phase transitions in heat capacity and thermal expansion, and revised thermodynamic data. Can. Mineral., 24, 425-434.

Hemingway, B.S., Krupka, K.M. and Robie, R.A. (1981) Heat capacities of the alkali feldspars between 350 and 1000 K from differential scanning calorimetry, the thermodynamic functions of the alkali feldspars from 298.15 to 1400 K, and the reaction quartz + jadeite = analbite. Amer. Mineral., 66, 1202-1215.

Hemley, J.J., Montoya, J.W., Christ, C.L. and Hostetler, P.B. (1977a) Equilibria in the $MgO-SiO_2-H_2O$ system: I. Talc-chrysotile-forsterite-brucite stability relations. Amer. J. Sci., 277, 322-351.

Hemley, J.J., Shaw, D.R. and Luce, R.W. (1977b) Mineral equilibria in the $MgO-SiO_2-H_2O$ system: II. Talc-antigorite-forsterite-anthophyllite-enstatite stability relations and some geologic implications in the system. Amer. J. Sci., 277, 353-383.

Hensen, B.J. (1972) Phase relations involving pyrope, enstatite and sapphirine in the system $MgO-Al_2O_3-SiO_2$. Yb. Carnegie Instn. Wash., 71, 421-427.

Hensen, B.J. and Green, D.H. (1973) Experimental study of the stability of cordierite and garnet in pelitic compositions at high pressures and temperatures. III. Synthesis of experimental data and geological applications. Contr. Mineral. Petrol., 38, 151-166.

Herzberg, C.T. (1983) The reaction forsterite+cordierite = aluminous orthopyroxene+spinel in the system $MgO-Al_2O_3-SiO_2$. Contr. Mineral. Petrol., 84, 84-90.

Herzberg, C.T. (1976) The plagioclase spinel-lherzolite facies boundary; its bearing on corona structure formation and tectonics of the Norwegian caledonides. In: "Progress in Experimental Petrology". London: NERC publications, D 3233-3235.

Hewitt, D.A. and Wones, D.R. (1984) Experimental phase relations of the micas, In "Reviews in Mineralogy, v.13", Ed: S.W. Bailey, Mineralogical Society of America, 201-256.

Holdaway, M.J. (1971) Stability of andalusite and the aluminosilicate phase diagram. Amer. J. Sci., 271, 97-131.

Holdaway, M.J. and Lee, S.M. (1977) Fe-Mg cordierite stability in high-grade pelitic rocks based on experimental, theoretical, and natural observations. Contr. Mineral. Petrol., 63, 175-198.

Holland, T.J.B. (1981) Thermodynamic analysis of simple mineral systems. In "Advances in Physical Geochemistry I", Newton, R.C., Navrotsky, A. and Wood, B.J. (eds.). New York: Springer-Verlag, 19-34.

Holland, T.J.B. (1980) The reaction albite = jadeite + quartz determined experimentally in the range 600-1200°C. Amer. Mineral., 65, 129-134.

Holland, T.J.B. (1979) Experimental determination of the reaction paragonite = jadeite + kyanite + H_2O, and internally consistent thermodynamic data for part of the system $Na_2O-Al_2O_3-SiO_2-H_2O$, with applications to eclogites and blueschists. Contr. Mineral. Petrol., 68, 293-301.

Holland, T.J.B., Navrotsky, A. and Newton, R.C. (1979) Thermodynamic parameters of $CaMgSi_2O_6-Mg_2Si_2O_6$ pyroxenes, based on

regular solutions and cooperative disordering models. Contr. Mineral. Petrol., 75, 305-306.

Huang, W.L. and Wyllie, P.J. (1974) Melting relations of muscovite with quartz and sanidine in the K_2O-Al_2O_3-SiO_2-H_2O system to 30 kilobars and an outline of paragonite melting relations. Amer. J. Sci., 274, 378-395.

Huckenholz, H.G., Holzel, E. and Lindhuber, W. (1975) Grossularite, its solidus and liquidus relations in the CaO-Al_2O_3-SiO_2-H_2O system upto 10 kbar. N. Jb. Mineral. Abh., 124, 1-46.

Irving, A.J., Huang, W.L. and Wyllie, J. (1977) Phase relation of portlandite, $Ca(OH)_2$ and brucite, $Mg(OH)_2$ to 33 kilobars. Amer. J. Sci., 277, 313-321.

Ivanov, I.P. and Gusynin, V.F. (1970) Stability of paragonite in the system SiO_2-$NaAlSi_3O_8$-Al_2O_3-H_2O. Geochem. Intern., 7, 578-587, Trans. from Geokhimiya, 7, 801-811.

Ivanov I.P., Potekhin, V.Y., Dmitriyenko, L.T. and Beloborodov, S.M. (1973) An experimental study of T and P conditions of equilibrium of reaction: muscovite - K-feldspar + corundum + H_2O at $P(H_2O) < P(total)$. Trans. from Geokhimiya, 9, 1300-1310.

Jamieson, H.E. and Roeder, P.L. (1984) The distribution of Mg and Fe^{2+} between olivine and spinel at 1300 C. Amer.Mineral., 69, 283-291.

Jenkins, D.M. and Newton, R.C. (1979) Experimental determination of the spinel peridotite to garnet peridotite inversion at 900° C and 1000° C in the system CaO-MgO-Al_2O_3-SiO_2 and at 900° C with natural garnet and olivine. Contr. Mineral. Petrol., 68, 407-419.

Johannes, W. (1968) Experimental investigation of the reaction forsterite + H_2O = serpentine + brucite. Contr. Mineral. Petrol., 19, 309-315.

Kalinin, D.V. and Zubkov, M.Y. (1981) Kinetic investigation of the MgO-SiO_2-H_2O system, reaction: serpentine = forsterite + talc + water. Soviet. Geol. Geophys., 22, 61-68.

Kawasaki, T. (1979) Thermodynamic analyses on the Fe-Mg exchange equilibrium between olivine and garnet: An application to the estimation of P-T relations of ultramafic rocks. J. Japan. Assoc. Mineral. Petrol. Econ. Geol. 74, 395-405.

Kawasaki, T. and Matsui, Y. (1983) Thermodynamic analysis of equilibria involving olivine, orthopyroxene and garnet. Geochim. Cosmochim. Acta 47, 1661-1680.

Kawasaki, T. and Matsui, Y. (1977) Partioning of Fe^{+2} and Mg^{+2} between olivine and garnet. Earth Planet. Sci. Lett. 37, 159-166.

Kerrick, D.M. (1972) Experimental determination of muscovite + quartz stability with $P(H_2O) < P(total)$. Amer. J. Sci., 272, 946-958.

Kerrick, D.M. and Ghent, E.D. (1979) P-T-XCO_2 relations of equilibria in the system: CaO-Al_2O_3-SiO_2-CO_2-H_2O. In: Zharikov, V.A., Fonarev, V.I., Korikovshii, V.A., (eds.) Problems in Physico-Chemical Petrology, Academy of Sciences of the USSR, 2, 32-52.

King, E.G., Ferrante, M.J. and Pankratz, L.B. (1975) Thermodynamic data for $Mg(OH)_2$ (brucite). U.S. Bur. Mines Rep. Invest. 8041, 13 pp.

King, E.G., Barany, R., Weller, W.W. and Pankratz, L.B. (1967) Thermodynamic properties of forsterite and serpentine. U.S. Bur. Mines Rep. Invest. 6962, 19 pp.

Kiseleva, I.A., Ogorodova, L.P., Topor, N,D, and Chigareva, O.G. (1979) A thermochemical study of the CaO-MgO-SiO_2 system. Geokhimiya, 12, 1811-1825 (in Russian).

Kitihara, S., Takenouchi, S. and Kennedy, G.C. (1966) Phase relations in the system MgO-SiO_2-H_2O at high temperatures and pressures. Amer. J. Sci., 264, 223-233.

Klein, C. and Waldbaum, D.R. (1967) X-ray crystallographic properties of the cummingtonite-grunerite series. J. Geol., 75, 379-392.

Koziol, A.M. and Newton, R.C. (1988a) Redetermination of the anothite breakdown reaction and improvement of the plagioclase-garnet-Al_2SiO_5-quartz geobarometer. Amer. Mineral., 73, 216-223.

Koziol, A.M. and Newton, R.C. (1988b) Experimental determination of almandine-grossular and (Ca, Fe, Mg) ternary garnet solid solution relations. EOS Trans., AGU, 69, no. 16, pp. 498.

Krupka, K.M., Hemingway, B.S., Robie, R.A. and Kerrick, D.M. (1985a) Low temperature heat capacities and derived thermodynamic properties of anthophyllite, diopside, enstatite, bronzite and wollastonite. Amer. Mineral., 70, 249-260.

Krupka, K.M., Hemingway, B.S., Robie, R.A. and Kerrick, D.M. (1985b) High temperature heat capacities and derived thermodynamic properties of anthophyllite, diopside, dolomite, enstatite, bronzite, talc, tremolite and wollastonite. Amer. Mineral., 70, 261-271.

Krupka, K.M., Robie, R.A. and Hemingway, B.S. (1979) High-temperature heat capacities of corundum, periclase, anorthite, $CaAl_2Si_2O_8$ glass, muscovite, pyrophyllite, $KAlSi_3O_8$ glass, grossular and $NaAlSi_3O_8$ glass. Amer. Mineral., 64, 86-101.

Kunze, G. (1961) Antigorit: Strukturtheoretische Grundlagen und ihre praktische Bedeutung fuer die weitere Serpentin-Forschung. Fortschr. Mineral., 39, 206-324.

Kushiro, I. and Yoder, H.S. (1966) Anorthite-forsterite and anorthite-enstatite reactions and their bearing on the basalt-eclogite transformation. J. Petrol., 7, 337-362.

Lane, D. and Ganguly, J. (1980) Al_2O_3 solubility in orthopyroxene in the system $MgO-Al_2O_3-SiO_2$. A reevaluation of the mantle geotherm. J. Geophys. Res., 85, 6963-6972.

Lee, H.Y. and Ganguly, J. (1987) Fe^{2+}-Mg fractionation between garnet and orthopyroxene: experimental determination in the FMAS system and application to geothermometry. J. Petrol., in press.

Leitner, B.J., Weidner, D.J. and Liebermann, R.C. (1980) Elasticity of single crystal pyrope and implications for garnet solid solution series. Phys. Earth Planet. Inter. 22, 111.

Liebermann, R.C. (1974) Compressional velocities of polycrystalline olivine, spinel and rutile minerals. Earth Planet. Sci. Lett. 17, 263-268.

Liebermann, R.C. and Ringwood, A.E. (1976) Elastic properties of anorthite and the nature of the lunar crust. Earth Planet. Sci. Lett., 31, 69-74.

Lindsley, D.H. (1983) Pyroxene thermometry. Amer. Mineral., 68, 477-493.

Lindsley, D.H., Grover, J.E. and Davidson, P.M. (1981) The thermodynamics of the $Mg_2Si_2O_6$-$CaMgSi_2O_6$ join: a review and an improved model. In: Newton, R.C., Navrotsky, A. & Wood, B.J. (eds.), "Advances in Physical Geochemistry, 1". New York: Springer-Verlag.

Matsui, Y. and Nishizawa, O. (1974) Iron (II)-magnesium exchange equilibrium between olivine and calcium-free pyroxene over a temperature range 800 to 1300°C. Bull. Soc. fr. Mineral. Crystallogr., 97, 122-130.

Mel'nik, Yu.P. and Radchuk, V.V. (1977) The stability of grunerite-$Fe_7Si_8O_{22}(OH)_2$. Geokhimiya, 5, 693-704 (in Russian).

Metz, G.W., Anovitz, L.M. and Essene, E.J. (1983) The heat capacity and phase equilibria of almandine. EOS Trans., AGU, 64, no. 18, pp. 346.

Mirwald, P.W. and Massonne, H.J. (1980) The low-high quartz and quartz-coesite transition to 40 kbar between 600 and 1600°C and some reconnaissance data on the effect of $NaAlO_2$ component on the low quartz-coesite transition. J. Geophys. Res., 85, 6983-6990.

Miyano, T. and Klein, C. (1986) Fluid behavior and phase relations in the system Fe-Mg-Si-C-O-H: Application to high grade metamorphism of iron-formations. Amer. J. Sci., 286, 540-575.

Miyano, T. and Klein, C. (1983) Phase relations of orthopyroxene, olivine and grunerite in high-grade metamorphic iron-formation. Amer.

Mineral., 68, 699-716.

Mukhopadhyay, D.K. and Lindsley, D.H. (1983) Phase relations in the join kirschsteinite ($CaFeSiO_4$)-fayalite (Fe_2O_4). Amer. Mineral., 68, 1089-1094.

Nekvasil, H. (1986) A theoretical thermodynamic investigation Ab-Or-An-Qz-H_2O and implications for melt speciation. Ph.D. Thesis, Penn State Univ., 268 pp.

Newton, R.C. (1969) Some high-pressure hydrothermal experiments on severely ground kyanite and sillimanite. Amer. J. Sci., 267, 278-294.

Newton, R.C. (1966) Some calc-silicate equilibrium relations. Amer. J. Sci., 264, 204-222.

Newton, R.C., Geiger, C.A., Kleppa, O.J. and Brousse, C. (1986) Thermochemistry of binary and ternary garnet solid solutions. IMA Abstr. Prog. p.186.

Newton, R.C., Charlu, T.V. and Kleppa, O.J. (1977) Thermochemistry of high pressure garnets and clinopyroxenes in the system CaO-MgO-Al_2O_3-SiO_2. Geochim. Cosmochim. Acta, 41, 369-377.

Nickel, K.G. and Brey, G. (1984) Subsolidus orthopyroxene-clinopyroxene systematics in the system CaO-MgO-SiO_2 to 60 kb, a reevaluation of the regular solution model. Contr. Mineral. Petrol., 87, 35-42.

O'Neill, H.S.C. and Wood, B.J. (1979) An experimental study of Fe-Mg partitioning between garnet and olivine and its calibration as a geothermometer. Contr. Mineral. Petrol. 70, 59-70.

Patera, E.S. (1982) Phase equilibria in the upper Martian mantle, calculation and experiments. Ph.D. thesis, Arizona State University.

Perchuk, L.L. and Lavrent'eva, I.V. (1983) Experimental investigation of exchange equilibria in the system cordierite-garnet-biotite, In "Advances in Physical Geochemistry, v.3", Ed: S.K. Saxena, Springer-Verlag, New York, 199-239.

Perkins, D. (1983) The stability of Mg-rich garnet in the system CaO-MgO-Al_2O_3-SiO_2. at 1000 to 1300°C and high pressure. Amer. Mineral., 68, 355-364.

Perkins, D., Holland, T.J.B. and Newton, R.C. (1981) The Al_2O_3 content of enstatite in equilibrium with garnet in the system MgO-Al_2O_3-SiO_2 at 15-40 kbar and 900-1600°C. Contr. Mineral. Petrol., 78, 99-109.

Presnall, D.C. (1976) Alumina content of enstatite as a geobarometer for plagioclase and spinel lherzolites. Amer. Mineral., 61, 582-588.

Richardson, S.W. (1968) Staurolite stability in a part of the system Fe-Al-Si-O-H. J. Petrol., 9, 468-488.

Richardson, S.W., Gilbert, M.C. and Bell, P.M. (1969) Experimental determination of kyanite-andalusite and andalusite-sillimanite equilibria; the aluminum silicate triple point. Amer. Journ. Sci. 267, 249.

Richardson, S.W., Bell, P.M. and Gilbert, M.C. (1968) Kyanite-sillimanite equilibrium between 700 and 1500 . Amer. Journ. Sci. 266, 513-541.

Robie, R.A. and Bethke, P.M. (1963) Molar volumes and densities of minerals. U.S. Geol. Surv. Rept. TEI-822, open-file report.

Robie, R.A. and Hemingway, B.S. (1984a) Heat capacities and entropies of phlogopite ($KMg_3[AlSi_3O_{10}](OH)_2$) and paragonite ($NaAl_2[AlSi_3O_{10}](OH)_2$) between 5 and 900 K and estimates of the enthalpies and Gibbs free energies of formation. Amer. Mineral., 69, 858-868.

Robie, R.A. and Hemingway, B.S. (1984b) Entropies of kyanite, andalusite, and sillimanite: additional constraints on the pressure and temperature of the Al_2SiO_5 triple point. Amer. Mineral., 69, 298-306.

Robie, R.A. and Stout, J.W. (1963) Heat capacity from 12 to 305 K and entropy of talc and tremolite. J. Phys. Chem., 67, 2252-2256.

Robie, R.A., Finch, C.B. and Hemingway, B.S. (1982a) Heat capacity and entropy of fayalite (Fe_2SiO_4) between 5.1 and 383 K: comparison of calorimetric and equilibrium values for the QFM buffer reaction. Amer. Mineral., 67, 463-469.

Robie, R.A., Hemingway, B.S. and Takei, H. (1982b) Heat capacities and entropies of Mg_2SiO_4, Mn_2SiO_4 and Co_2SiO_4 between 5 and 380 K. Amer. Mineral., 67, 470-482.

Robie, R.A., Hemingway, B.S. and Fisher, J.R. (1978) Thermodynamic properties of minerals and related substances at 298.15 K and 1 bar (10^5 Pascals) pressure and at higher temperatures. US Geol. Survey Bull. 1452.

Sack, R.O. (1982) Spinels as petrogenetic indicators: Activity-composition relations at low pressures. Contr. Mineral. Petrol., 79, 169-186.

Saxena, S.K. (1989a) Personal communication.

Saxena, S.K. (1989b) Assessment of bulk modulus, thermal expansion and heat capacity of minerals. Geochim. Cosmochim. Acta, 53, in press.

Saxena, S.K. (1982) Computation of multicomponent phase equilibria. In: "Advances in Physical Geochemistry, 2". New York: Springer-Verlag, 353 pp.

Saxena, S.K. (1973) "Thermodynamics of rock-forming crystalline solutions". New York: Springer-Verlag.

Saxena, S.K. and Chatterjee, N. (1986) Thermochemical data on mineral phases: the system $CaO-MgO-Al_2O_3-SiO_2$. J. Petrol., 27, 827-842.

Saxena, S.K. and Eriksson, G. (1985) Anhydrous phase equilibria in the earth's upper mantle. J. Petrol., 26, 378-390.

Saxena, S.K. and Eriksson, G. (1983a) Theoretical computation of mineral assembalges in pyrolite and lherzolite. J. Petrol., 24, 538-555.

Saxena, S.K. and Eriksson, G. (1983b) High temperature phase equilibria in a solar composition gas. Geochim. Cosmochim. Acta, 47, 1865-1874.

Saxena, S.K. and Fei, Y. (1988a) The pressure-volume-temperature equation of hydrogen. Geochim. Cosmochim. Acta, 52, 1195-1196.

Saxena, S.K. and Fei, Y. (1988b) Fluid mixtures in the C-H-O system at high pressure and temperature. Geochim. Cosmochim. Acta, 52, 505-512.

Saxena, S.K. and Fei, Y. (1987a) Fluids at crustal pressures and temperatures I. Pure species. Contr. Mineral. Petrol., 95, 370-375.

Saxena, S.K. and Fei, Y. (1987b) High pressure and high temperature fluid fugacities. Geochim. Cosmochim. Acta, 15, 783-791.

Saxena, S.K. and Ghose, S. (1971) Mg^{2+}-Fe^{2+} order-disorder and the thermodynamics of the orthopyroxene crystalline solution. Amer. Mineral. 56, 532-559.

Saxena, S.K., Sykes, J. and Eriksson, G. (1986) Phase equilibria in the pyroxene quadrilateral. J. Petrol., 27, 843-852.

Scarfe, C.M. and Wyllie, P.J. (1967) Experimental redetermination of the upper stability limit of serpentine up to 3 kb pressure. Trans. Am. Geophys. Union, 48, 255.

Schramke, J.K., Kerrick, D.M. and Blencoe, J.G. (1982) The experimental determination of the brucite = periclase + water equilibrium with a new volumetric technique. Amer. Mineral., 67, 269-276.

Seifert, F. (1974) Stability of sapphirine: a study of the aluminous part of the system $MgO-Al_2O_3-SiO_2-H_2O$. J. Geol., 82, 173-204.

Sharp, A.D., Essene, L.M., Metz, G.W., Westrum, E.F., Hemingway, B.S. and Valley, J.W. (1986) The heat capacity of a natural monticellite and phase equilibria in the system $CaO-MgO-SiO_2-CO_2$. Geochim. Cosmochim. Acta, 50, 1475-1484.

Shaw, H.R. and Wones, D.R. (1964) Fugacity coefficients for hydrogen gas between 0° and 1000°C., for pressures to 3000 atm.. Amer. J. Sci., 262, 918-929.

Shmulovich, K.I. (1974) Phase equilibria in the CaO-Al_2O_3-SiO_2-CO_2 system. Geochem. Int., 11, 883-887.

Skinner, B.J. (1966) Thermal expansion. In "Handbook of physical constants", Clark, S.P., (ed.). Geol. Soc. Am. Memoirs, 97, 75-96.

Skinner, B.J. (1956) Physical properties of end-members of the garnet group. Amer. Mineral. 41, 428-436.

Smith, W.R. and Missen, R.W. (1982) Chemical reaction equilibrium analysis. New York; Wiley-Interscience.

Soga, N. (1968) The temperature and pressure derivatives of isotropic sound velocities of α-quartz. J. Geophys. Res., 73, 827-829.

Soga, N. (1967) Elastic constants of garnet under pressure and temperature. J. Geophy. Res. 72, 4227-4234.

Staudigel, H. and Schreyer, W. (1977) The upper stability limit of clinochlore, $Mg_5Al[Si_3Al_{10}](OH)_8$, at 10-35 kbar $P(H_2O)$. Contr. Mineral. Petrol., 61, 187-198.

Sumino, Y. (1979) The elastic constants of Mn_2SiO_4, Fe_2SiO_4 and Co_2SiO_4 and the elastic properties of olivine group minerals at high temperature. J. Phys. Earth, 27, 209-238.

Sumino, Y., Nishizawa, O., Goto, T., Ohno, I. and Ozima, (1977) Temperature variation of elastic constants of single-crystal forsterite between 190 and 400°C. J. Phys. Earth, 28, 273-280.

Suzuki, I. (1975) Thermal expansion of periclase and olivine and their anharmonic properties. J. Phys. Earth, 23, 145-159.

Suzuki, I., Seya, K., Takei, H. and Sumino, Y. (1981) Thermal expansion of fayalite, Fe_2SiO_4. Phys. Chem. Mineral, 7, 60-63.

Syono, Y., Akimoto, S. and Matsui, Y. (1971) High pressure transformations in zinc silicates. J. Solid State Chem., 3, 369-380.

Velde, B. (1966) Upper stability of muscovite. Amer. Mineral., 51, 921-929.

Wagner, V.H. (1932) Zur Thermochemie der Metasilikate des Calciums und Magnesiums und des Diopsids. Z. Anorg. Allgemeine Chemie, 208, 1-22.

Wang, H. and Simmons, G. (1972) Elasticity of some mantle crystal structures. I. Pleonaste and hercynite spinel. J. Geophy. Res. 77, 4379.

Watanabe, H. (1982) Thermochemical properties of synthetic high-pressure compounds relevant to the earth's mantle. In "High pressure

research in geophysics", Akimoto, H. and Manghani, M.H. (eds.). Center for Academic Publications, Tokyo, Japan. 441-464.

Weeks, W.F. (1955) Heats of formation of metamorphic minerals in the system $CaO-MgO-SiO_2-H_2O$ and their petrological significance. J. Geol., 64, 456-473.

Weidner D.J. (1986) Mantle model based on measured physical properties of minerals. In "Advances in Physical Geochemistry" (ed. Saxena, S.K.), Springer-Verlag, New York, 251-274.

White, W.P. (1919) Silicate specific heats. Amer. J. Sci., 47, 1-21.

Windom, K.E. and Boettcher, A.L. (1981) Phase relations for the joins jadeite-enstatite and jadeite-forst at 28 kb. Amer. J. Sci., 281, 335-351.

Windom, K.E. and Boettcher, A.L. (1976) The effect of reduced activity of anorthite on the reaction grossular + quartz = anorthite + wollastonite: a model for plagioclase in the earth's lower crust and upper mantle. Amer. Mineral., 61, 889-896.

Wones, D.R. (1972) Stability of biotite: a reply. Amer. Mineral., 57, 316-317.

Wones, D.R. and Dodge, F.C.W. (1977) The stability of phlogopite in the presence of quartz and diopside. Thermodynamics in Geology. D.G. Fraser (ed.), Dordrecht-Holland: D.Reidel Pub. Co., 229-247.

Wones, D.R. and Eugster, H.P. (1965) Stability of biotite: experiment, theory, and application. Amer. Mineral., 50, 1228-1272.

Wood, B.J. (1978) Reactions involving anorthite and $CaAlSi_2O_6$ pyroxene high pressures and temperatures. Amer. J. Sci., 278, 930-942.

Wood, B.J. (1976) The reaction phlogopite + quartz = enstatite + sanidine + H_2 Progress in Experimental Petrology, Natural Environment Research publication series D, No. 6, 17-19.

Wood, B.J. and Holloway, J.R. (1984) A thermodynamic model for subsolidus equilibria in the system $CaO-MgO-Al_2O_3-SiO_2$. Geochim. Cosmochim. Acta 48, 159-176.

Wood, B.J. and Kleppa, O.J. (1981) Thermochemistry of forsterite-fayalite olivine solutions. Geochim. Cosmochim. Acta, 45, 529-534.

Wood, B.J. and Nicholls, J.W. (1978) The thermodynamic properties of reciprocal solid solutions. Contr. Mineral. Petrol., 66, 389-400.

Wood, B.J., Kirkpatrick, R.J. and Montez, B. (1986) Order-disorder phenomena in $MgAl_2O_4$ spinel. Amer. Mineral. 71, 999-1006.

Woodhead, J.A. (1977) The crystallographic and calorimetric effects of Al-Si distribution of the tetrahedral sites of melilite. Ph.D. dissertation, Princeton Univ. Microfilms, Ann Arbor, Michigan.

Yoder, H.S. (1968) Akermanite and related melilite-bearing assemblages. Yb. Carnegie Instn. Wash., 66, 471-477.